



Høgskulen på Vestlandet

Master Thesis

ING5002

Predefinert informasjon

Startdato:	25-05-2019 09:00	Termin:	2019 VÅR
Sluttdato:	03-06-2019 14:00	Vurderingsform:	Norsk 6-trinns skala (A-F)
Eksamensform:	Masteroppgave		
SIS-kode:	203 ING5002 1 MOPPG 2019 VÅR Haugesund		
Intern sensor:	(Anonymisert)		

Deltaker

Kandidatnr.: 110

Informasjon fra deltaker

Engelsk tittel *: Study of the influence of particle size and moisture content on the explosibility of dusts

Egenerklæring *: Ja **Inneholder besvarelsen** Nei
konfidensiell materiale?:

Jeg bekrefter at jeg har Ja
registrert oppgavetittelen
på norsk og engelsk i
StudentWeb og vet at
denne vil stå på
vitnemålet mitt *:

Jeg godkjenner avtalen om publisering av masteroppgaven min *

Ja

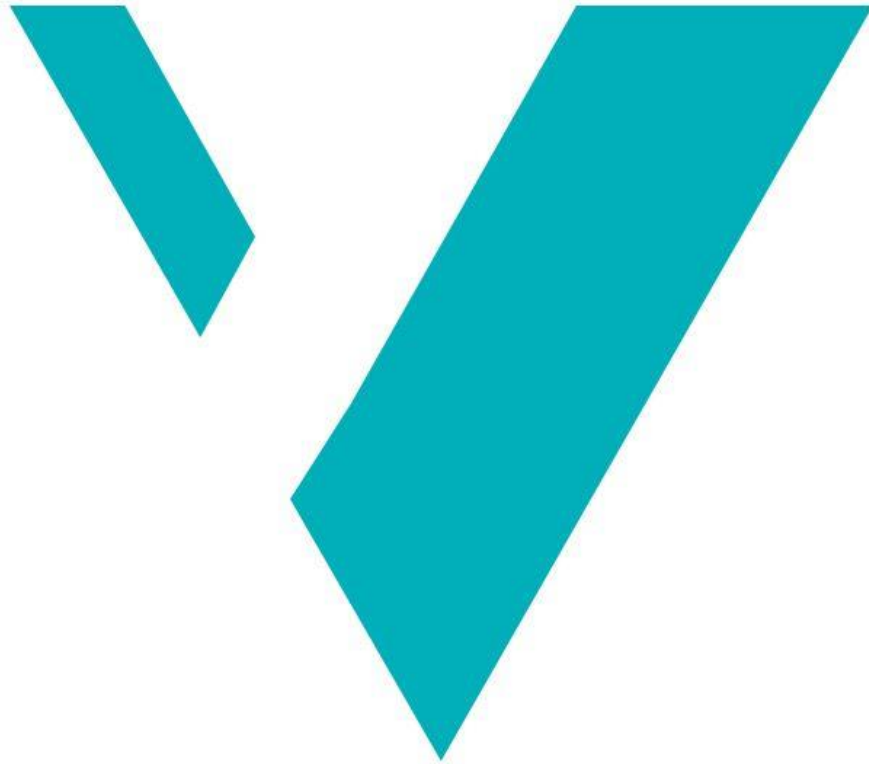
Er masteroppgaven skrevet som del av et større forskningsprosjekt ved HVL? *

Nei

Er masteroppgaven skrevet ved bedrift/virksomhet i næringsliv eller offentlig sektor? *

Nei

Study of the influence of particle size and moisture on the explosibility of dusts



Inger Marie Fanebust

WESTERN NORWAY UNIVERSITY OF APPLIED SCIENCES

Master Thesis in Fire Safety Engineering

Haugesund

June 2019



Western Norway
University of
Applied Sciences

Study of the influence of particle size and moisture on the explosibility of dusts

Master thesis in Fire Safety Engineering

Author:
Inger Marie Fanebust

Author sign.

Inger Marie Fanebust

Thesis submitted:

Spring 2019

Open thesis

Tutor: Dr. Nieves Fernandez-Anez

External tutor:

Keywords:

Dust explosions, NFPA 664, literature review,
statistical analysis, particle size, particle size
distribution, particle shape, biomass, wood
dust, coal, 20L sphere, 1m³ sphere, moisture

Number of pages: 96

+

Appendix: 16

Haugesund, June 3rd, 2019

This thesis is a part of the master's program in Fire Safety engineering at Western Norway University of Applied Sciences. The author(s) is responsible for the methods used, the results that are presented, the conclusion and the assessments done in the thesis.

Preface

It is a pleasure to finally be able to present this thesis that I have been working towards for the better part of a year. This is the final part of my Master of Science in fire safety engineering, and it has been quite a journey. I started out knowing next to nothing about dust explosions and now I think I'm quite ready to join the cult.

This project has been funded as part of a collaboration with the NFPA Research Foundation. The collaboration results in a report named *Influence of particle size and moisture content of wood particulates on deflagration hazard* and a poster that was presented at the European Geoscience Union's general assembly. The conference took place in Vienna in April and was sponsored by the Research Foundation. The content, opinions and conclusions contained in this report are solely those of the authors and do not necessarily represent the views of the Fire Protection Research Foundation, NFPA, Technical Panel or Sponsors.

I would like to give my sincerest thanks to my supervisor Dr Nieves Fernandez-Anez who has been with me every step on the way. Your encouragement and undying optimism have been so much appreciated, and your enthusiasm for the subject is contagious. This would have been a very different project without your help and guidance.

I would also like to direct my thanks to the NFPA Research Foundation who first suggested the topic and presenting the problem. In particular to Sreenivasan Ranganathan, who has been our liaison at the Research Foundation, and who has been most helpful and forthcoming whenever I had any queries. It's the Research Foundation's sponsorship that let me present my work at an international conference. I would also like to acknowledge the rest of the panel, for sharing their insight on the challenges facing businesses that work with wood particulates, and their advice on the article

Henrik, your love and support and willingness to cook have been absolutely lifesaving. Thank you.

And to my family, most importantly my parents: You are great, I'm lucky to have and without you, none of this would ever have happened (literally). I would also like to give a shout out to my grandmother who has called me on a near weekly basis. I appreciate your concern.

Abstract

This project was started on the behest of the NFPA Research Foundation. It consists of a literature review and a statistical analysis. The aim has been to uncover whether the median particle size limit given in the standard NFPA 664 is supported by scientific literature. The standard applies to woodworking industries and considers dust with a mass median particle size greater than 500 μm and moisture content above 25% to be non-deflagrable.

The literature review focuses on finding the effect of particle size and particle size distribution as well as moisture content. In addition, since shape is a defining attribute of biomass dusts, particle shape has also been studied. A major point in scientific literature is that smaller particles are considered more dangerous because they are more easily ignited, more easily dispersed and will give more violent explosions. Larger particles require more energy to heat to the point of devolatilization and leading to a decrease in maximum explosion pressure and maximum rate of pressure rise. Explosion severity's dependence on particle size is considered well-established through explosion tests. Such tests should, according to standards, be executed in a 1 m^3 explosion chamber. The explosion chambers are equipped with instruments to measure and record pressure development. There is also a more affordable version of the explosion chamber, the 20 L-sphere. It can be calibrated to match the results from the 1 m^3 - chamber and is widely used.

As part of the literature review a data collection was also conducted. The original intention was to only collect data from research on wood. This quickly proved a challenge as there were limited amounts of data available. To have enough data to perform an analysis, other biomasses was added to the collection, then coal dust was added as well. The samples were first considered all together, then coal and biomass were considered separately, finally biomass was split in to wood and non-wood biomasses. This enabled comparison between coal and biomass, and between wood and other biomasses. The data has been used to look for correlations between attributes of the dusts (d_{10} , d_{50} , d_{90} , PDI and moisture content) and the explosion properties (P_{max} , $(dP/dt)_{\text{max}}$, K_{St} and MII). To examine particle size distributions histograms and boxplots were used. Biomass and coal were compared and among the samples, biomass show a wider range of particle sizes. The average biomass particle is also larger than the corresponding coal particle. Despite this P_{max} is higher for biomass than coal.

Some findings were in line with the expectations set by the literature review, while other where surprising. Like in cases where the correlation analysis showed opposite trends between coal and biomass. This would suggest that drawing conclusions for biomass based on what is known about coal is not optimal, neither is using standard equipment or procedures developed for coal.

The main conclusion is that there is a great need for further work. There need to be an agreed upon standard for how to measure particle size, especially biomass. In addition, finding out which dust parameters is most useful to predict explosion outcome is urgent.

Sammendrag

Dette prosjektet er initiert på forespørsel fra amerikanske NFPA Research Foundation og består av en litteraturstudie og en dataanalyse. Målet har vært å avdekke om grenseverdiene for median partikkelstørrelse som er gitt i standarden NFPA 664 er understøttet av eksisterende forskningslitteratur. Standarden regulerer tiltak for å unngå brann og eksplosjoner i trevareindustrien. Den anser at støv med median partikkelstørrelse på over 500 μm og med fuktighet over 25% ikke utgjør en eksplosjonsfare.

Litteraturstudien forsøker å bestemme hvilken effekt partikkelstørrelse og sammensetning av partikkelstørrelser, og innhold av fuktighet har på eksplosjonsscenarioer. I tillegg, siden partikkelens form er en viktig, definerende egenskap for støv av biomasse, har dette også blitt undersøkt. Et viktig poeng er at mindre partikler er ansett som en større trussel fordi de er lettere å antenne, har lettere for å danne støvskyer og gir mer voldsomme eksplosjoner. Større partikler krever mer energi før pyrolyse kan inntreffe noe som vil gi mindre hurtig trykkøkning ved eksplosjon og et lavere maksimaltrykk. Denne sammenhengen mellom trykkutvikling og partikkelstørrelse er ansett som veletablert og bekreftet ved hjelp av eksplosjonstester. Slike tester skal, i følge standarder, utføres i et 1 m^3 eksplosjonskammer. Eksplosjonskammeret skal være utstyrt med trykkmålere som registrerer trykkutviklingen. Et alternativ til 1 m^3 -kammeret er 20-literskammeret. Dette er i utstrakt bruk da den er billigere i drift og kan kalibreres så resultatene samsvarer med dem fra det større kammeret.

Som en del av litteraturstudien er det også foretatt en datainnsamling. Intensjonen var opprinnelig å bare samle inn data fra forsøk med trematerialer. Dette viste seg raskt å være en utfordring ettersom det var sært begrenset med tilgjengelige data. For å ha nok data til å kunne utføre en statistisk analyse ble andre biomasser lagt til, deretter ble også data for kull inkludert. I analysen ble materialprøvene først vurdert som en helhet, deretter delt opp slik at biomasse og kull kunne vurderes hver for seg. Videre ble biomassen delt opp i tre og andre biomasser. Dette gjorde det mulig å sammenligne materialene og se etter ulikheter mellom biomasse og kull, samt tre og andre biomasser. Dataene ble brukt til å se etter korrelasjon mellom egenskaper i støvprøvene (d_{10} , d_{50} , d_{90} , PDI og væskeinnhold) og eksplosjons egenskaper (P_{max} , $(\text{dP}/\text{dt})_{\text{max}}$, K_{St} og MIT). Histogrammer og boksdiagram ble brukt for å undersøke fordelingen av partikkelstørrelser. En sammenligning av dataene for kull og biomasse viser at biomassepartiklene generelt er større enn kullpartiklene og har samtidig en bredere fordeling av størrelser. Til tross for dette er P_{max} høyere for kull.

Noen av funnene i dataanalysen var i tråd med forventningene satt av litteraturstudien, mens andre funn var mer overraskende. Eksempelvis i tilfellene hvor korrelasjonsanalysen viste motsatte trender for kull og biomasse. Forklaringen på dette er usikker, men det antyder at det kan være ugunstig å trekke konklusjoner om biomasse basert på kunnskap om kull. Det samme gjelder det å bruke standard testutstyr og prosedyrer utviklet for kullstøv.

Hovedkonklusjonen i dette arbeidet er at det er et stort behov for videre forskning. Det trengs en standard for hvordan partikkelstørrelse skal måles, særlig biomasse. I tillegg, må det undersøkes videre hvilke parametre i for støvet som korrelerer best med eksplosjonsparameterne.

Table of contents

Preface.....	V
Abstract.....	VII
Sammendrag.....	IX
Table of contents.....	XI
Table of figures.....	XV
Figures.....	XV
Tables.....	XVI
Definitions.....	XVII
1. Introduction.....	1
1.1. Historical dust explosions.....	1
1.2. The problem at hand.....	3
1.3. NFPA 664: Standard for the Prevention of Fires and Explosions in Wood Processing and Woodworking Facilities.....	5
2. Theory.....	7
2.1. Dust explosions.....	7
Main factors influencing dust explosions.....	8
2.2. The effect of particle size.....	10
Particle size distribution.....	14
2.3. The importance of particle shape.....	17
Agglomeration.....	18
2.4. The influence of moisture.....	21
3. Methods.....	23
3.1. Available testing methods.....	23
For particle size.....	23
For explosion characteristics.....	30
For moisture content.....	33
3.2. Statistical analysis.....	34

Data collection.....	34
Histograms and boxplots.....	34
Scatterplots.....	35
Sources of error.....	36
4. Results.....	37
4.1. Attributes of the samples.....	37
4.2. Attributes of the explosion tests.....	39
4.3. The scatterplots.....	43
P_{\max} and d10.....	43
P_{\max} and d50.....	44
P_{\max} and d90.....	45
P_{\max} and the polydispersity index.....	46
P_{\max} and moisture.....	47
K_{St} and d10.....	48
K_{St} and d50.....	49
K_{St} and d90.....	50
K_{St} and the polydispersity index.....	51
K_{St} and moisture.....	53
dP/dt and d10.....	54
dP/dt and d50.....	55
dP/dt and d 90.....	56
dP/dt and the polydispersity index.....	57
dP/dt and moisture.....	58
MIT and d10.....	59
MIT and d50.....	60
MIT and d90.....	61
MIT and the polydispersity index.....	62
MIT and moisture.....	63

Specific surface area	64
5. Discussion	65
6. Conclusion.....	69
7. Further work	71
8. References	73
9. Appendix A – data collection.....	A
10. Appendix B – EGU poster and abstract.....	N
10.1. Abstract.....	N
10.2. Poster	P

Table of figures

Figures

Figure 1. Explosion pentagon	7
Figure 2. Influence of particle size on the maximum pressure of explosion of wood dust [28]	11
Figure 3. Influence of median particle size in MIE [22]	13
Figure 4: Particle size distributions in the experiments of Gao et al. [36].....	15
Figure 5. Influence of particle shape on the sieving method	17
Figure 6. Equivalent spherical diameters [14]	17
Figure 7. Effect of agglomeration in dust particles [23].....	19
Figure 8: Explosion severity of coal dust at different moisture content in the size range 125-550 μm [52].....	22
Figure 9: Example of particles with different kinds of shapes [53].....	24
Figure 10: Tunnel separator schematic diagram (fig. 2 in article [56]).....	27
Figure 11: Evolution of the overpressure in the sphere during the explosion [28]	30
Figure 12: Leeds ISO 1 m ³ vessel [59].....	31
Figure 13: A general boxplot	35
Figure 14: Boxplot showing the particle sizes for biomass and coal (note: one outlier for d90 biomass has been excluded for readability)	37
Figure 15: Histogram for d10, biomass and coal	38
Figure 16: Histogram for d50, biomass and coal	38
Figure 17: Histogram for d90, biomass and coal	38
Figure 18: Boxplot showing maximum explosion pressure for biomass and coal	39
Figure 19: Boxplot showing maximum rate of pressure rise for biomass and coal.....	39
Figure 20: Boxplot showing explosion indexes (K_{St}) for biomass and coal.....	40
Figure 21: Scatterplots showing correlations between maximum pressure and d10	43
Figure 22: Scatterplots showing correlations between maximum pressure and d50	44
Figure 23: Scatterplots showing correlations between maximum pressure and d90	45
Figure 24: Scatterplots showing correlations between maximum pressure and the polydispersity index.....	46
Figure 25: Scatterplots showing correlations between maximum pressure and moisture content	47
Figure 26: Scatterplots showing correlations between the explosion index and d10	48
Figure 27: Scatterplots showing correlations between the explosion index and d50	49
Figure 28: Scatterplots showing correlations between the explosion index and d90	50
Figure 29: Scatterplots showing correlations between the explosion index and the polydispersity index.....	51
Figure 30: Scatterplots showing correlations between the explosion index and moisture content	53
Figure 31: Scatterplots showing correlations between the maximum rate of pressure rise and d10	54

Figure 32: Scatterplots showing correlations between the maximum rate of pressure rise and d50	55
Figure 33: Scatterplots showing correlations between the maximum rate of pressure rise and d90	56
Figure 34: Scatterplots showing correlations between the maximum rate of pressure rise and the polydispersity index	57
Figure 35: Scatterplots showing correlations between the maximum rate of pressure rise and moisture content	58
Figure 36: Scatterplots showing correlations between the minimum ignition temperature and d10.....	59
Figure 37: Scatterplots showing correlations between the minimum ignition temperature and d50.....	60
Figure 38: Scatterplots showing correlations between the minimum ignition temperature and d90.....	61
Figure 39: Scatterplots showing correlations between the minimum ignition temperature and the polydispersity index	62
Figure 40: Scatterplots showing correlations between the minimum ignition temperature and moisture content	63
Figure 41: Scatterplots for specific surface area and explosion parameters.....	64

Tables

Table 1: Examples of some historical dust explosions.....	2
Table 2: Summary of the available testing methods for particle size	29
Table 3: Summary of the results from the data analysis.....	42
Table 4: Data collection part 1/2 – dust parameters.....	A
Table 5: Data collection part 2/2 – combustion properties of the dusts.....	H

Definitions

Materials	
Dust	Finely divided solid material.
Biomass	Plant/organic material that can be used for fuel.
Wood	A type of biomass.
Coal	A type of fossil fuel.
Particle characteristics	
D ₅₀	The median diameter. Used for reporting particle size, 50% of particles have a smaller diameter than the given value for d ₅₀ . Usually in µm.
D _{XX}	The diameter at the XX th percentile of a distribution.
Polydispersity index, PDI	An index for how large the span of a distribution is. A higher number indicates a wider distribution. $PDI = \frac{d_{90} - d_{10}}{d_{50}}$
SSA	Specific surface area. Total superficial area of a particle.
Explosion characteristics	
P _{max}	Maximum explosion pressure, usually given in bar. Measured in explosions chambers, such as the 20L-sphere or 1 m ³ -chamber.
(dP/dt) _{max}	Maximum rate of pressure rise in an explosion, usually given in bar/s. Measured in explosions chambers, such as the 20L-sphere or 1 m ³ -chamber.
K _{St}	Dust explosion index/deflagration index. Measure the relative severity compared to other dusts. Higher index means more severe explosion. [bar m/s] $K_{St} = \left(\frac{dP}{dt}\right)_{max} \cdot V^{1/3}$
MIT	Minimum ignition temperature.
MEC	Minimum explosible concentration.
Statistics	
Median	The median value in a distribution is a value half of the population is below.
Mean	Average.

Correlation factor, R	A number between -1 and 1 that indicates whether two variables are correlated.
p-value	A number between 0 and 1 indicating the strength of the correlation factor R.

1. Introduction

1.1. Historical dust explosions

Dust explosions are a threat to human lives, material property and commercial interests. The first documented dust explosion happened in Italy at Giacomelli's Bakery Warehouse in 1785 in a bakery. A cloud of flour dust was ignited by a lamp. Two workers were injured in the explosion [1]. After the first dust explosion was recorded more followed suit, and for the first couple of hundred years or so incidents overwhelmingly involved grains and flour.

In more recent history, one explosion that has been thoroughly investigated by the U.S. Chemical Safety Board is the incident at Imperial Sugar Company on February 7th, 2008. 14 workers were killed and 36 injured, 70 other workers escaped unharmed. In the investigation report it can be read that the first explosion was likely caused by a packing material being dropped off a forklift, resulting in a cloud of sugar in the air that few seconds later was ignited. This set off a series of fireballs across a large area of the facility. The secondary explosions were dust explosion where sugar dust had been dislodged for overhead equipment had been dislodged and dust from floors and other horizontal surfaces were disturbed and blasted into the by the pressure waves from the primary explosion. The CBS thinks the secondary explosions could have been largely avoided had good cleaning and maintenance procedures been practiced. The violence of the explosions also caused ruptures in the waterpipes, disabling the sprinkler system. [2].

In 2012, Canada had two sawdust explosions. The first one, on January 20th at Babine Forest Productions, cost two human lives and 20 people were injured. Later that year on April 24th, an explosion at Lakeland Sawmill claimed another two lives and left 22 people with injuries. Both incidents had wood as the fuel of the explosions.

Another wood dust explosion claimed 4 lives. In 2015 a dust explosion in Bolsey wood mill in the United Kingdom. The incident occurred on June 17th, but the following fires took several weeks to put out, due to difficult access to the burning material and the smouldering character of the fire [3].

It turns out even oregano can give explosions. 5th of April 2016 suspended oregano dust ignited and a grinding hopper was destroyed in the following explosion. None of the workers at High Quality Organics were injured in the incident. [4].

Table 1: Examples of some historical dust explosions

Year	Location	Company/business	Material	Loss	Ref.
1785	Italy	Giacomelli's Bakery Warehouse	Flour	2 injured.	[1]
1858	Stettin, Poland	Roller mill	Grain dust	Mill building destroyed	[1]
1893	Litchfield, IL, USA	Great Planet Flouring Mill	Grain dust	1 killed, 12 injured, 40 houses destroyed	[5] [1]
1916	Peterborough, ON, Canada	Quaker Oats Cereal Factory	Grain dust	23 killed, entire plant destroyed	[1]
2008	Port Wentworth, GA, USA	Imperial Sugar Company	Sugar	14 killed, 36 injured	[2]
2011	Atchison, KS, USA	Barlett grain co	Grain dust	6 killed, 2 injured	[6]
2012	Burns Lake, BC, Canada	Babine Forest Productions	Wood dust	2 killed, 20 injured	[7]
2012	Prince George, BC, Canada	Lakeland Sawmill	Wood dust	2 killed, 22 injured	[8]
2013	Våler, Hedmark, Norway	Forestia Braskereidfoss	Wood dust	Production building destroyed	[9]
2015	Bosley, UK	Wood Treatment Limited	Wood dust	4 dead, 4 injured	[3]
2015	New Taipei, Taiwan	Formosa fun coast festival	Starch dust	15 dead, 497 injured	[10]
2016	Reno, NV, USA	High Quality Organics	Oregano	Damaged equipment	[4]
2018	Aqaba Port, Jordan	Abu Ghraib Trading Co/unknown	Grain dust	7 killed, 2 injured	[11]

1.2. The problem at hand

The influence of particle size and moisture content on the behaviour of dust explosions has been thoroughly studied for coal, and it is well known that smaller and drier products cause easier-to-ignite clouds and that the resulting explosions are more violent. Several researchers have satisfactorily worked on describing these influences, both experimentally and computationally. However, with the increase on the use of new energy materials such as biomass, this behaviour needs to be revised and reconsidered to ensure safe working spaces.

When starting to look at the available data for the wood industry, it became evident how scarce this data is. Companies and facilities are testing these materials, but the data is not available, and the general public cannot access it.

However, this lack of availability is not the only problem that needs to be solved. Biomass was treated as any previous studied fuels, mainly fossil fuels, and assumptions were made in order to use the already established knowledge in this case. However, there is a fundamental difference between coal and biomass particles that leads to several gaps of knowledge that need to be filled: sphericity. Coal particles have always been treated as spherical particles, and all the studies regarding their deflagration behaviour is based on this. Nevertheless, biomass particles are not spherical, one of the dimensions often being much larger than the other two. This implies the need of a change in the parameters used to define the particle size of these materials, and a new complete study on how this change influences the deflagration behaviour of dusts.

Finally, and no less important, the lack of consensus on the use of a determined experimental procedure to measure the particle sizes increases the uncertainty around the values, and the impossibility of comparing the obtained results.

The influence of moisture is clearer in this case. Moisture can promote the explosibility of certain materials, but in the case of wood, an increase on the moisture content causes a decrease of both the tendency to ignite and the severity of the explosions.

The process to fill these research gaps has already started, but it needs to accelerate, and to be prioritized, because it is the only way of ensuring safe working spaces.

The standard NFPA 664 defines the values of particle size and moisture content of wood particulates that cannot be surpassed in order to avoid explosions.

In the present document the existing knowledge will be examined, focusing on particle size, shape and distribution, and moisture content in dust explosions; this report studies the different experimental procedures used to determine the particle size, which lead to an inconsistency of the obtained results; reports the data collected regarding the particle size; and finish with some advice on future needs.

Furthermore, the available data has been examined with regards to data of explosions depending on particle size and moisture content. The data has been analysed with an aim to understand the behaviour of dusts, and for this purpose the correlations existing between these data and parameters defining the particle size has also been studied. The data collected from literature shows a wide range of values that, analysed together, does not provide the expected results that can be found in literature.

1.3. NFPA 664: Standard for the Prevention of Fires and Explosions in Wood Processing and Woodworking Facilities.

The NFPA (National Fire Protection Association) is a non-profit organisation based in the USA whose declared mission is to eliminate death, injury, material or economic loss due to fire, electrical or related hazards. This work includes having published 300 codes and standards. [12]

The NFPA 664 is, as the name suggests, focused on preventing fires and explosions in wood processing and woodworking industries. Its purpose is to provide minimum requirements for the design, operations and maintenance with regards to the safety of life, property protection and mission continuity from fire and explosion. The standard applies to all new facilities and to new processes in existing facilities. It does not apply to facilities that were built or approved to be built before the standard were published in 2017.

Chapter 3 of the standard gives some definitions of relevant terminology. A deflagration is “propagation of a combustion zone at a velocity less than the speed of sound”. And a deflagration hazard is determined to exist either if a certain amount of deflagrable wood dust covers upward facing surfaces or if deflagrable wood dust is suspended in the air under normal operating conditions in amounts greater than 25 % of the MEC. There is also included a wide definition of wood: Cellulosic materials derived from trees, wheat straw, flax, bagasse, coconut shells, corn stalks, hemp, rice hulls, paper or other fibres used as a substitute or additive to wood.

The most relevant of the definitions (at least as concerns to this project) are perhaps the definitions of deflagrable and non-deflagrable wood dust. Deflagrable wood dust is any dust that will propagate a flame front, thus presenting a fire or explosion hazard, when suspended in air or other oxidizing medium. Wood particulate with a mass median particle size of 500 µm or less, with a moisture content of less than 25 % are considered deflagrable. A non-deflagrable dust is a dust with the same moisture content (25 %), but a mass median particle size greater than 500 µm.

Chapter 4.4 determines when a deflagration hazard exists. This is when the average thickness of a layer of flammable dust is over 3,2 mm or, for smaller areas if the layer exceeds 3,2 mm in at least 5 % of the area. There is some flexibility in the 3,2 mm criteria should the dust in question have a settled bulk density other than 230 kg/m³. The following equation is to be used for finding the correct allowable dust layer thickness (this is eq. 4.4.2b in the standard, eq. 4.4.2a is the same equation, but using U.S. customary units):

$$T = \frac{(3,2 \text{ mm})(320 \text{ kg/m}^3)}{(\text{Settled Bulk Density, kg/m}^3)} \quad (1)$$

where:

T = the allowable thickness (mm)

Chapter 8 follows up stating that there is also a deflagration hazard anywhere deflagrable wood dust is, or could be, suspended in air during operation at a maximum concentration above 25 % of the MEC. The appendix to this chapter warns that all wood waste in an enclosed dust collector should be considered as potentially deflagrable. According to the standard, wood waste usually has a deflagration risk if the mean particle size is less than 420 μm and where as little as 10 % of the dust has a diameter of less than 80 μm . However, the standard claims that if the mean particle size exceeds 420 μm , only weak deflagrations are likely.

The following is a list from Ch. 8.4.1.2 of the physical properties of particulates that should be considered when evaluating the hazard of particle size reduction equipment.

1. Minimum explosible concentration (MEC)
2. Minimum ignition energy (MIE)
3. Particle size distribution
4. Moisture content as received and tested
5. Maximum explosion pressure at optimum concentration
6. Maximum rate of pressure rise at optimum concentration
7. K_{St} (normalized rate of pressure rise) as defined in ASTM E1226, *Standard Test Method for Pressure and Rate of Pressure Rise for Combustible Dusts*
8. Layer ignition temperature
9. Dust cloud ignition temperature
10. Limiting oxidant concentration (LOC) to prevent ignition
11. Electrical resistivity
12. Charge relaxation time
13. Chargeability

2. Theory

2.1. Dust explosions

Even though the most known explosions are those caused by combustible gases, dust explosions are as frequent and damaging as the first one, and *“both types of explosions have the potential to cause loss of life, personal injury, property damage, business interruption, and environmental degradation”* [13].

A dust explosion happens when an ignition source is introduced to a cloud of combustible dust. The phenomenon that follows can be described as a “ball of flame”. The flame front will propagate out in all directions from the ignition point and create a volume of hot combustion products. The high temperature combustion gases will typically expand into the unburnt dust and preheat it. This will make the combustion zone expand more quickly and create even more combustion gases that will again contribute to preheating unburnt material accelerating the process further. [14].

In the study of dust explosions, the first obstacle is the definition of dust. As Amyotte points out in his book [13], NFPA 68 [15] defines dust as any finely divided solid, 420 μm or less in diameter. However, they define combustible dust as a combustible particulate solid that presents a fire or deflagration hazard when suspended in air or some other oxidizing medium over a range of concentrations, regardless of particle size. And this is only scraping the surface of the problems that arise when attempting to quantify the data.

In order for a dust explosion to occur, five factors have to come together to make what has been called the dust explosion pentagon [16]:

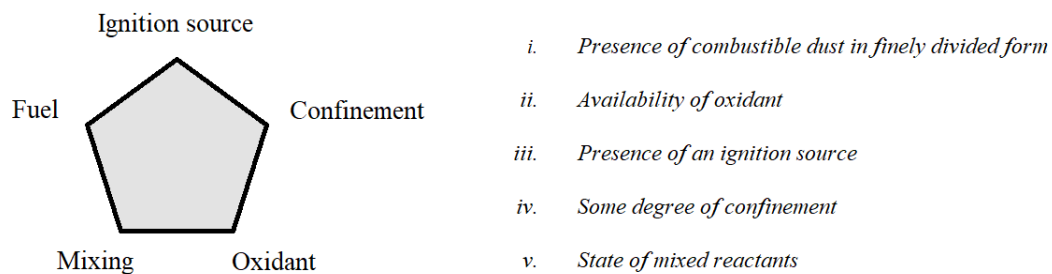


Figure 1. Explosion pentagon

Furthermore, it is known that any combustible material that poses a fire hazard in its solid form, will also pose an explosion hazard if dispersed in air as dust. In addition, some materials that are not normally considered combustible can still be explosible when in dust form, such as metals [17]. This makes a long list of hazardous materials that need to be studied, characterised and classified.

Main factors influencing dust explosions

The main factors that influence the characteristics and consequences of dust explosions have been previously studied, mainly for fossil fuels. However, even when their importance is well-known, it is difficult to quantify it and their relative influence needs to be further studied, as well as how a combination of several factors affects these processes. Moreover, some of these parameters may present unexpected behaviours for different materials. That is why, due to the rise of new fuels, they need to be deeply studied and characterised. The parameters listed below represent the main ones that always need to be determined in order to understand the characteristics and consequences of dust explosions.

Chemical composition

Volatiles, ash and moisture contents are basic parameters influencing the explosibility of dust clouds. An increase on the first one produces an increase on the explosibility of clouds, while the effect of an increase of ash or moisture are just the opposite. [18] [19].

Particle size

Fine particles facilitate the flame propagation, and both the easiness of ignition and the severity of the explosion increases with their presence.

Dust concentration

The concentration of a fuel in air must be in the range formed by the lower explosive limit and the upper explosive limit (flammable range) to be ignitable. In the case of dusts, the upper explosive limit is not very often used. [20].

Ignition source

The type of ignition source, amount of energy, exposure time, volume of the sample affected by this energy and its spatial distribution can affect the characteristics of the explosion.

Initial temperature and pressure

A higher initial temperature or pressure cause a reduction of the mass of air available for combustion and a reduction of the moisture of the sample, which produces an increase on the explosion severity [21].

Turbulence

Turbulence will remove heat from the ignition zone by rapid convection, so ignition requires higher energies and temperature. On the other hand, turbulence increases the violence of the explosion [22].

Gas presence

Depending on the gas mixed with the dust, the explosion can be prevented (hydrogen) or promoted (methane).

2.2. The effect of particle size

The explanation of the differences between dust and gas or vapour explosions can be simplified by the heterogeneity of the clouds that are formed. Dispersed dust is continuously in a movement-deposition situation, caused by air currents and turbulence, which largely depends on the particle size.

The quantitative and qualitative dependence of the violence of explosion on particle size is strongly affected by the interplay of phenomena controlling the combustion/heating of solid material [23]. Eckhoff observed that the general trend in dust deflagrations shows that a decrease on the particle size causes an increase on the deflagration risk. However, this trend does not continue indefinitely as the particles get smaller. Deflagration of dust clouds consists on three consecutive processes: devolatilization, gas-phase mixing, and gas-phase combustion. Particle size influences the devolatilization rate, so that the lower the particle size, the higher the devolatilization rate. However, a lower limit in this depends on the ratios between the three processes, and not in any of them individually. Above this critical particle size, the devolatilization process becomes the critical factor in the flame propagation, but below it, devolatilization is so fast that the combustion is controlled by gas mixing and gas combustion.

Gao et al. [24] theoretically proved that the flame propagation mechanisms during dust explosions transitioned from kinetics-controlled to devolatilization-controlled as increasing the particle size. They observed that when kinetics controls the flame propagation, the flame front formed was smooth and its shape is similar to the premixed gas explosions. The flame zone consisted of premixed blue flame at the leading zone and luminous flames behind it. Opposite, when devolatilization controls the flame propagation, the flame front had a complicated structure. The flame zone consisted of blue spot flames at the leading zone and luminous flames behind them. The yellow luminous zone formed in the two different flame propagation regimes was explained as follows: around the particles, local high-concentration regions of fuel existed; when those particles burned without sufficient oxygen, soot particles were formed, and these particles emitted yellow flame. Because the particles were scattered, the pyrolysis fuel concentration was not uniform. The Damkoler number defines the transition between kinetics-controlled and devolatilization-controlled, which is proportional to the particle size. Dobashi and Senda [25] pointed out that the flame structure was dependent on the relation between gasification rate and flame propagation velocity.

In general, it can then be said that smaller particles pose a greater deflagration risk than larger particles. Small particles are more easily dispersed and will stay suspended for longer. Moreover, because the particles are small, they are heated to the point of devolatilization or pyrolysis by less energy, are therefore more easily ignited, and can better propagate a flame. Based on the assumption that pyrolysis or devolatilization is very fast when the particle size is small enough, gas combustion becomes the controlling factor [26].

On the other hand, larger particles require more heat to devolatilize, often resulting in incomplete combustion and a continued risk of deflagration. The controlling factor for what speed a flame can propagate through a dust cloud will therefore be devolatilization, once the particle size passes a critical value [26]. The severity of the explosion will decrease as the particle size increases. As an example, Rice et al. [27] observed that coal dust particles above 850 μm ceased to take part in the explosion.

This dependence on particle size has been observed in relation to several used to characterise the ignition sensitivity and explosion severity of dusts. The effects of an increase in explosible dusts' particle size are numerous and well-established; these include, for example, a decrease in the maximum explosion pressure, P_{max} , potentially significant decrease in the maximum rate of pressure rise, $(dP/dt)_{\text{max}}$, and an increase in the minimum explosive concentration (MIE) [23]. "Increasing particle size is a classic application of inherent safety". Some other effects are explained below.

Calle et al. [28] observed the influence of particle size on the maximum pressure of explosion of wood dust, as shown in Figure 2, with a decrease of explosion pressure when the range of particle size increases.

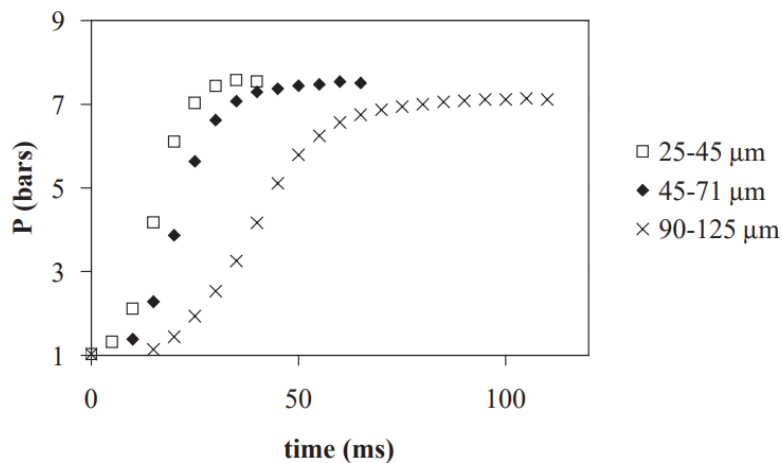


Figure 2. Influence of particle size on the maximum pressure of explosion of wood dust [28]

Fumagalli et al. [29] developed a model that shows the strong reduction of the explosion index K_{St} when the dust mean diameter increases.

The minimum ignition temperature (MIT) is affected due to the inefficient exchange of heat between the gas and dust particles when the dust particles are coarser, requiring more temperature to undergo devolatilization and thereby ignition. Eckhoff [23] studied this influence in coal dust and observed that there is also a limiting particle size (38 to $<75 \mu\text{m}$) below which there is no significant change in MIT. He then determined that the limiting size for coal dust is in the order of 50 μm , but several factors affect this limiting size, such as oxygen concentration, moisture content, porosity, discharge pressure, etc.

The minimum explosive concentration (MEC) for combustible dusts is the concentration of dust in air that is just enough to support flame propagation. MEC corresponds to the lower flammability limit (LFL) used for fluid fuels. Lower and upper flammability limits (LFL and UFL) for flammable gases and vapours are easily found in standardized laboratory test [14]. For dusts, the MEC can also be determined in laboratory tests by observing the success or failure of a flame propagating through dust suspended in a tube. It is possible then to observe which concentrations can support the combustion, and therefore may pose a deflagration risk. Some discrepancies in the results have occurred when comparing tests with the same concentration, but different direction of flame propagation [14] (these tests are often performed in a vertical tube). This is believed to be due to gravity, when the suspended dust is ignited at the top the flame will be moving downward as the dust particles fall away from the flame front, thus making the effective concentration lower. The opposite is true when dust is ignited at the bottom, it will then be falling towards the flame, increasing the effective concentration.

For combustible dusts the MEC can be determined with some certainty, however the maximum explosible concentration is more difficult. Theoretically there is an upper concentration limit, or rich limit, though experiments in a 20 L-sphere have showed that it is possible to get an explosion from both coal dust and polyethylene at concentrations above 4000 g/m³ [30]. For comparison the rich limit for methane is 200-300 g/m³ [30].

The inter-particle distance in a dust cloud will also be larger at lower concentrations, leading to inefficient particle to particle heat transfer and explosion propagation. Hence, more heat will be required to be transferred to the dust cloud for ignition and explosion propagation. In other words, in the case of lower dust concentrations, the MIT will be higher than that of the higher concentrations. Conversely, as the dust concentration increases, the number of particles per unit volume increases, leading to a decrease in inter-particle distance and efficient heat transfer between the particles. As a result, there will be more particles at a raised temperature causing a vigorous explosion even at a lower MIT. However, there is a restriction to the MEC, which is not clearly defined, probably due to its dependence on a number of factors [31].

Particle size also heavily influences the minimum ignition energy (MIE) of dust clouds, as Eckhoff reported in his book for three materials: aluminium, optical brightener and polyethylene [23]. In 1979, Kalkert and Schecker [32] developed a theory indicating that the MIE is proportional to the cube of the particle diameter. However, this relationship has not been confirmed, and different researches have obtained different results, probably due to the presence of fine size fractions in the dusts, which shows the need for considering the entire size distribution rather than just a mean size [23].

Nevertheless, the influence of particle size in MIE cannot be neglected, as Figure 3 shows with the results of three different dusts whose MIE decreases systematically with particle size. [33]

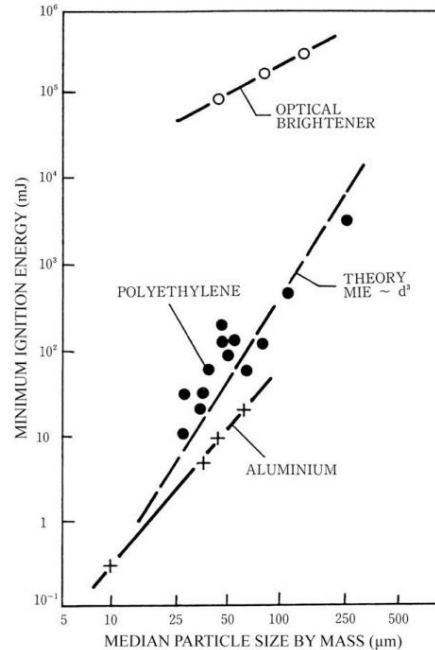


Figure 3. Influence of median particle size in MIE [22]

Focusing on the wood processing industry, the influence of particle size was observed at the wood processing industry, and reported by Amyotte et al. [34] from a facility that suffered a dust explosion. Trying to investigate the accident, explosibility analyses on a Siwek 20-L sphere were developed. They observed the inadequacy of designing the safety measurements of the facility only taking into account the coarse particles, even when they are present much more frequently. In this case, pockets of fine dust were found in a dead-space in the process unit header, and these fine particles present almost twice the value of maximum pressure of explosion and the K_{St} increased from 9 for coarse particles to 130 for the fine ones. This shows the importance of detecting and analysing small particle sizes, and designing the measurements always considering these parameters to avoid non desirable consequences.

In general, it is considered that bulk materials do not present that high risk, since they are difficult or even impossible to put into suspension, so dust clouds are not expected. However, it is important to keep two facts in mind. First, bulk materials can break into smaller particles or into dust from just being handled, so they should always be treated as a potential dust when prevention and protection measurements are considered. Second, there is an important risk of ignition from layers that can act as ignition sources. In that case, both dust and bulk materials can ignite, in some cases with the same probability and risk [35].

Particle size distribution

A dust sample is rarely composed of mono-particles, which is the term used for particles with the same shape and/or size. Therefore, not only particle size is important, but also the size distribution of the dust sample or deposit, which defines the relative amount of particles present according to the size. Particle size distribution (PSD) is an important factor for determining the deflagration risk of a dust cloud. If the fraction of very small particles is substantial this will carry an increased explosion hazard, as was explained in the section before. However, this is not the only characteristic that influences the risk of explosion, reason that leads in the definition of new parameters.

PSD has commonly been determined only by the parameter D_{50} , known as the median particle size. D_{50} is defined as the diameter below which 50 % of the cumulative mass or volume is present. Clearly, D_{50} by itself does not reflect the true shape of the distribution curve as it is only one value. To compensate for this, researchers are using D_{10} and D_{90} along with the D_{50} to get a more complete description of the dust in question, representing the diameter below which 10 % and 90 % of the cumulative mass is present, respectively.

The influence of PSD in flame propagation was studied in 2013 by Wei Gao et al. [36], using octadecanol dust of different size distributions. The dust was heated and sprayed (in liquid form, though it cooled quickly and solidified) into a testing chamber. 50 ms after spraying the dust was ignited and the flame propagation was captured by a high-speed camera. The experiment was repeated with 3 different particle size distributions, each one with a concentration of 142 g/m^3 . Figure 4 shows the PSDs used in the experiments, where they have named the different distribution types A, B and C, being type C the one with the largest portion of larger particles. Results showed that for type A (smaller particles) the flame propagated with an even front, leaving nothing behind. The assumption is that all the particles were pyrolyzed or evaporated before the flame passed, and so acting very similar to a pre-mixed gas explosion. The propagation through type B was more complex: blue spot flames appeared ahead of the main flame front, and some of the particles were not fully burnt.

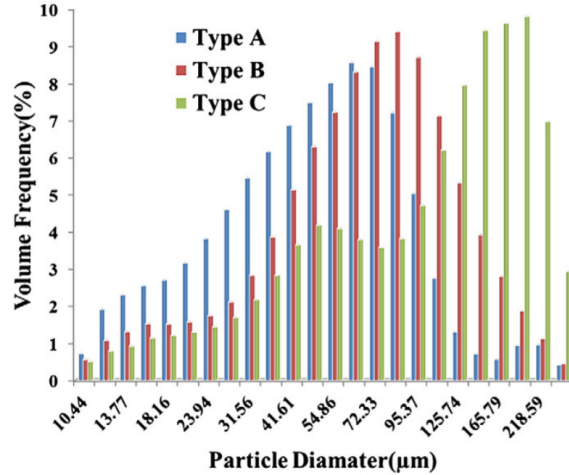


Fig. 3. Particle size distributions in the experiments.

Figure 4: Particle size distributions in the experiments of Gao et al. [36]

During a long time, these three parameters were used as independent numbers in order to provide the PSD of dusts. Furthermore, these values can be used to express the span of particle sizes, a factor known as the polydispersity index, σ_D , and defined by equation 1.

$$\sigma_D = \frac{D_{90} - D_{10}}{D_{50}} \quad (2)$$

Castellanos et al. [37] adopted a novel approach in the field of dust explosion research showing the high correlation existing between polydispersity and P_{max} and K_{st} . Defining polydispersity as a measure of the width of the particle size distribution characterized by the span of the size distribution, they observed an increase on the severity of the explosions with increasing the polydispersity.

However, comparing different researcher, Tascon observed that the polydispersity index has not been found to correlate consistently with explosion severity [38]. It only takes into account the width of the distribution (and the D_{50}) and fails to consider if for example a wider span is due to an increase in D_{90} or a decrease in D_{10} . In other words, two distributions can have the same poly-dispersity index and still be vastly different.

Additionally, these terms were appropriate while the studied particles had round or almost-round shapes, but it became a problem when new materials started being on the spot. Biomass materials have generally elongated shapes, making difficult to determine a mean diameter that represents all the particles.

Another approach has been to use the surface weighted mean ($d[3,2]$) and the volume weighted mean ($d[4,3]$) to define the particle size distribution. $D[3,2]$ is the diameter of the sphere that has the same volume/surface area ratio as the particle of interest, and $d[4,3]$ is the diameter of the sphere of equal volume to the particle.

These are parameters that can be determined directly by some equipment, like laser diffraction, but they have not shown strong correlations with the dust explosion's parameters that are being studied here.

This made the need for new definitions of parameters that should be used clear, but there is still no agreement on which one(s) will provide the best information.

A well-known parameter that has been used before and has showed a correlation with the behaviour of dust explosions is the specific surface area. Specific surface area is defined as the total superficial area that a particle has. It is an important parameter regarding explosions of dusts because many of the reactions that occur during an explosion take place in the surface of the particle, so the bigger these areas are, the more probable reactions are, and the more likely a deflagration is.

Another parameter that has shown a coherent relation to both maximum pressure and pressure rise is skewness. Skewness is how the distribution graph compares to a normal distribution; it expresses the degree of asymmetry. The skewness index $[-1, 1]$ indicates which way the distribution is skewed. A negative skew means the distribution curve has a tail to the left, in the negative direction. If the skew is positive, the distribution curve had the tail on the right, a tail of coarse particles. A perfectly symmetric distribution curve has skewness index $Sk = 0$. In a study from 2013, Tascón [38] compared the skewness index with the polydispersity index by using two existing studies (Castellanos et al. [39] and Li et al. [40]) that focused on the polydispersity index. They both found that there was a relation between explosion severity and polydispersity, however, their results are contradictory: Castellanos et al. found that an increase in the polydispersity index gives an increase in P_{\max} and $(dP/dt)_{\max}$, while Li et al.'s results indicated that a *decrease* in size polydispersity increases the explosion severity. Tascón applied a graphic skewness index to the data sets collected in the two studies, and found a coherent relation to P_{\max} and $(dP/dt)_{\max}$. Equation (3) shows the formula for finding the graphical skewness. The equation was implemented in a program called GRADISTAT.

$$Sk_G = \frac{\ln D_{16} + \ln D_{84} + 2 \ln D_{50}}{2(\ln D_{84} - \ln D_{16})} + \frac{\ln D_5 + \ln D_{95} + 2 \ln D_{50}}{2(\ln D_{95} - \ln D_5)} \quad (3)$$

It is important to note that Tascón points out that the median diameter is still a significant factor. Its effect on explosion parameters is far more evident than that of the skewness index. Skewness only has a notable effect when comparing dust samples with a very similar D_{50} . Tascón also insists that while particle size determination is certainly important, the diverging results and lack of repeatability is also a common problem. The main reason for this is the use of different instruments that are based on different physical properties, other factors include sampling methods, particle dispersion or agglomeration as well as software settings. [38].

2.3. The importance of particle shape

While coal dust particles may be considered spherical, this is commonly not true for biomass particles. This causes some difficulties since a lot of testing equipment and procedures seems to be designed to handle spherical particles. Particle size measurements also treat spheres as the standard shape, since the diameter is very often the parameter that is reported. Biomass can be fibrous, needle-like or any other shape, which can make it difficult for the particles to fit through holes such as in testing equipment or when sieving.

This causes an enormous inaccuracy on the definition of D_{10} , D_{50} and D_{90} as the parameters describing the particle size. The influence of particle shape in the definition of these parameters can be easily seen by the determination of particle size through sieving. If the studied particle has one of its dimensions larger than the sieve's size and the other two smaller, depending on how it falls on the sieve, the particle will go through it, or will not. If the movement is helped by a vibrational system, the probabilities of this particle going through the sieve are even larger. However, the particle's size could be considered bigger than the sieve's size, as illustrated in figure 6, which illustrates how a particle with length a and width b can or cannot pass through a sieve with a size mesh d (bigger than b but smaller than a) depending on the relative position to the mesh.

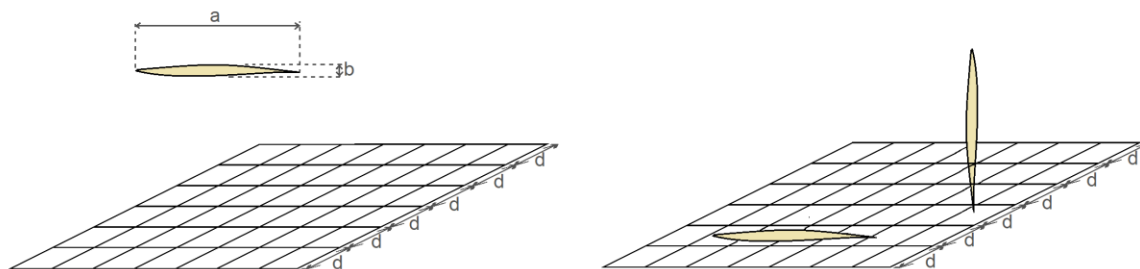


Figure 5. Influence of particle shape on the sieving method

For unevenly shaped particles an equivalent diameter is sometimes used. Meaning simply that the diameter is given as it would have been had the particle been a perfect sphere. However, to find a particle's equivalent diameter one must choose what parameter to keep constant. One can use the same surface-to-volume ratio, the same volume or the same projected area and the result is likely to vary significantly, as observed in figure 6.

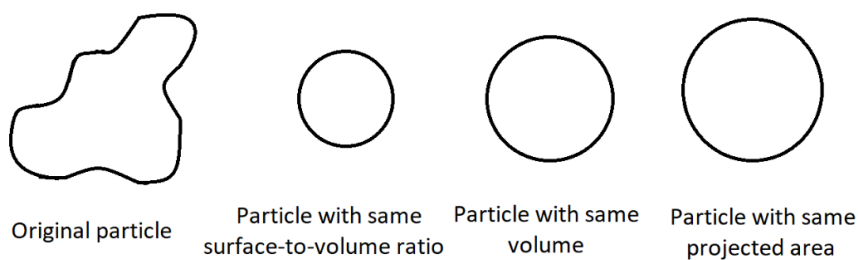


Figure 6. Equivalent spherical diameters [14]

In his book [13], Amyotte refers to a study [41] of dusts' dispersibility properties, which is described as a "dust's tendency to form clouds". This tendency is affected by several parameters, chiefly particle size, particle specific surface area, dust area moisture content, dust density, particle shape, and agglomeration. Klippel et al. [41] divided dust into six groups of "dustiness", that is how easily dispersed a dust is. Group 1 have a minimal tendency to stay airborne, while group 6 is the opposite. Examples of dusts from the different groups are given in the book, and include sanding dust in group 2, and potato starch in group 6, thus saying that potato starch is likely to stay airborne longer than the sanding dust [13].

And so, the particle shape is an important factor in dust's dispersibility properties as it affects both the specific surface area and the agglomeration process of the dust, as well as directly affecting the dispersibility itself. The specific surface area is thought of as increasing with decreasing particle size, however it will also increase when considering any other particle shape than spherical. This is because spheres have the lowest surface to volume ratio of any shape, therefore all other shapes must have higher specific surface area. With increased specific surface area, whether due to small particle size or uneven particle shape, a dust's dispersibility will increase because of greater drag force, or air resistance, acting on the particles. The same is true for particles with a textured surface. Asymmetric shape and uneven surface have been shown to give lower terminal settling velocity due to rotational settling and eddy formation [13]. For dusts that consists of fibrous or flake-like particles the rate of settling would depend on the particles' orientation.

In the case of biomass dust, the particles' shape complicates testing procedures. For example, the 1 m³ ISO chamber that among other things is used to find the minimum explosible concentrations for dusts, does not function optimally for biomass or other particles of a more uneven shape. The mechanism for feeding fuel into the explosion chamber consists of a fuel container and a tube. The tube is shaped like a 'C' and is lining the periphery of the sphere and has 5 mm openings. In a research article from 2013 Huéscar Medina et al. outlines the problems of the ill adapted testing equipment [42]. Fibrous and elongated biomass particles do not fit well through the holes and can clog the pipe, hindering effective flow. There is also an issue with the low mass density of many biomass dusts. Around 750 g/m³ have been found to be the most reactive concentration for biomass dusts. The dust pot that holds the fuel prior to injection has a volume of 5 litres. To hold 750 g/m³ of a 100 kg/m³ material the dust pot would need to be 8,5 litres.

Agglomeration

Particle size, moisture content, particle size distribution and particle shape are the main factors affecting the agglomeration of dusts, pointing out the importance of this factor on the risk of explosions of organic dusts.

When particles are suspended (or not), they will often collide and stick together in lumps. This is referred to as agglomeration, or sometimes coagulation. In this situation, the particle size determined in a laboratory for this sample would still be the same, but the effective particle size will increase, reducing the ignition tendency of the

sample, in other words the agglomerates will act as larger particles. Finer dust and dust with more moisture, have a higher tendency to form agglomerates and thus modifying their ignition behaviour [31].

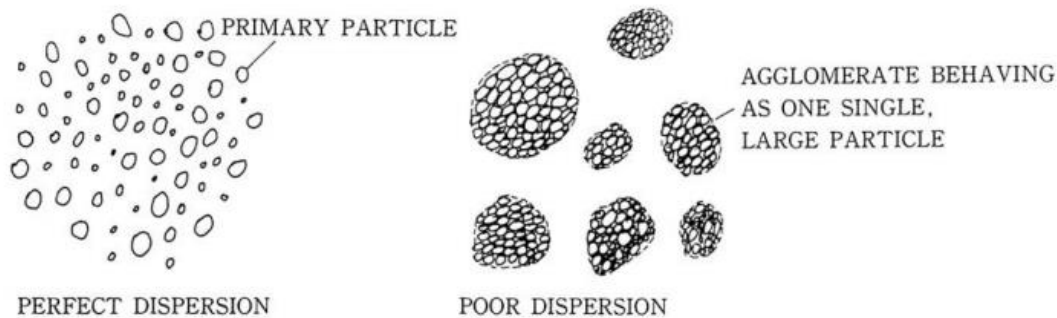


Figure 7. Effect of agglomeration in dust particles [23]

Agglomeration of dust particles has two aspects that are important to consider: attraction forces between particles in dust layers, and rapid coagulation in dust clouds. Agglomeration in dust layers will make dispersing the dust more difficult, and the dust is less likely to form a dust cloud of primary particles (single particles, not agglomerates). The second aspect, coagulation taking place in dust already suspended, means that even if the dust is well dispersed larger agglomerates may still form [13].

Interparticle forces that cause agglomeration of dust particles:

- Van Der Waals forces
- Electrostatic forces
- Interparticle forces due to moisture

Interparticle forces due to moisture is what makes agglomeration more present when moisture content is higher. Electrostatic forces depend on the material and whether or not it is conductive. Van der Waals' forces is affected by particle size. As the dust gets finer the importance of van der Waals' increases. In a 2011 article [33] Eckhoff gives several equations, one of them for calculating van der Waals' forces, F_W , between two particles:

$$F_W = \frac{A}{a^2} * \frac{x_1 x_2}{x_1 + x_2} \quad (4)$$

In the equation above A is a constant, a is the smallest distance between the sphere surfaces and x_1 and x_2 are the diameters of the two particles.

The following equations are found in Eckhoff's article *Influence of dispersibility and coagulation on the dust explosion risk presented by powders consisting of nm-particles* from 2013 [43]. n is the number of particles per cm^3 at the time t , and n_0 is the number of particles in the moment the cloud was formed. The coagulation constant K is material dependent, table 1 in the article gives examples for some materials and the values range between 0,49 and 0,83

· $10^9 \text{cm}^3 \text{s}^{-1}$. The equation was first resolved experimentally in the 1930s, Whytlaw-Gray and co-workers were able to count the number of particles per unit volume of dust cloud and plotted this against time. For a wide range of materials this plot formed a straight line.

$$\frac{1}{n} - \frac{1}{n_0} = Kt \quad (5)$$

$$-\frac{dn}{dt} = Kn^2 \quad (6)$$

The equations are not valid in the earliest stages of coagulation, this is because the agglomeration will happen much more rapidly than the coagulation constant predicts. The initial stage is also difficult to follow experimentally, especially for very small particles.

It should also be noted that the original coagulation equations were assumed all particles were spherical, which is rarely the case, especially for biomass dusts. However, minor irregularities will not significantly impact the mobility of a suspended particle and should therefore only have a minor on the coagulation rate. It has been experimentally confirmed that coagulation rates in dust clouds are not very affected by particle shape, though there are exceptions (like for chain-like structures). [43].

As a dust cloud will never be 100 % mono-disperse, it will instead consist of particles in a variety of sizes, often a wide variety. According to research referenced by Eckhoff it has been experimentally found that the wider the range of the size distribution the faster a dust cloud will coagulate. [43]. It has however, proven quite difficult to precisely calculate the effect of polydispersity.

Moisture has a significant impact on a dust's dispersibility properties. Experience suggests that dry dusts are more easily dispersed than moist dust. Any amount of liquid will increase the interparticle forces, sometimes increasing the attraction by a great deal. As the moisture level rise the excess water will start to form "liquid bridges" between particles and eventually these bridges will completely fill the space between particles. At this point the capillary forces between the particles are the main source of the cohesion. Further increase of moisture content will result in the dust being suspended in liquid. [33].

Agglomeration is generally not taken into account when the risk of explosion of solid materials is studied. It is true that, regarding safety, the worst scenario should always be considered, which in this case means the drier and with smaller particle size. However, by moisturizing the samples, the risk can decrease, and the amount of water needed in order to reduce it highly depends on the agglomeration tendency of the dusts.

2.4. The influence of moisture

Water has been widely used in the suppression of gas fire and explosions [44, 45], being a low cost alternative for inert materials, with no environment impact, no toxicity and relatively high availability. It has been normally used as a way of preventing dust explosions. Amyotte et al. [46] proposed the control of moisture in pipes and silos as one of the measurements to prevent dust explosions [47, 48].

However, moisture is one of the main parameters due to its antagonistic effect in the dust explosion mechanism. Depending on the chemical composition of the dust, the moisture can inhibit or promote the ignition of dusts and the severity of the explosion. On the one hand, the inhibition can be caused by agglomeration, heat sink effect, water vapour inerting or inhibition of mass transfer at particle surface. On the other hand, an increase of the ignition and explosion characteristics could be observed when the water presence leads to violent chemical reaction with the dust or when its adsorption chemically modified the particle surface and improves the species diffusion, which can lead to explosion risks higher than for the dry dust [49].

At lower moisture content, the moisture would mainly consume the reaction heat of dust explosion by temperature rise and phase change. In this situation, because the heat consumption is proportional to the mass of moisture, the measured explosion severity reduces gently and linearly with the rising moisture content. Nevertheless, as the moisture content continues to rise, due to the stronger interparticle cohesion between particles, besides consuming heat, the existence of moisture would also cause the agglomerations of dust particles and, thereby, increase the effective particle size of dusts and weaken dispersion of dust clouds, so that the reduction of explosion becomes more remarkable and even dust cloud cannot ignite [50].

When increasing the moisture content, an increase on the MIT, an increase on the MEC and a decrease on the P_{max} can be observed, causing a decrease both on the ignition sensitivity and on the explosion severity: explosions would occur less easily, and their consequences would be less dramatic. However, there is not a consensus on the limit of moisture content that would ensure the non-occurrence of explosions, being difficult to find any fix number at this respect. Lees [51] established that the explosibility of the dust decreases significantly with dust moisture content above 30%.

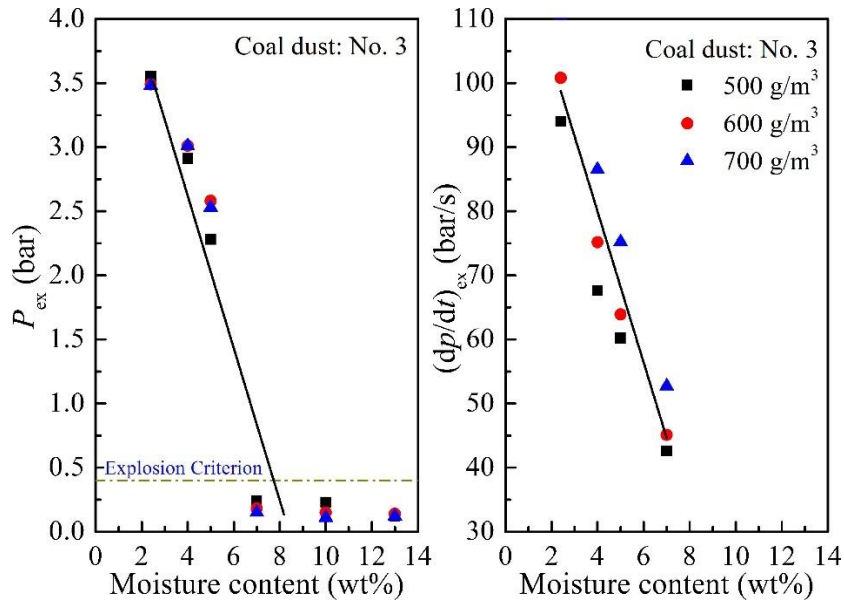


Figure 8: Explosion severity of coal dust at different moisture content in the size range 125-550 μm [52].

It is also a general practice in industry to treat moist dust as less dangerous than the dry one, and it is generally correct to do so. However, it is difficult to define the limiting value at which a dust has to be considered wet or dry. First, solid particulates have four different types of water associated: intracellular water, floc water, capillary water and free water. The methods used to determine the moisture content make a differentiation on the type of water that is actually being measured, making the first need to characterise, define and determine these types of moisture. By moisturising the dust, the moisture content that is probably mainly affected is the free water, but this hypothesis should be tested and the influence of this moisturising in the particles and the explosion risk should be studied.

3. Methods

3.1. Available testing methods

In this chapter follows a description of methods used for finding particle size, explosion characteristics and moisture content for dusts.

For particle size

The methods used for finding and defining particle size and size distribution are diverse. Sieving is a recurring method and is often used in combination with other methods, such as laser diffraction or image analysis. Possibly because sieving does not give a definite particle size, but rather a range or size distribution. There are at least three standards regulating sieving procedures.

EN 15149-2:2010 is a European standard for how to determine the particle size distribution of solid biofuels using a vibrating sieve tower. The aperture is described as a stack of seven sieves with a collection pan below. The sieve openings are given in mm as 3,15; 2,8; 2,0; 1,4; 1,0; 0,5; 0,25.

The standard also gives an equation to calculate the median particle size, D_{50} , by linear interpolation:

$$D_{50} = C_2 + (50 - S_2) \times \frac{C_3 - C_2}{S_3 - S_2} \quad (7)$$

Image analysis has two steps, first take a picture or scan of a prepared sample and then interpret the image, this is usually done by a computer.

Following in this chapter are the methods used to measure particle size and particle size distribution of biomasses described in different research articles.

Analysis of standard sieving method for milled biomass through image processing. Effects of particle shape and size for poplar and corn stover [53]

For this 2014 paper Gil, Teruel and Arauzo has tested two types of biomass: SRF poplar and corn stover. Poplar is described as a woody material, while corn stover is herbaceous. The authors do not go into detail about their method, but instead refer to the standards they followed for the different procedures. The samples were collected and prepared according to standards EN 14778-1:2011 for poplar and EN 14780:2011 for corn stover. European standards EN 14774-1:2009 and EN 15149-2:2010 were followed when analysing the samples' moisture content and particle size respectively.



Figure 9: Example of particles with different kinds of shapes [53]

A vibrating screen machine with six sieves was used for particle size distribution, according to standard ISO 3310-1. The sieves had opening sizes of (0,1; 0,25; 0,5; 1; 2; 5) mm. Before sieving a series of trials were made to determine sieving time, to ensure that the sieving was complete. The material was weighed on an electronical balance with $\pm 0,001$ gram accuracy. The sieving was deemed complete when the mass change between two sieves was less than 0,3 % of the total mass per minute. ($0,3 \text{ \% min}^{-1}$). This happened after 20 minutes.

For each size range two samples were taken for image analysis. The particles were dispersed, attempting to avoid overlapping. 24 2D-images were obtained by a scanner. For the smallest particles (those that fell through the bottom sieve) the resolution was 3200 dpi, for all other size-groups 600 dpi was used. The images were analysed to find morphological characteristics of the 100s to 1000s of scanned particles. The original colour images were enhanced and turned black and white. A filter was applied to automatically remove blobs that may correspond to more than one particle. Particles not fully in the picture were also removed.

Machine vision-based particle size and size distribution determination of airborne dust particles of wood and bark pellets [54]

Airborne dust samples from pelleting operations were collected from a baghouse deposit. The samples were of pine in the shape of pelleting sawdust and pelleting ground bark. The two materials are treated separately throughout the study. Each of the materials were made into three subsamples by sieving them. A sieve with mesh 230 ($63 \mu\text{m}$) were used to divide the samples in two, the third subsample was unseparated. Each of the total 6 subsamples were kept in separate bags (in an air-conditioned lab, at $22 \text{ }^\circ\text{C}$ and 55 \% RH) before the tests.

To perform the test the samples were shaken and about a spoon's worth (2-3 g) were heaped onto clear paper. A thin piece of cardboard was used to spread out the material into a thin layer. (cardboard was chosen because there is no electrostatic attraction of the particles). Using the cardboard still, a small squared area was separated

out then moved over to a flatbed scanner (Cano-scan 4400F) with a $\frac{3}{4}$ " flat art brush. The scanner bed was lined with a "high quality overhead projector transparent sheet", making removing the sample easy. Once on the scanner bed a pointy knife was used to assure that no particles were touching or overlapping. This was described as time-consuming but practically achievable. For a black background an oil painted art paper (with a normal quality paper the fibre would be visible in the image, and could possibly affect the results) were placed carefully on top of the *singulated arrangement* of wood dust. For each layout like this, 10 pictures were taken, each focusing on a small square (50,8 mm \times 50,8 mm). With three layouts per material this makes 60 pictures to be processed.

In chapter 2.7 in the paper the authors state that particles can easily be measured accurately and separated based on any selected parameter (e.g. length width, area) with image processing methods, but not by standard mechanical sieving.

Influence of the size distribution and concentration on wood dust explosion: Experiments and reaction modelling [28]

In this 2005-study by Callé et al. the explosibility of wood dusts with different particle size distributions and concentrations are tested. The material was produced by sanding pieces of beech and oak. The sanding resulted in a very wide size distribution and the dust was sieved into four ranges: 25-45 μm , 45-71 μm , 71-90 μm and 90-125 μm . A mean diameter was found for each of the ranges, though the report does not specify by which method.

Use of tube flow fractionation in wood powder characterisation [55]

In this research paper, by Laitinen and Karinkanta, tube flow fractionation was used to determine particle size of sawdust from Norwegian Spruce (*picea abies*). After the wood material was collected it was stored in a freezer. Later the saw dust was dried in an oven at a temperature below 105 °C. The dried material was sieved using a vibrating screen with aperture size of 4 mm. Any particles too large to pass through the sieve were discarded and not used in the research. The remaining material was sent through a milling system consisting of an air classifier mill (100 ATP) and an integrated rotor impact mill (50 ZPS).

To dilute the milled material, 1 g of wood powder were mixed in deionised water to a 0,2 % particle concentration. Before dilution a dispersant was added to the wood powder, to keep the powder from forming agglomerates. Laser diffraction was used to measure volumetric particle size distribution according to ISO13320.

For the tube flow fractionation, a sample is injected into a tube, and initially the particles are randomly distributed in the flow, but they are intended to sort themselves. Particles with one or multiple long dimensions are more likely to be caught by the faster middle flow, thus the larger particles tend to concentrate at the front of the flow and exit the tube first.

In the tests a 5 cm² sample at consistency 0,2 % was fractioned for 100 s at an average flow rate of 7,3-8,5 cm³/s in a long plastic tube (D=4mm). Based on 23 parallel sample analyses the standard deviation of the combined sample fractionation and optical image analysis was determined to be 4,5 %. The variables of interest in the fractionation procedure are flow velocity, pressure, temperature, sample volume and consistency. These were to be kept constant.

Effects of particle shape and size on devolatilization of biomass particle [56]

This study from 2008 has made a considerable effort to categorize and separate biomass particles by shape and size. Two types of biomass were used: hardwood sawdust particles ($\leq 300\mu\text{m}$) and poplar dowels ($\geq 2\text{mm}$). The particles were categorized as either spherical, cylindrical or flakes. Particles were supposed to have different shapes, but similar volume/mass. The preparation of the samples consisted of four steps:

1. Separation with sieve shaker: A series of sieves were stacked with the finest mesh on the bottom and the coarsest one on top, mesh sizes ranging from 25-80. A sample is poured on to the top sieve and the shaking last for 40-45 minutes. The material collected from each sieve is bagged separately. This step is mainly to separate the particles by size.
2. Aerodynamic classification: Figure 10 is a schematic illustration of the tunnel separator they built. In the bottom of the tunnel four trays are placed to collect the dust. The dust is injected through an opening at the top of the tunnel. Compressed air enters through a vertical distribution pipe and spreads the dusts as it enters. Each particle's trajectory is determined by its shape. More drag forces work on particles with a bigger surface area or lower density, these will end up in tray 4, furthest from the distributor. Trays 2 and 3 collect cylinder and flake-like particles, while tray 1 gets the more equant particles. Samples collected in the trays are sometimes run through the tunnel separator more than once.
3. Shape separation by sieve: samples collected in trays 1, 2 and 3 in the aerodynamic classifier are separated into near-spherical, flake-like and cylinder-like particles. The samples are put in a new sieve shaker, in this step time is the variable. The particles with smaller aspect ratio will fall through more quickly, leaving the flakes and cylinders behind for longer. By lengthening the shaking time, more particles with higher aspect ratio will pass the sieve.
4. Further shape separation by friction plate: This was done by placing a 2-foot-long board clad in 600 grit sandpaper at a 30° angle. One or two samples were then poured onto the high end of the board to allow the sawdust to fall the length of the board. Only the most spherical make it all the way down, thus the different shapes will sort themselves along the board.

After the samples had been through all four steps (sometimes repeatedly) particles were individually photographed from orthogonal angles. As part of the project the researchers developed an algorithm for

reconstructing particle shapes based on the three images taken from different angles. The algorithm includes three major steps: image acquisition and processing, image contour alignment, and surface generation.

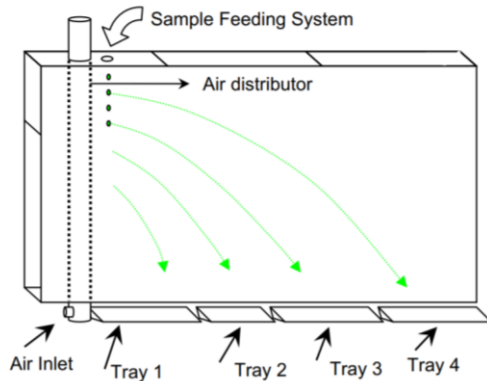


Figure 10: Tunnel separator schematic diagram (fig. 2 in article [56])

Experimental research on shape and size distribution of biomass particle [57]

This study from 2011 looks at 4 different kinds of biomass: pine, bean stalk, rice straw and reed. In preparation for the test, each sample was dried and ground for 3 minutes in a batch knife mill pulveriser FW177. The samples were then sieved into 5 particle size ranges: 83-106 μm , 106-150 μm , 150-180 μm , 180-300 μm and 300-425 μm . The content of the sieves was weighed to find the particle size distribution. The sieving process was repeated three times for all the materials and the average value (amount of material in the sieves) was used. From each of the ranges, 300 particles were randomly chosen for examination. Using a Nikon E200 microscope the chosen particles were magnified 300 times, and the images was analysed by Image J software. The software was able to measure the length and width for each individual particle.

Sieve analysis of biomass: accurate method for determination of particle size distribution

A recent study [58] of three different biomasses (hemp, miscanthus and pine sawdust) concluded that sieve analysis only gave a reliable result for one of the materials (pine sawdust). In the test they used a horizontal vibrating sieve shaker Retsch 2000. The experimental set up consisted of seven sieves and a collection pan at the bottom. The opening sizes for the sieves were 0.63, 1.5, 3.15, 4.5, 6.7, 8 and 10 mm. The sieves were sorted so that the coarsest, with the largest openings, was on top and then decreasing opening size for each sieve. The bottom pan would collect any particles sufficiently small to fall through all the sieves.

Before performing the test, the sieves were individually weighed. The material sample were placed in the top sieve and the sieve tower were then shaken for 30 minutes, with an amplitude of 30 mm/g applied. After

shaking, each of the sieves were weighed again and the weight of the sieve were subtracted to find the amount of material the sieves had collected. Each material was tested twice, and the arithmetic median value was used.

For hemp the result was that more than half (56,16 %) of the material were left on the top sieve. The authors believed this to be due to the elongated fibrous characteristics of hemp particles.

The miscanthus particles were described as needle-shaped. This resulted in the top four sieves capturing a total of less than 1,3 % of the material. Normally (for spherical particles), this would indicate that almost all the particles had a diameter of less than 3,15 mm (the opening size of the 3rd sieve), which is not entirely untrue, however it is inaccurate.

The test worked well for sawdust. The pine particles are described as more spherical and the results show a greater disparity, that is more even distribution among the sieves.

Summary

The following table gives a short summary of some of the opportunities and limitations of each of the methods described in this chapter.

Table 2: Summary of the available testing methods for particle size

Method	Opportunities	Problems/limitations
Sieving	Widespread use, several standards, can be used in combination with other methods, finds PSD, multiple sieve sizes available.	Not ideal for non-spherical particles; does not give the size of individual particles, but rather a range.
Image analysis	Good for different shapes, can be used to find several parameters length, width, diameter SSA, aspect ratio etc. Often used as a second step, after separating the dust into size ranges	Usually a 2D image. Not standardized. Best suited for relatively small samples.
Laser diffraction	Gives volumetric particle size and other parameters directly	
Aerodynamic classification	Separates by shape/surface area	Not commonly used.
Friction board	Separates by shape/surface area more than size	Not very accurate, no standard, no defining limits (like sieves have), not commonly used.
Tube flow fractionation	Separates by shape/surface area	Not commonly used.

For explosion characteristics

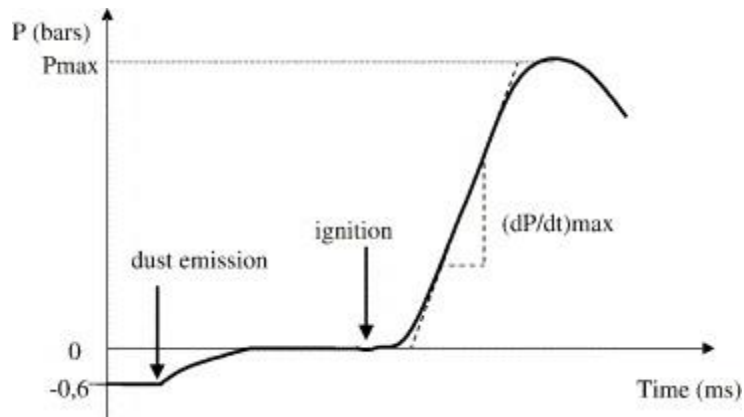


Figure 11: Evolution of the overpressure in the sphere during the explosion [28]

The 1 m³ sphere

The 1 m³ sphere is a constant volume explosion vessel used for finding P_{max} and K_{St} . It is also the method preferred by standards and the method other methods are calibrated against. Use of the 1 m³ sphere is outlined in the standard EN BS 14034.

The apparatus consists of an external 5 L fuel container, linked to the explosion chamber by a 19 mm diameter tube. There is also equipment to record the pressure development over time. From the recorded information the deflagration index K_{St} can be derived by using equation (8). [59]. The testing procedure starts with filling the dust container and pressurising it to 20 bar. On activation a fast-acting valve releases the dust into the explosion chamber through a multi-hole ‘C’ tube. The dispersed dust is then ignited.

$$K_{St} = \left(\frac{dP}{dt} \right)_{max} \cdot V^{1/3} \quad (8)$$

Through literature review and some experiments of their own, a group of researchers, Medina et al. [42], saw that the fuel dispersion system in the standard sphere was not ideal for biomass, and sought to modify the equipment to be more suitable for biomasses. The original dispersion system, the ‘C’ ring, did not allow fibrous biomass to pass through, even when it was milled down to a diameter of less than 63 μm , (openings in the ‘C’ ring are 5 mm each [42]). Among all the cases they studied only one presented a type of biomass that could pass through the standard dispersion system. These were found by Sattar et al. and were nut shells from walnuts, pine nuts and pistachios. For their own experiments the researchers swapped the ‘C’ ring with a spherical nozzle, they also changed the fuel container for a 10 L version to accommodate low bulk density biomass. The

new set up was calibrated for its ignition delay using cornflour to give the same K_{St} with the standard 'C' ring disperser and the 10 L external dust store and spherical nozzle disperser.



Figure 12: Leeds ISO 1 m³ vessel [59]

The 20L sphere

As the 1 m³ sphere was quite expensive both to build and to operate, researchers started experimenting with smaller versions of the explosion chamber. This resulted in the Siwek 20L explosion chamber. Testing showed that vessels smaller than 20 litres were not suitable, likely because the heat loss from the flame front to the walls of the chamber would be relatively greater than for a larger vessel. [60]. The ISO 1 m³ explosion chamber is the reference standard for finding K_{St} and P_{max} , however as the 20 L sphere can be calibrated to give the same results it is recognised by standards as well. In addition, it only needs the dust sample to be 1/50 of the mass compared to the larger sphere, which is a significant contributing factor to the 20L sphere being more commonly used than the 1 m³ sphere. [59].

United States Bureau of Mines (USBM) developed their own version of the 20L sphere. The USBM vessel is operated by placing the dust sample in the dispersion nozzle instead of in a separate fuel container, the dust is then dispersed by an air pulse [61]. And later the University of Bergen made a hybrid sphere, combining the USBM vessel with the Siwek dispersion system. [60].

The Hartmann tube

The Hartmann tube is an explosion chamber which operates on mainly the same principles as the spherical explosion chambers described above but has the shape of a cylinder. The cylinder has an internal diameter of 61 mm and length 322 mm giving it a volume of about 1,96 L, which is significantly smaller than even the 20 L sphere [62]. Originally, the Hartmann tube was the apparatus for testing carbonaceous dusts' explosibility. Now it is used for finding the minimum ignition energy and can also be used to investigate the minimum explosible concentration as it gives similar results as the spherical explosions chambers. On P_{max} and K_{St} the

tube apparatus does not give reliable results, this is in large part due to the extensive contact between the flame and the tube walls, which leads to heat loss and a lowering of both the peak pressure and the rate of pressure rise. [59].

Customized explosion chamber

In 2018 a group of researchers constructed and calibrated a 36L to give results corresponding to both the 1 m³ and the 20L dust explosion chambers [60]. The paper details the process of calibrating the apparatus, as well as simulating the airflow inside both the 36L-sphere and the 20L-sphere by using CFD. The newly constructed dust explosion chamber had a maximum allowable working pressure and a maximum allowable temperature of 70 bar and 260 °C. The apparatus was equipped with vacuum, dispersion, ignition and data acquisition systems. Operation of the apparatus was based on the ASTM E1226-12a standard: First a known mass of dust is placed in the fuel container, then the vessel is closed and evacuated. The air reservoir is pressurized, and a fast-acting valve opens for 50 ms to let the air flow disperse the dust into the explosion chamber. There is a delay time of 25 ms before the dust is ignited. The explosions pressure development is recorded.

For moisture content

Finding the moisture content of any dust is simply a matter of drying a wet sample and comparing the weights to find out how much water was originally in the sample.

To find the moisture content a 25 g wet sample is placed in an oven on 103°C for 24 hours. The sample is then weighed again, and the mass percentage of moisture can be found with the following equation. Equation (9) for moisture content is given by Yang in *Image and Sieve Analysis of Biomass Particle Sizes and Separation after Size Reduction* [63]:

$$MC = \frac{\text{Loss weight} \cdot 100}{\text{Wet sample weight}} \quad (9)$$

3.2. Statistical analysis

Based on the literature review data has been collected to explore some of the rules and correlations that the theory of dust explosions relies on.

Data collection

To perform the statistical analysis data had to be collected. The original objective was to do a data analysis specifically for wood. However, it quickly became clear that the available data was scarce. First any data concerning sizes of wood particulates, including those not linked to any explosion tests. Widening the search to include other biomasses and eventually coal, was necessary to get the amount of data needed for an analysis, (though more data would still be ideal). All the available data has been organised in a spreadsheet where all available information was recorded: d10, d50, d90, specific surface area, the polydispersity index, moisture content, volatile matter, fixed carbon, ash, P_{max} , dP/dt , K_{St} , minimum ignition temperature for layers and dust clouds, minimum explosible concentration, minimum ignition energy and which explosion chamber the test was performed in. Two more columns were added to define whether the material was biomass or coal, and wood or another biomass. This is to be able to separate these categories and create separate plots for them, thus visualizing any differences that may be between the materials. It is interesting to know whether biomass and coal act the same, and whether wood differ from other biomasses.

The K_{St} is dependent on dP/dt . Therefore, for all the tests where dP/dt was included in the report K_{St} could be calculated if the size of the explosion vessel is known by using equation (8). However, a problem arose. When trying to use the same equation to find dP/dt where the K_{St} was given the results came out surprising, significantly deviating from the values directly given. This was even more true for the 1 m³-vessel, and this made it necessary to consider if the volume was meant to always be 20L, regardless of the vessel used. As this question remains unanswered, the equation has not been used to calculate either K_{St} -values or dP/dt -values, and the statistical analysis is based entirely on data given in the reports.

Histograms and boxplots.

The histograms and boxplots in chapter 4.1 are meant to show attributes of the distribution of different particle sizes.

Six histograms have been made, two for each of d10, d50 and d90, one for biomass and coal. Biomass and coal could easily have been combined into the same histogram, and still conveyed the same information. The histograms show frequency: how many of the samples in the dataset has a d10 within a certain interval. [64].

A boxplot is a way of graphically depicting how the median and the 25- and 75-percentiles are distributed in a data set of a single variable. The box shows the quartiles and the whiskers mark the highest and lowest observations that are not outliers. Outliers are marked as dots or circles. [64].

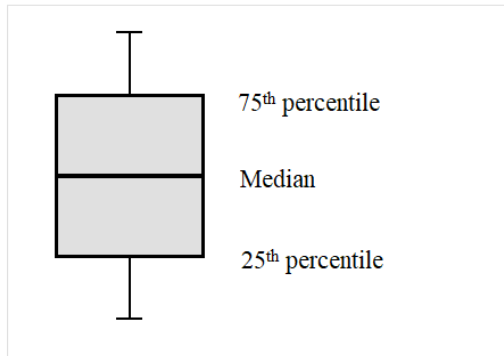


Figure 13: A general boxplot

Boxplots in Figure 14 are used to show and compare the particle size reported for the parameters d10, d50 and d90 for coal and biomass. Each box represents either d10, d50 or d90 for either coal or biomass. The y-axis shows the particle size, the size of the boxes indicates the median 50th percentile, meaning 50 % percent of the data falls inside the box. The whiskers fathom all the rest of the data except outliers. Outliers are marked as circles.

```
attach(data_for_explosions_R)
boxplot(
d10[Material=="biomass"],
d10[Material=="coal"],
d50[Material=="biomass"],
d50[Material=="coal"],
d90[Material=="biomass"],
d90[Material=="coal"],
las=1,
col = c(3,5),
ylim=c(0,800) )
```

choosing the dataset

naming the function

defining each of the boxes, in order from left to right

the orientation of the numbers on the y-axis

choosing colors number 3 and 5 for the boxes

setting limits on the y-axis

Scatterplots

The main investigation into the data was done with scatterplots. Plotting each of P_{max} , K_{St} , dP/dt and MIT against each of d50, d90, the polydispersity index and the moisture content for all the material categories (all data, biomass, coal, wood, and non-wood biomass), resulting in 80 plots. For each plot, in addition to the graphic two indexes were also given: R and p .

Pearson's correlation coefficient R will be between -1 and 1. If R is exactly -1 or 1 it means there is a perfect correlation. If R is 0 it means there is absolutely no correlation. The p -value is between 0 and 1 and indicates the strength of R . If p is closer to 0 then R is stronger, or more likely to be right. This is because p indicates the likeliness of the null-hypothesis. The null-hypothesis in this case is that there is no correlation. The p -value is therefore an indication of the likelihood of the given R -value to occur if there were no correlation. If the p -value is a very small number it means it is unlikely, and that the null-hypothesis can be rejected. The limit for this is difficult to set, 0,05 is sometimes used, but there is no universal limit that can be used for all cases. For the scatterplots made here the limit will probably differ since the number of datapoints vary between plots.

The code for the scatterplots:

<code>ggscatter(data_not_wood,</code>	<i>the name of the function (ggscatter) and the data set (data_not_wood)</i>
<code>x="d90",y="Pmax",</code>	<i>the names of the parameters to be plotted along each axis</i>
<code>add="reg.line",</code>	<i>the line that shows the trend</i>
<code>conf.int=TRUE,</code>	<i>the grey field that is the confidence interval</i>
<code>cor.coef=TRUE,</code>	<i>the correlation coefficient, R and p</i>
<code>cor.method="pearson",</code>	<i>specifies the correlation method to be Pearson's</i>
<code>title = "Non-wood biomasses")</code>	<i>the title of the plot</i>

Sources of error

Given the limited and incomplete dataset it is not realistic to expect a final answer to our enquiries. And this is probably the main source of error: there simply is not enough available data to be certain if any correlation that are found are statistically significant.

There are significant differences in measuring methods for particle size and other particle parameters. For the most part researcher give the particle size as a diameter,

There are also differences in the explosion equipment. The 20 L sphere is supposed to be calibrated to match the results of the 1 m³ sphere, however the results are not a perfect match, making this a variable of unclear impact. In addition, the explosion equipment is poorly suited to biomass which could mean the data for biomass are less reliable. Researchers are aware of this and some of them has chosen to make adaptations to the equipment (such as the 36 L sphere), which makes their results not compare well to others', as their experiments were not conducted under the same conditions.

The researchers have varying approaches and are investigating different angles of the dust explosion phenomena. This controls which parameters are relevant to them. They are therefore giving different parameters, some only give d50, some even neglect to say what they have measured when they give the particle size. When there is no information on what has been measured, it has been assumed that it is d50. The reasoning is that d50 is the most common parameter to give, and therefore hopefully the assumption is more likely to be right. Ideally such samples would be left out of the data collection, but with so little data available, quantity became a priority. Other times guessing has been called for is when the results of the explosion testing were not presented in a table with accurate values, but instead were presented graphically [40]. Efforts were made to read the figures accurately, though it is unlikely it was without some error.

Particle shape is not included as a variable, because this was not possible. It is of course assumed that the coal particles are near-spherical, but the biomass is very likely not. This makes the chosen parameters for size (d10, d50 and d90) an incomplete description of the actual sizes of particulates in a sample.

4. Results

The results in this chapter are presented as the outputs from R studio.

4.1. Attributes of the samples

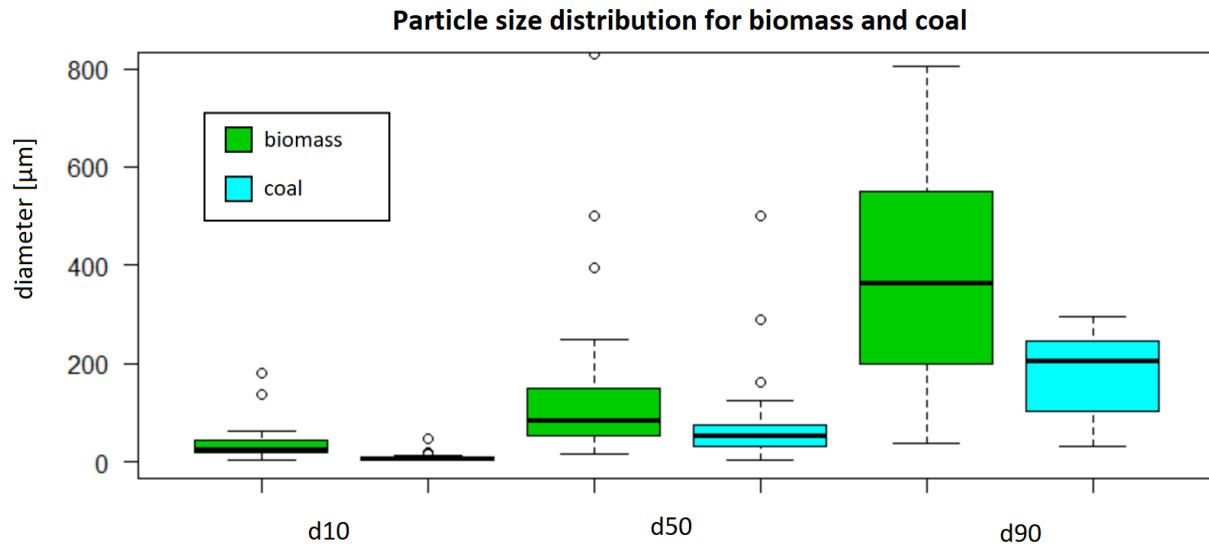


Figure 14: Boxplot showing the particle sizes for biomass and coal (note: one outlier for d90 biomass has been excluded for readability)

Figure 14 is the boxplot showing the distribution of the size of d10, d50 and d90 for the biomass and coal particles in the dataset. The y-axis is the particle size in μm . From the boxplot we can see that the distributions for d10 are very narrow for both materials, and that it widens for d50 and even further for d90. It is also evident that biomass has a much wider range for all three percentiles, especially d90.

The histograms show the frequency of the appearance of a diameter in the d10, d50 and d90 in the data collection. For each percentile there are two histograms, one for biomass and one for coal. The x-axis is the diameter and the y-axis show how many of the samples fall into that size range, or more precisely: how many times a sample has a d10, d50 or d90 in that size range.

For the most part the histograms have a normal distribution, skewed to the left. The exception is d90 for coal which is a bimodal distribution with the major mode on the right. Other than this biomass is more heterogenous than coal and is spread over bigger ranges. Particle size smaller for coal.

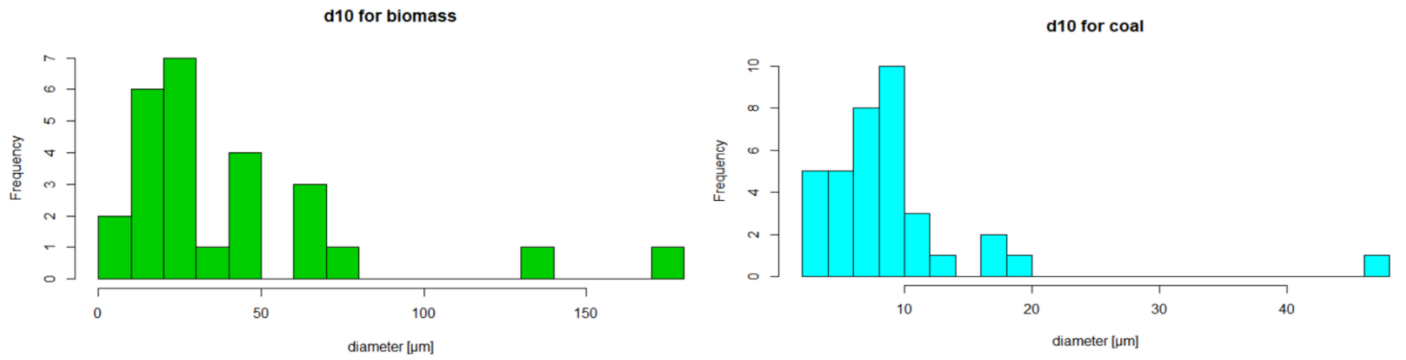


Figure 15: Histogram for d10, biomass and coal

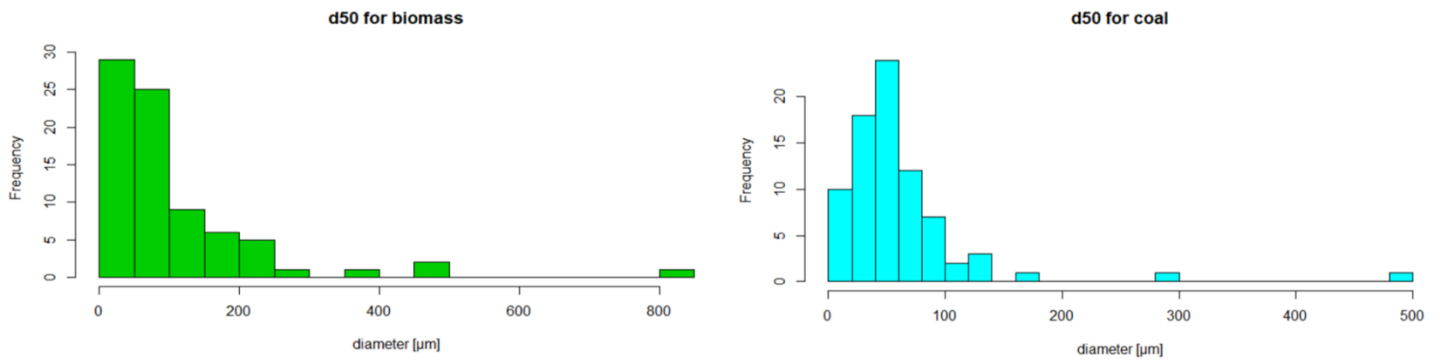


Figure 16: Histogram for d50, biomass and coal

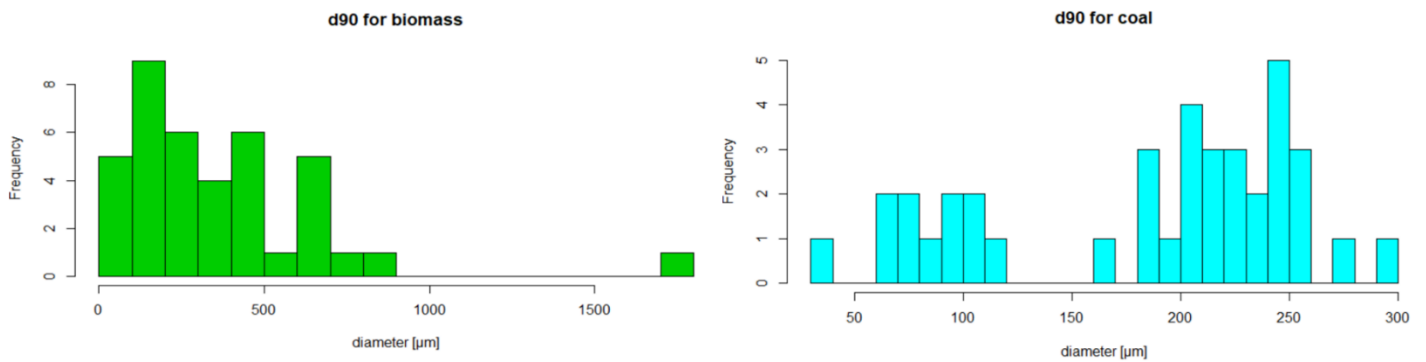


Figure 17: Histogram for d90, biomass and coal

4.2. Attributes of the explosion tests

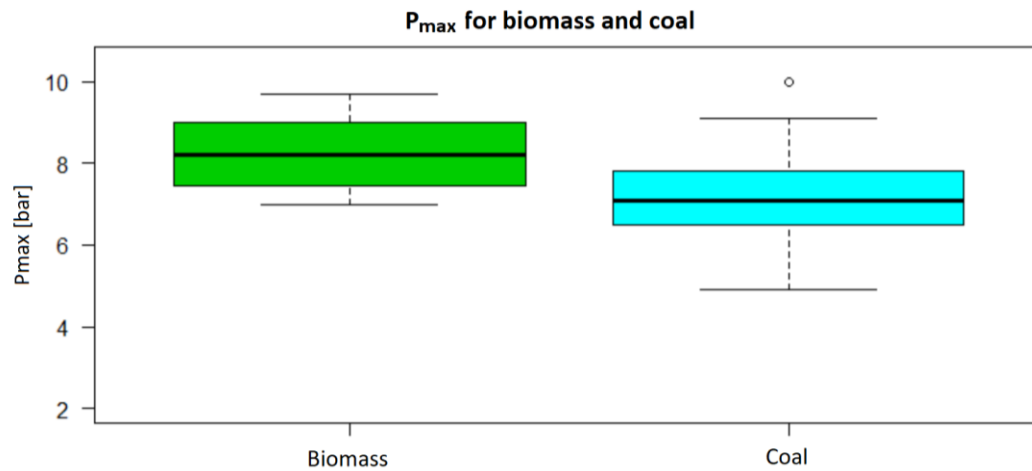


Figure 18: Boxplot showing maximum explosion pressure for biomass and coal

The boxplots above and below in Figure 18 and Figure 19 show the maximum pressures and the maximum rates of pressure rise from the data collection sorted by material. From Figure 18 we can see that biomass on average has a higher maximum explosion pressure than coal. Coal has a bigger range of P_{max} , and the highest value for P_{max} in the data collection is for coal.

It can be read from Figure 19 that coal has the highest median value for $(dP/dt)_{max}$, coal also has the highest and lowest values for this parameter in the data collection. Biomass' middle half has a larger span, while coal's is more concentrated, especially the third quartile, above the median.

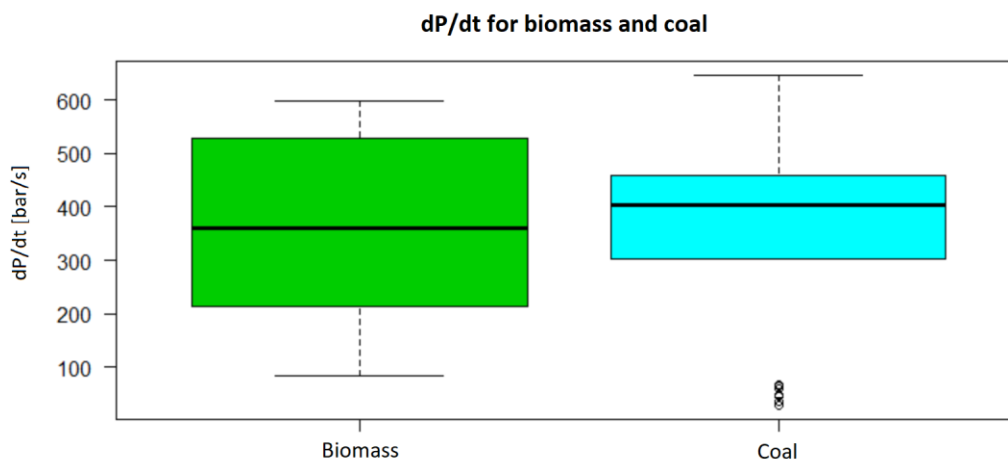


Figure 19: Boxplot showing maximum rate of pressure rise for biomass and coal

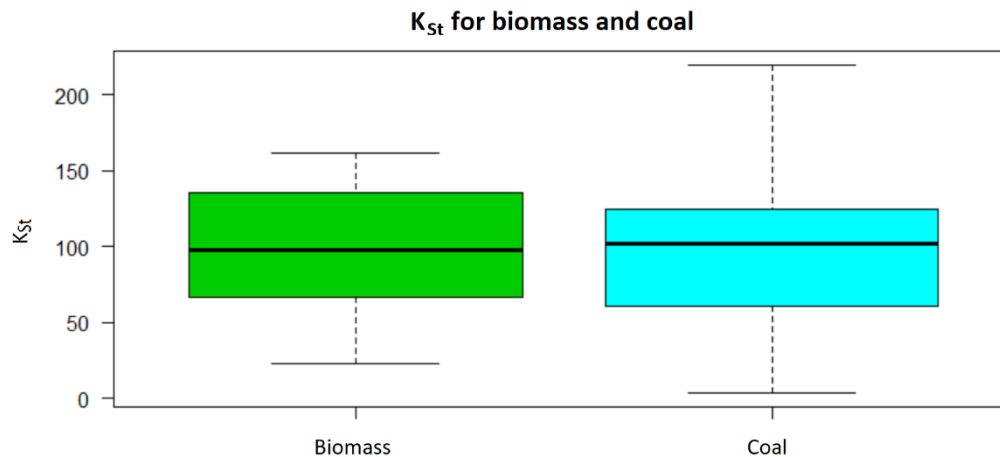


Figure 20: Boxplot showing explosion indexes (K_{St}) for biomass and coal

According to Figure 20 the median K_{St} for biomass and coal is almost the same, though slightly higher for coal, suggesting coal yield more severe explosions. This is in line with the results for dP/dt in Figure 19, which is to be expected as K_{St} is dependent on the rate of pressure rise. The reason they are not an even better match is probably that they are for the most part based on different samples; few researchers provided values for both K_{St} and $(dP/dt)_{max}$.

Table 3 is a summary of the scatterplots in chapter 4.3, in it the correlation factor R is given for all the plots, as well as the p -value. If R is close to 1 or -1, it indicates a strong correlation. It should be noted that some of the plots only consists of a few datapoints, so even though this table may suggest a strong correlation between some factors, there are too little data to draw any conclusions. The p -value ranges from 0 to 1 and indicates the significance of the correlation. A p -value closer to zero is a more significant R -value. The R -values larger than 0,5 or smaller than -0,5 have been marked in blue (along with their corresponding p -values). R -values exceeding $\pm 0,69$ are marked in a darker blue.

There are 7 cases of opposite correlations between biomass and coal (dP/dt and $d90$, dP/dt and $d50$, dP/dt and PDI , K_{St} and the polydispersity index, K_{St} and $d90$, MIT and $d10$, MIT and PDI). Sometimes wood and non-wood biomasses also show opposite correlation, however when this is the case, there is always a severe lack of data, especially for wood. In other words, there is at present no need to suspect that wood behaves radically different than other biomasses.

The correlations for polydispersity index and P_{max} , and polydispersity and K_{St} is showing promise, though most of the data does not have a known PDI . The results for $d50$ were not as expected. Mostly there were no or weak correlation to explosion parameters, $d50$ only shows some correlation when there is too little data.

Moisture is also surprising. According the correlation analysis there is a positive correlation between moisture content and both $(dP/dt)_{\max}$ and K_{St} . This indicates that as the moisture content increases the explosion will get more violent. There is a negative correlation between moisture content and both P_{\max} and MIT. Meaning that as moisture content increase the maximum explosion pressure will decrease and so will the minimum ignition temperature, making the dust easier to ignite.

Table 3: Summary of the results from the data analysis

x-axis	y-axis	All		Coal		Biomass		Wood		Non-wood biomass	
		R	<i>p</i>	R	<i>p</i>	R	<i>p</i>	R	<i>p</i>	R	<i>p</i>
d10	P _{max}	0,0037	0,98	-0,46	0,0049	-0,28	0,31	-0,88	0,048	0,57	0,18
	dP/dt	0,14	0,39	-0,49	0,0074	-0,13	0,71	0,96	0,19	-0,63	0,13
	K _{St}	-0,084	0,59	-0,48	0,0085	-0,27	0,33	0,57	0,32	-0,63	0,13
	MIT	-0,41	0,021	-0,19	0,4	0,23	0,52	-	-	0,14	0,77
d50	P _{max}	0,035	0,68	-0,1	0,37	-0,11	0,43	-0,01	0,97	0,44	0,085
	dP/dt	0,058	0,67	0,33	0,077	0,099	0,064	-0,76	0,017	0,08	0,72
	K _{St}	-0,11	0,26	-0,14	0,3	-0,14	0,3	-0,61	0,012	0,097	0,72
	MIT	-0,19	0,1	-0,12	0,49	-0,18	0,23	-0,39	0,61	-0,0098	0,97
d90	P _{max}	0,34	0,006	0,0093	0,96	0,26	0,19	0,54	0,087	0,27	0,37
	dP/dt	0,022	0,88	0,74	4,4e-06	-0,31	0,16	-0,13	0,73	-0,44	0,13
	K _{St}	-0,03	0,83	0,43	0,017	-0,23	0,24	-0,17	0,61	-0,44	0,13
	MIT	-0,45	0,005	-0,48	0,017	-0,48	0,098	-	-	0,22	0,64
PDI	P _{max}	0,36	0,015	0,38	0,041	0,61	0,034	0,95	0,015	-0,049	0,92
	dP/dt	0,26	0,11	0,57	0,0011	-0,41	0,24	-0,99	0,072	0,036	0,04
	K _{St}	0,27	0,11	0,63	0,00057	-0,52	0,084	-0,76	0,13	0,045	0,92
	MIT	0,33	0,072	-0,084	0,71	0,0049	0,99	-	-	0,14	0,77
Mois-ture	P _{max}	-0,51	2,9e-05	-0,28	0,11	-0,7	4,1e-05	-0,98	3,5e-06	0,2	0,48
	dP/dt	0,63	2,8e-06	0,76	2,1e-06	0,31	0,23	0,99	0,11	0,29	0,31
	K _{St}	0,33	0,015	0,3	0,14	0,33	0,09	0,85	0,0039	0,29	0,31
	MIT	-0,56	8,5e-05	-0,69	0,00031	-0,71	0,00051	-	-	-0,75	0,0018

4.3. The scatterplots

P_{\max} and d_{10}

P_{\max} doesn't show a significant correlation with fines. A large portion of the samples are located as a group below a d_{10} of about 40 μm . In this area P_{\max} is observed ranging from about 5 to 9 bar, without any tendency. This behavior is observed in all the studied groups of samples, concluding that there is not significant correlation between the finest 10th percentile and maximum explosion pressure.

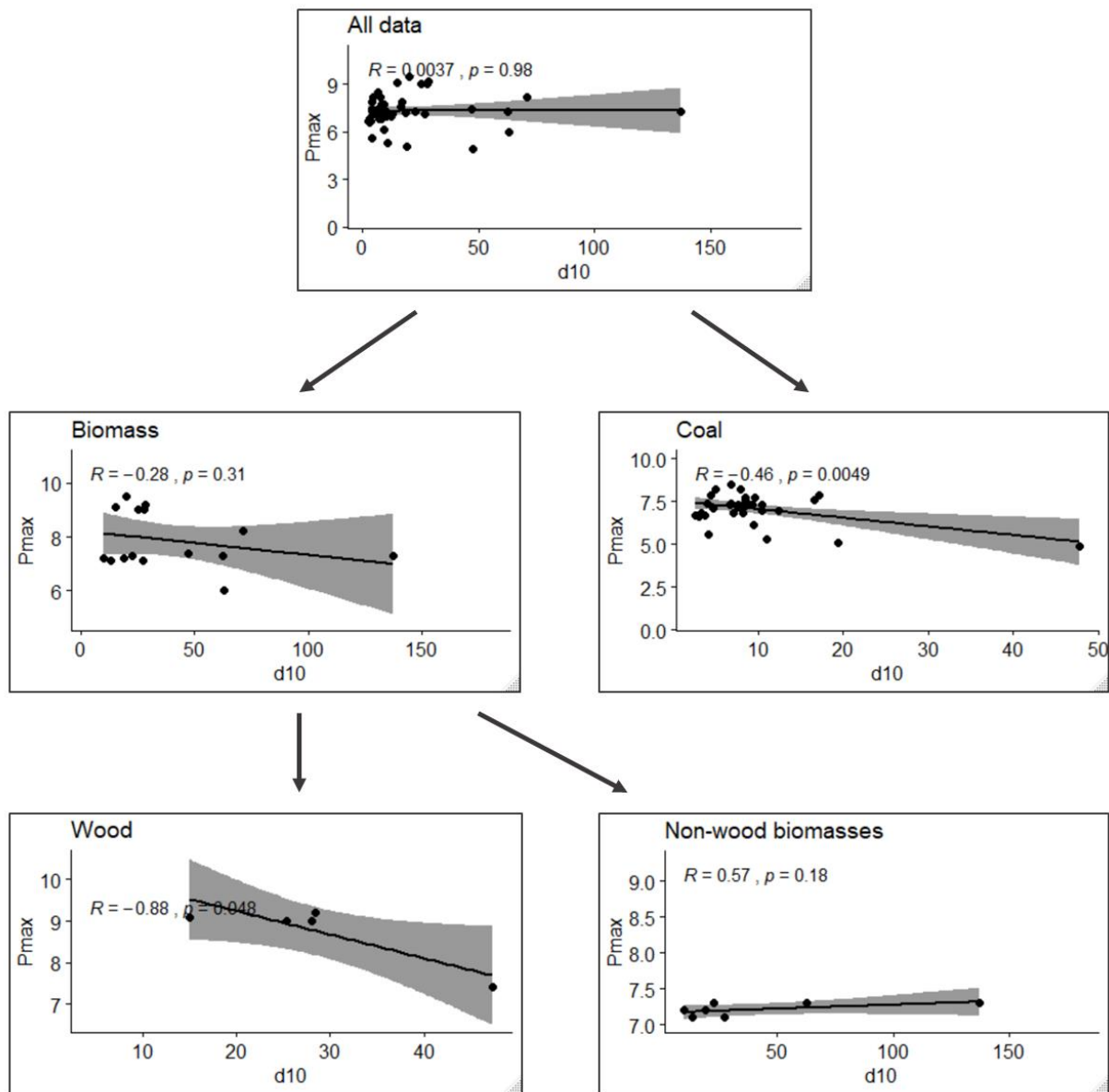


Figure 21: Scatterplots showing correlations between maximum pressure and d_{10}

P_{max} and d_{50}

Nearly all the samples are located in a group below approximately $150 \mu\text{m}$. This group is ranging from 0,40 to 10,9 bar and does not have any tendency or correlation. There are some samples with larger particle size that presents the same range of values for P_{max} giving an almost horizontal correlation line with no significance. When the data is divided into biomass and coal the same observation can be made for both groups, meaning that this lack of correlation is not dependent on material.

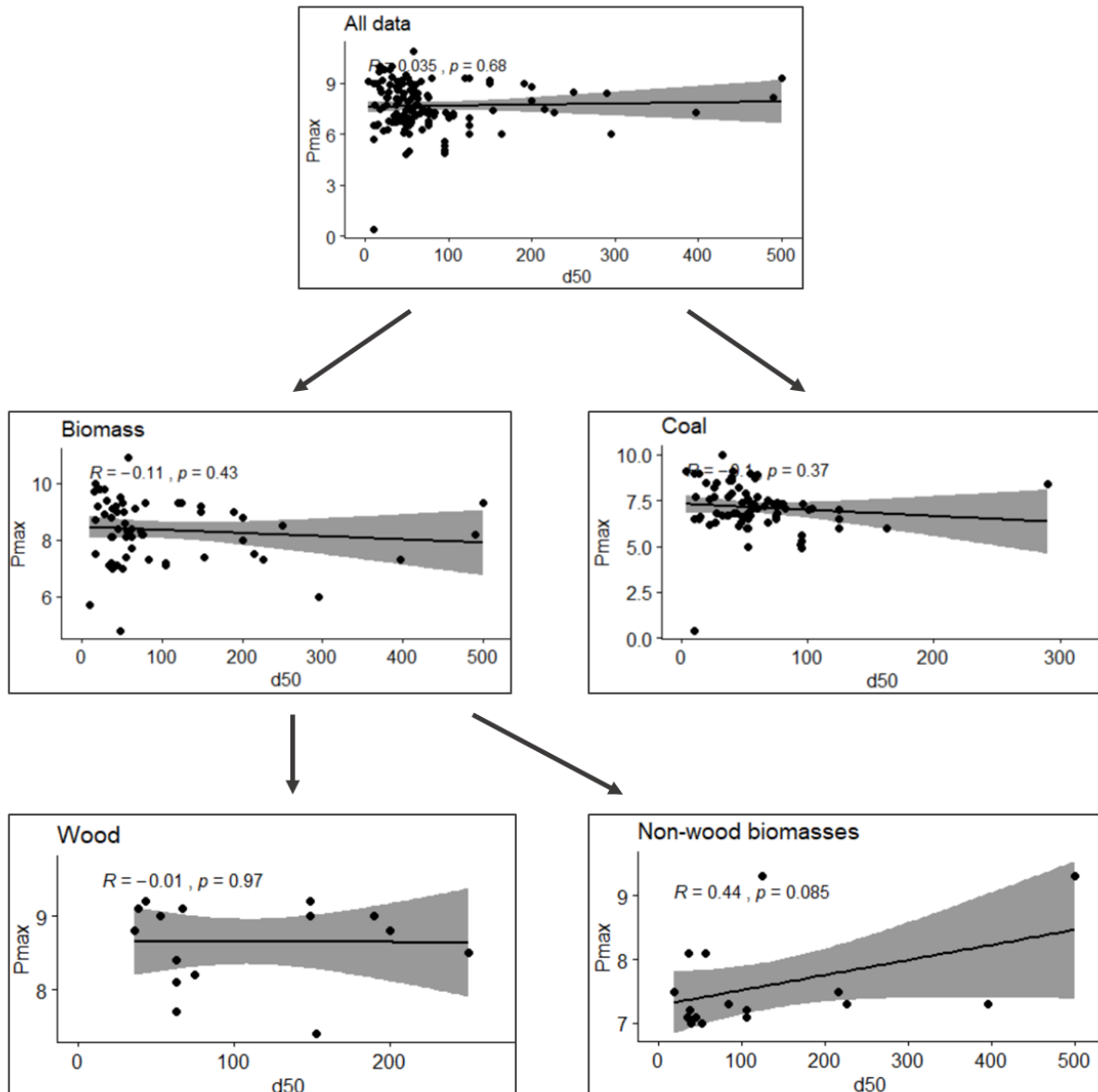


Figure 22: Scatterplots showing correlations between maximum pressure and d_{50}

P_{max} and d_{90}

The values of P_{max} have a narrow distribution in the complete dataset, all except one outlier lying close to the trendline. The trend is slight, but positive. This indicates that increased particle sizes give more violent explosions, which is opposite of what one would expect. For coal the trendline is very close to flat which would mean P_{max} is constant and not affected by particle size. Wood shows a stronger positive correlation than any of the other categories, including all biomasses and non-wood biomasses. The correlation is not very significant and it is based on few data points, it still does not align with expectations.

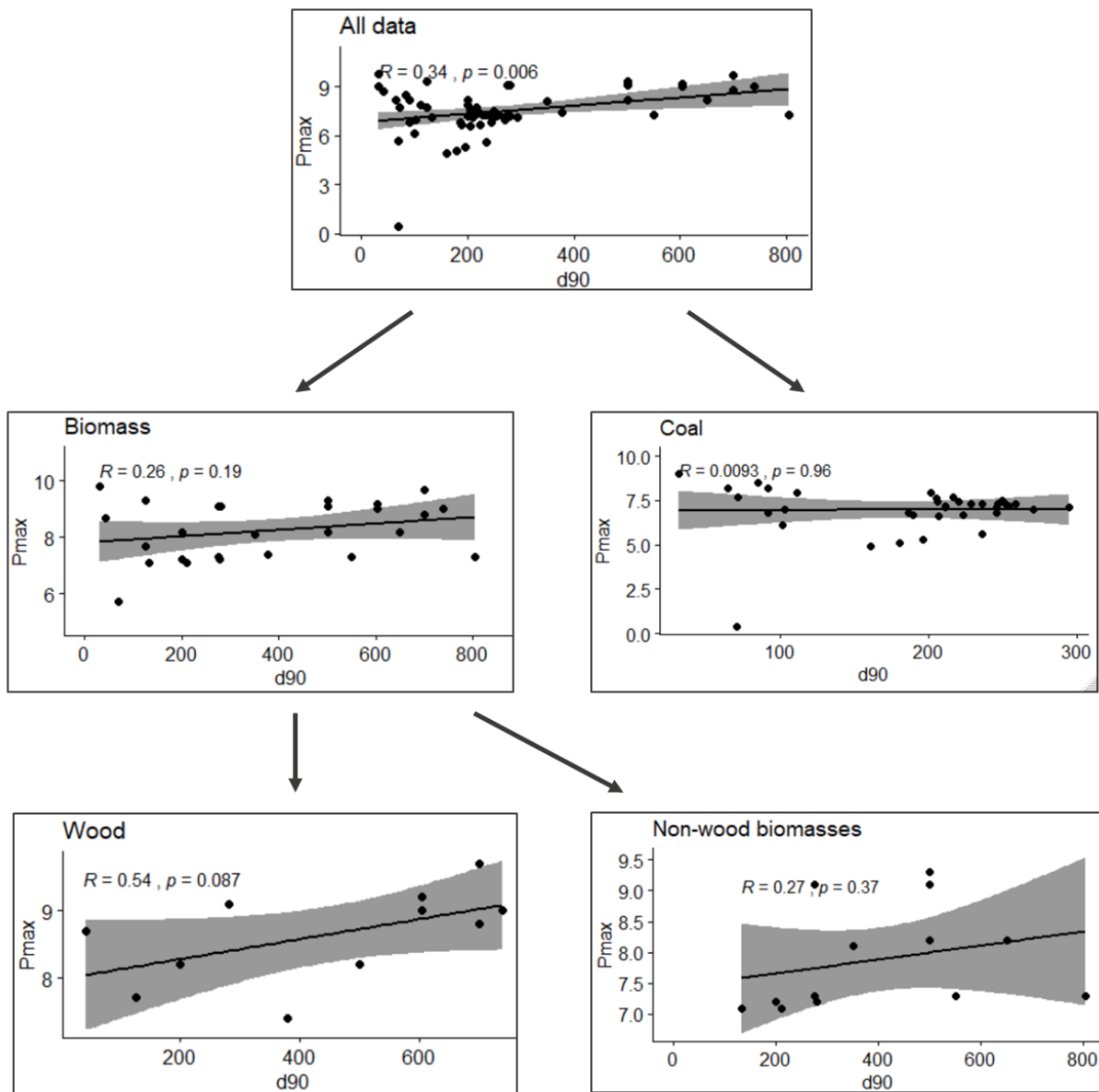


Figure 23: Scatterplots showing correlations between maximum pressure and d_{90}

P_{max} and the polydispersity index

There is some correlation between P_{max} and the polydispersity index. For the complete data set his correlations is significant, this is also true for coal. For biomass the correlation is stronger, and also significant, but the amount of data is small. There is a very strong correlation for wood, however there is only 5 data points, similarly there is too little data to conclude anything for the non-wood biomass as well.

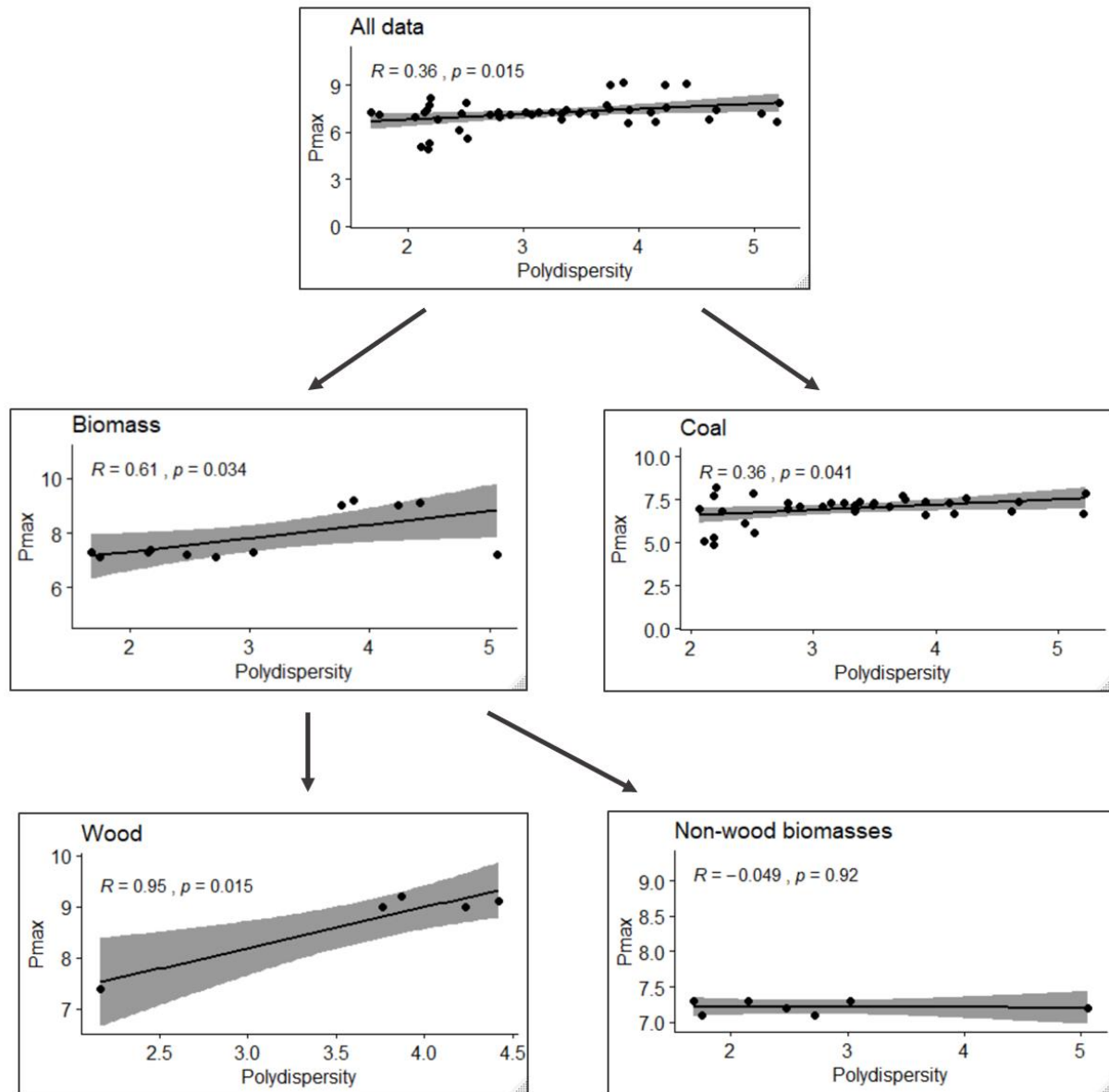


Figure 24: Scatterplots showing correlations between maximum pressure and the polydispersity index

P_{max} and moisture

The full dataset shows that there is some correlation between the maximum pressure and moisture content. This correlation is negative and has very high significance. It is in line with expectations that more moisture will lead to less severe explosions. For coal the correlation is weaker and less significant. The data for biomass show a strong correlation, with high significance, but when it is split up into wood and non-wood, it is clear that the result for wood (although a strong, significant correlation) is inconclusive due to too few point, and the data for non-wood biomass shows very weak and insignificant correlation. Non-wood biomass is the only one where the correlation is positive.

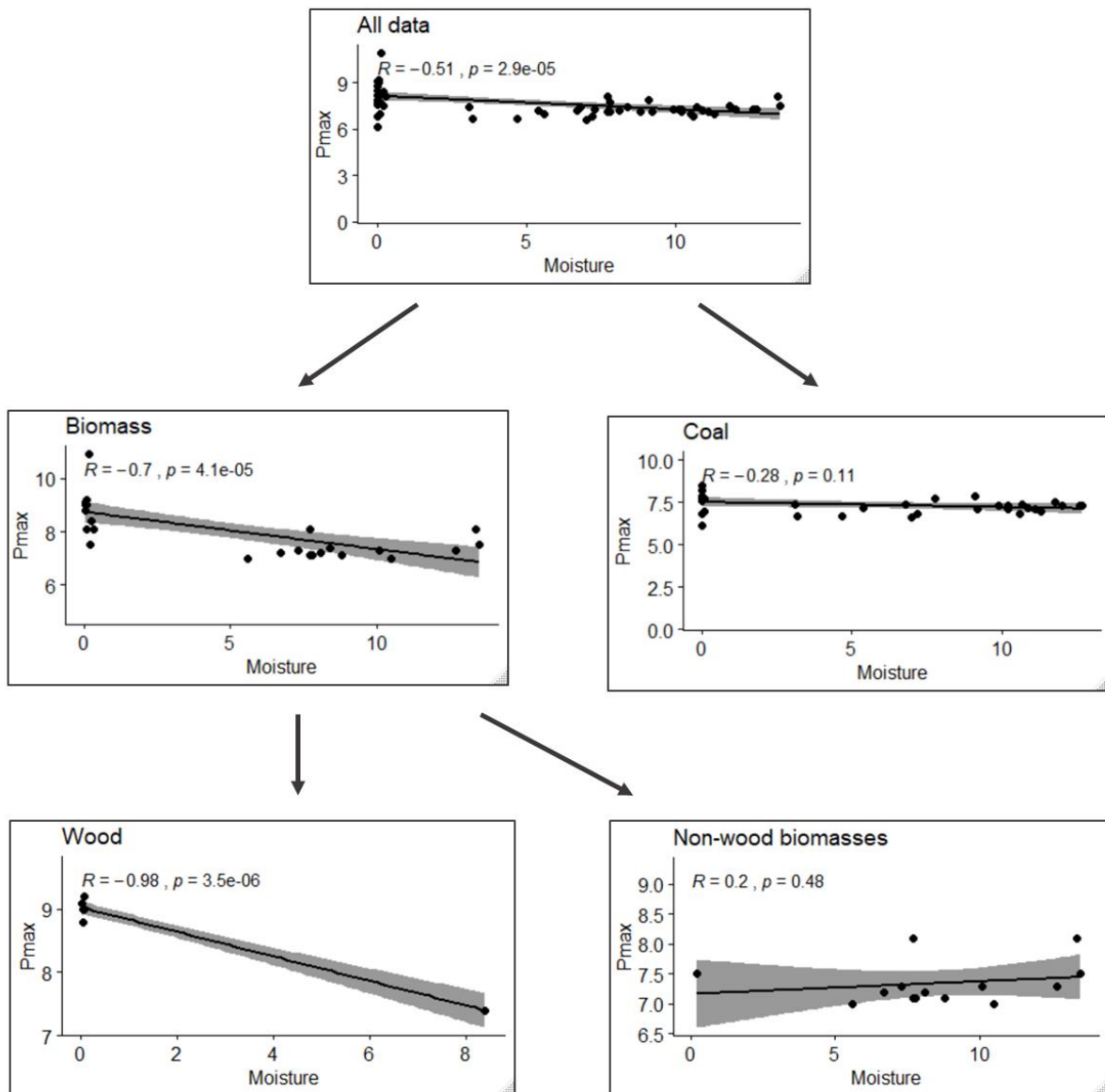


Figure 25: Scatterplots showing correlations between maximum pressure and moisture content

K_{St} and d₁₀

None of these plots have enough data to make any satisfactory conclusions. Still, a tendency of clustering to the left sides of the plots can be observed, meaning most of the samples have a d₁₀ of less than about 30 μm. The declining trendlines suggest that a larger value for d₁₀ will give a less severe explosion. However, none of the correlations are strong, and only the data for coal shows significance.

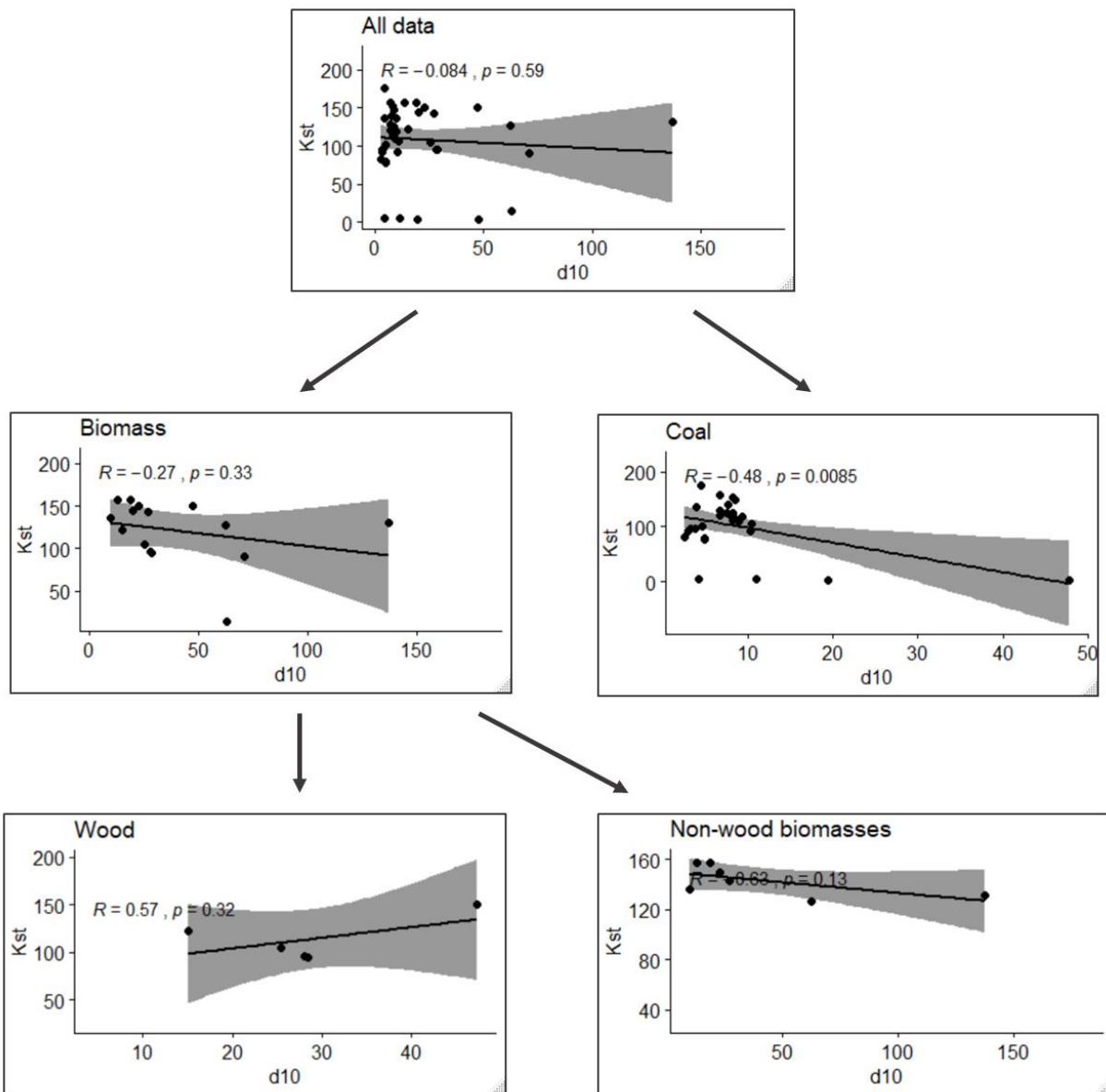


Figure 26: Scatterplots showing correlations between the explosion index and d₁₀

K_{St} and d₅₀

The complete dataset shows very weak, negative correlation and very low significance. Most of the data is gathered below about 150 μm in a cluster of no apparent correlation. All of this is also true for the biomass and coal plots, coincidentally these two plots have the same R- and p-values of -0,14 and 0,3, respectively. In the breakdown of the biomass plots the wood plot shows a significant negative correlation, while the other biomasses have a very weak positive correlation with low significance.

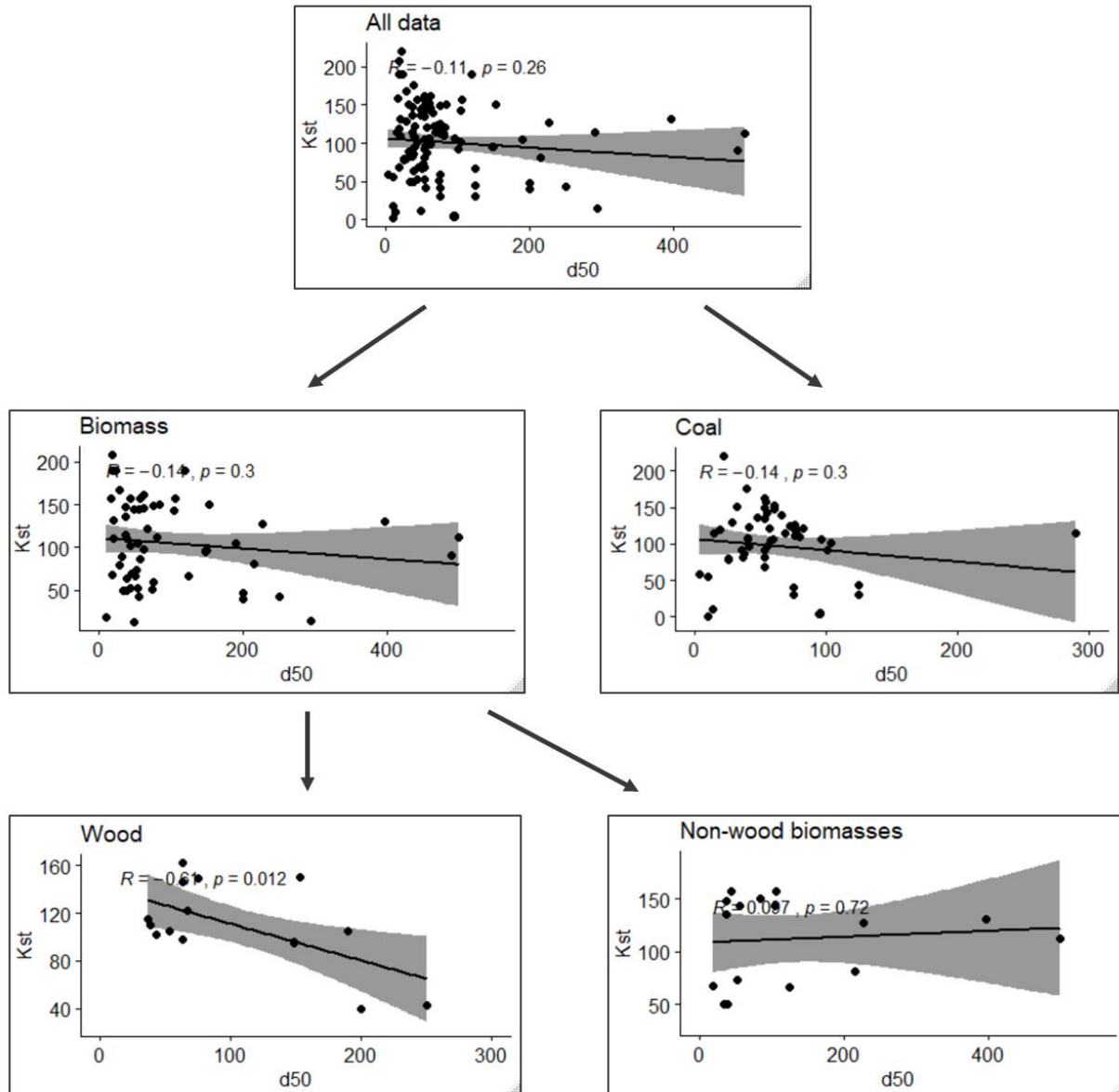


Figure 27: Scatterplots showing correlations between the explosion index and d₅₀

K_{St} and d₉₀

In plot for the complete dataset the data points have a wide distribution, the K_{St} ranging between 0 and 200 bar m/s and d₉₀ ranging between 0 and 800 μm. There is no apparent correlation. The plot for biomass is very similar to the complete dataset, though with a somewhat stronger and more significant negative correlation. The non-wood biomasses show a notable but insignificant negative correlation and the wood a weak insignificant negative correlation. Both biomass groups have quite few datapoints. The second strongest, but most significant correlation among these plots is for coal. The coal correlation is also the only one that is positive, indicating that larger particles (a higher d₉₀) leads to more violent explosions.

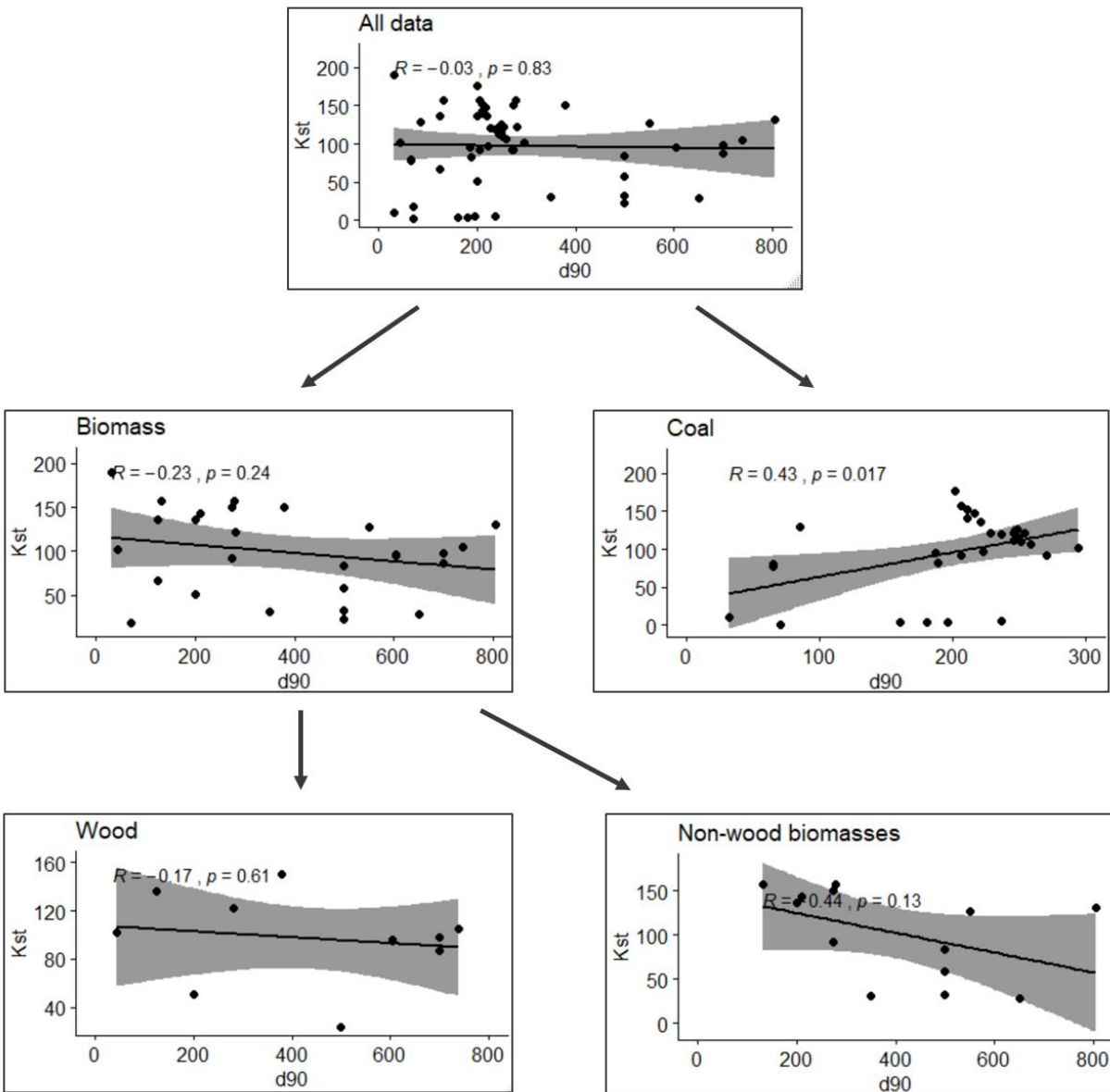


Figure 28: Scatterplots showing correlations between the explosion index and d₉₀

K_{St} and the polydispersity index

For the complete data set there is a weak positive correlation between the K_{St} and polydispersity index, indicating that a wider size distribution can lead to a more severe explosion. The data for coal supports this with a stronger positive correlation and a very high significance. Biomass unexpectedly shows the opposite tendency: a negative correlation of some significance. When breaking the data further down, it appears the negative correlation may be caused by the wood samples as they show a strong negative correlation. The non-wood biomasses show no correlation. It should be noted that the biomass plots are made up of a total of twelve datapoints.

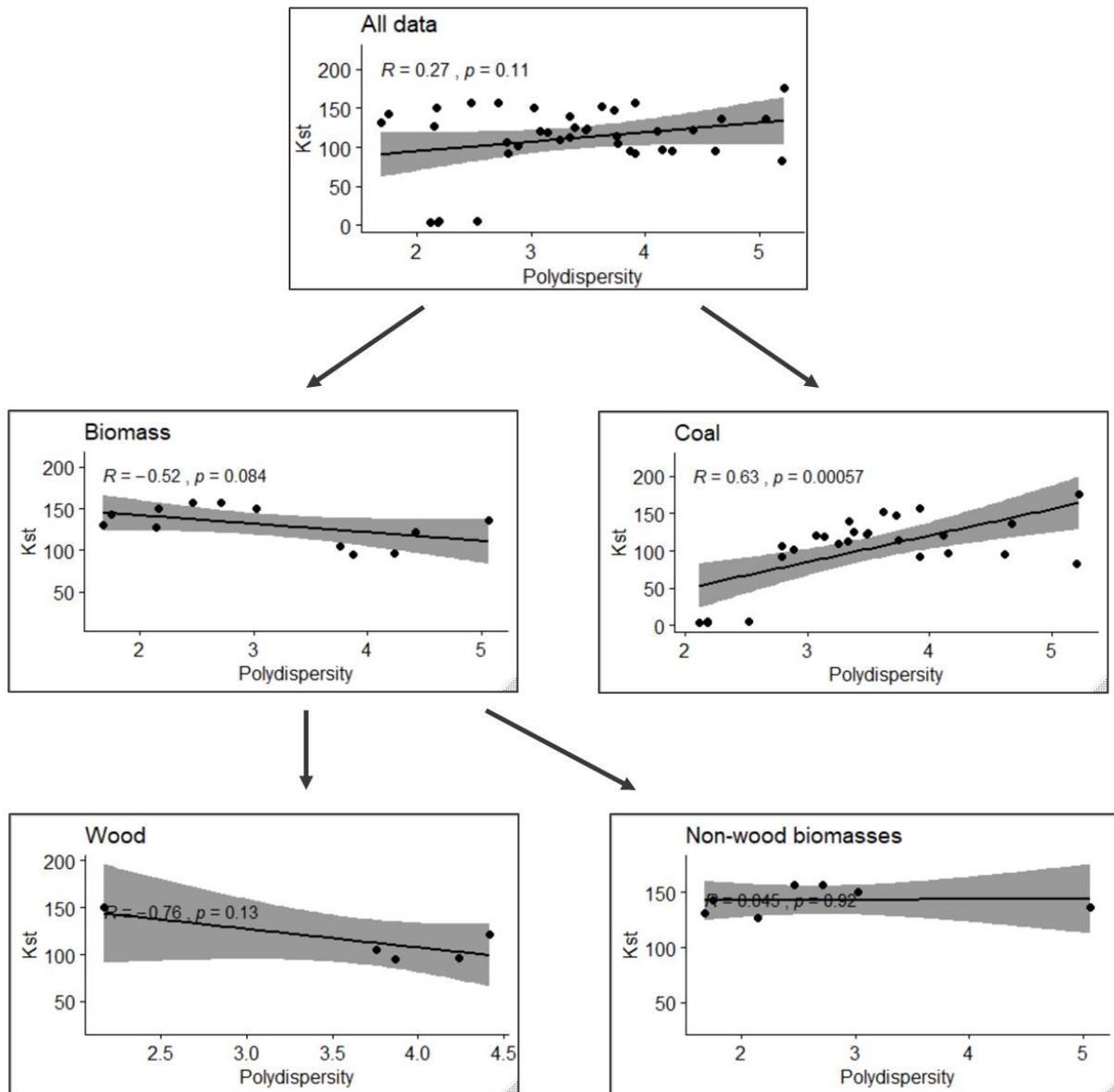


Figure 29: Scatterplots showing correlations between the explosion index and the polydispersity index

K_{St} and moisture

K_{St} and moisture show weak positive correlation when considering the complete data set. This is also the case for biomass, coal and non-wood biomasses, but the correlation for these are less significant. There is too little data for wood, but the data that there is suggest a strong, positive correlation with high significance.

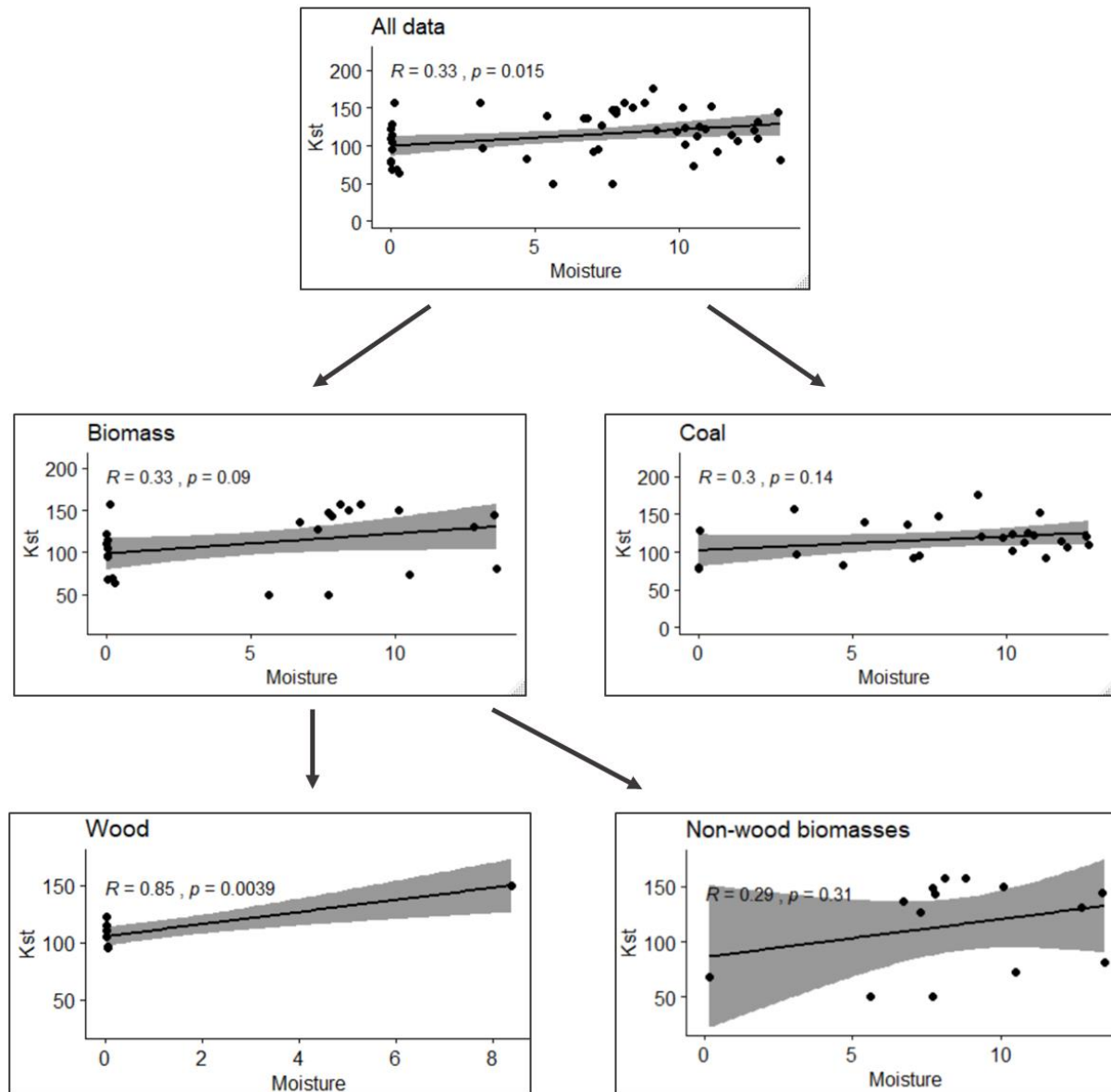


Figure 30: Scatterplots showing correlations between the explosion index and moisture content

dP/dt and d10

Like with the previous plots containing d10 there is a cluster of datapoints for in the lower end of d10, below 20 μm , and from the coal plot we can see that these dots are mostly coal and that they show a significant, negative correlation. In fact, the plots for biomass, coal and non-wood biomass all show negative correlation. Despite wood being the only one with a positive correlation, and this is a correlation based on three samples, the complete dataset still comes out with a positive correlation. Three datapoints is the minimum needed to have a correlation-factor. The plot for non-wood biomasses is identical (except for the values on the y-axis) to the non-wood biomass plot for K_{St} and d10.

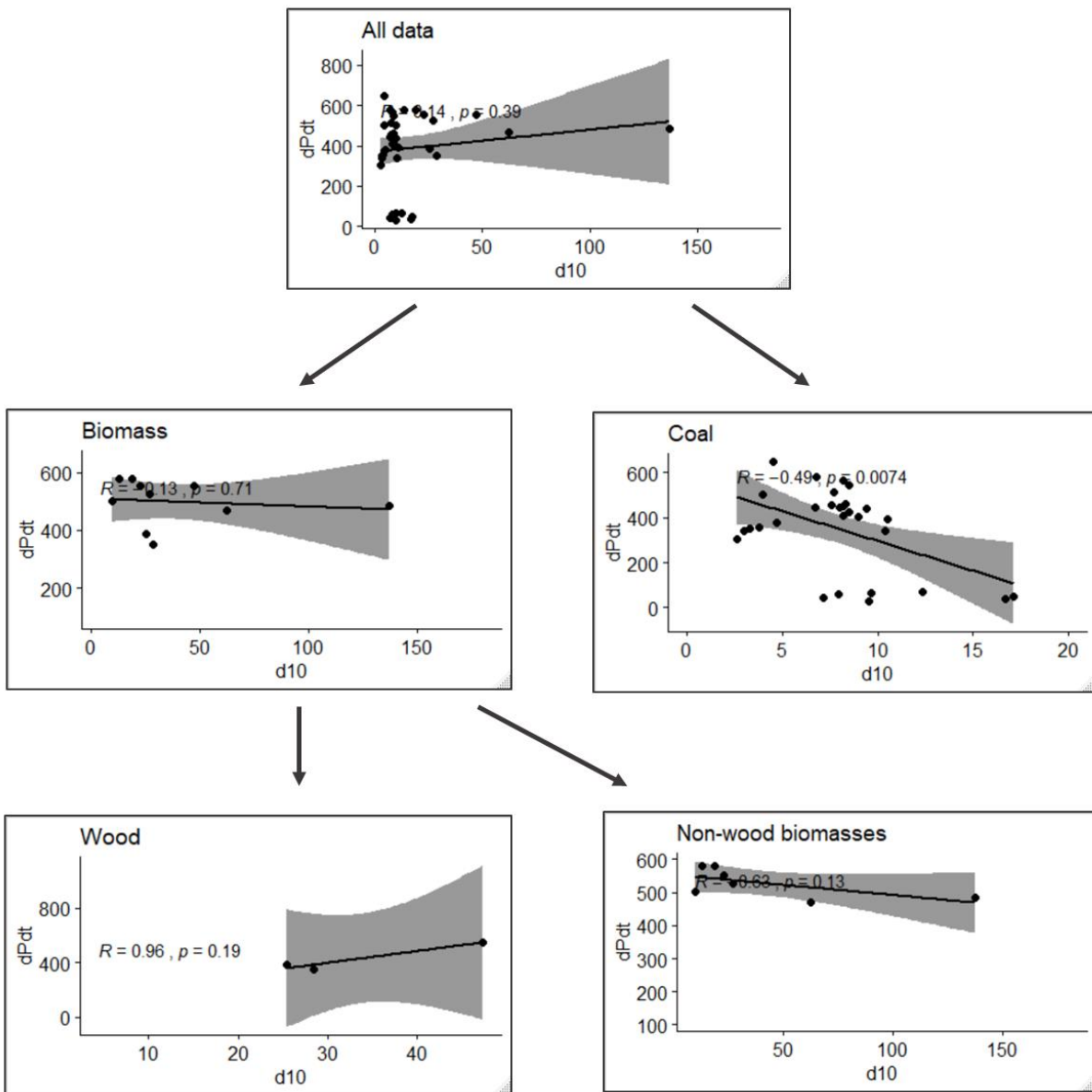


Figure 31: Scatterplots showing correlations between the maximum rate of pressure rise and d10

dP/dt and d50

Much of the data are concentrated in the lower end of the d50, though in that area the data is spread widely across the y-axis.

Again, there is opposite correlations for biomass and coal. The plot for coal is positive, indicating larger particles will cause a more rapid pressure rise. Both biomass in general and non-wood biomass show very little correlation, while wood show a significant negative correlation. This would mean a higher d50 should give a less severe explosion, or less rapid pressure rise, which is more in line with expectations.

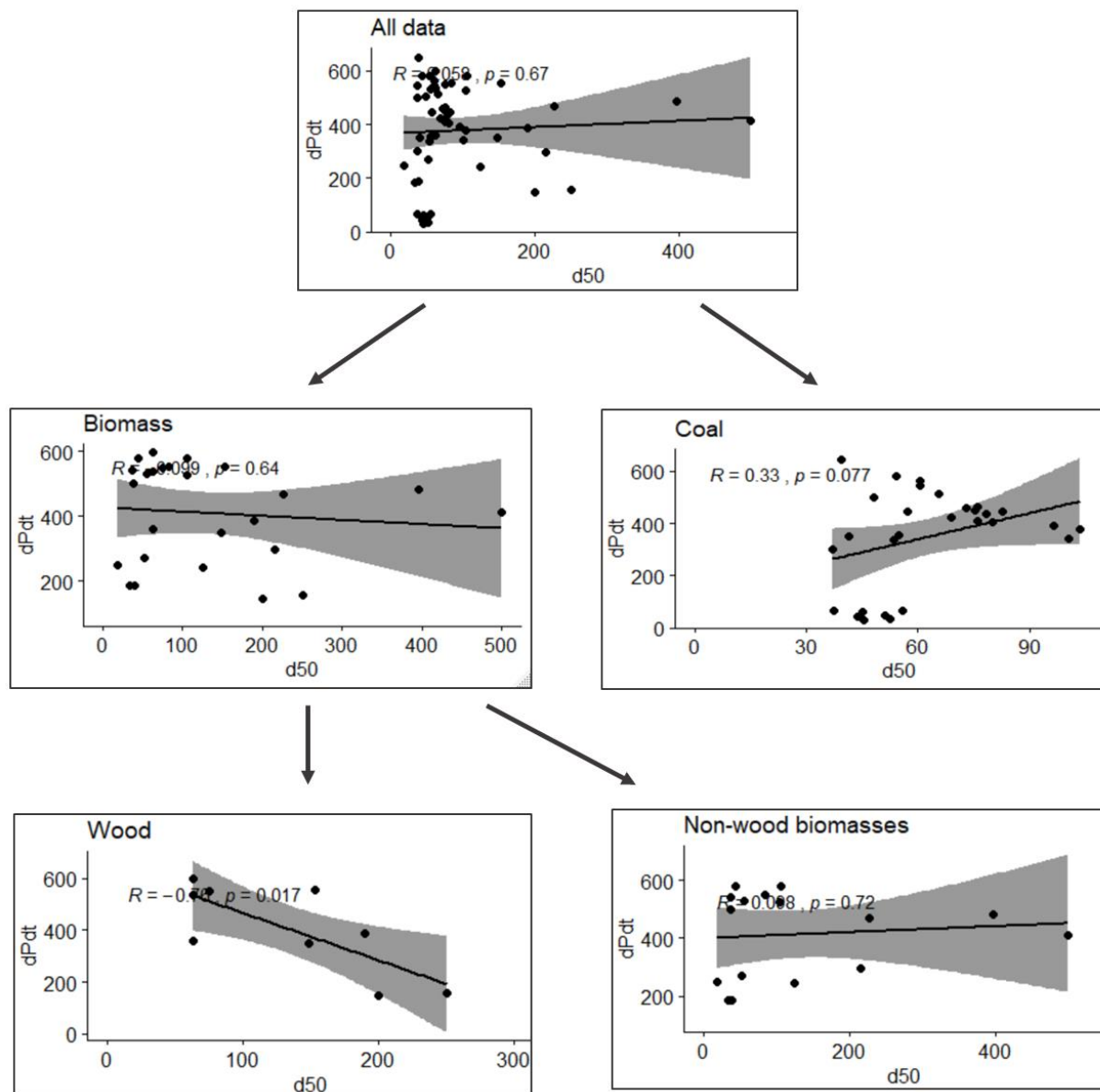


Figure 32: Scatterplots showing correlations between the maximum rate of pressure rise and d50

dP/dt and d 90

The only plot that shows any notable correlation is the coal plot. Coal show a strong very significant positive correlation between rate of pressure rise and d90, meaning a higher d90 will give more rapid pressure rise. For the remaining plots there are only weak correlations with low significance, though it should be noted that for the biomass plot the correlation is negative, contrary to the coal plot.

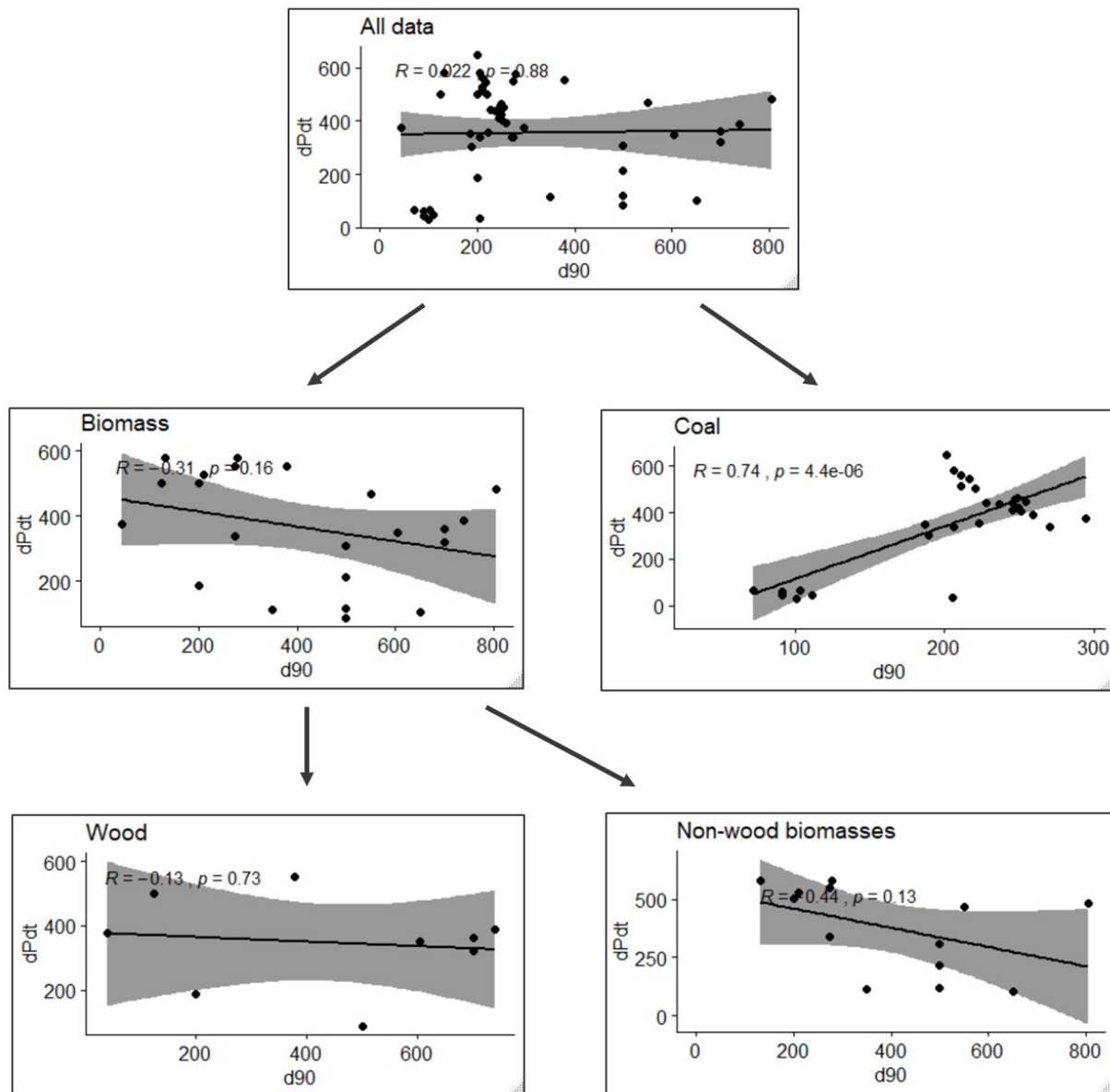


Figure 33: Scatterplots showing correlations between the maximum rate of pressure rise and d_{90}

dP/dt and the polydispersity index

The data in the plot for all data is very spread out, both in x- and y-directions. This shows some positive correlation with low significance. For coal there is a marked positive correlation between rate of pressure rise and the polydispersity index, indication that a wider spread of particle sizes in a sample will give a more rapid pressure rise. For biomass there is again an opposite trend, but still based on very little data, particularly for wood where there is only three datapoints. The non-wood biomasses show no correlation.

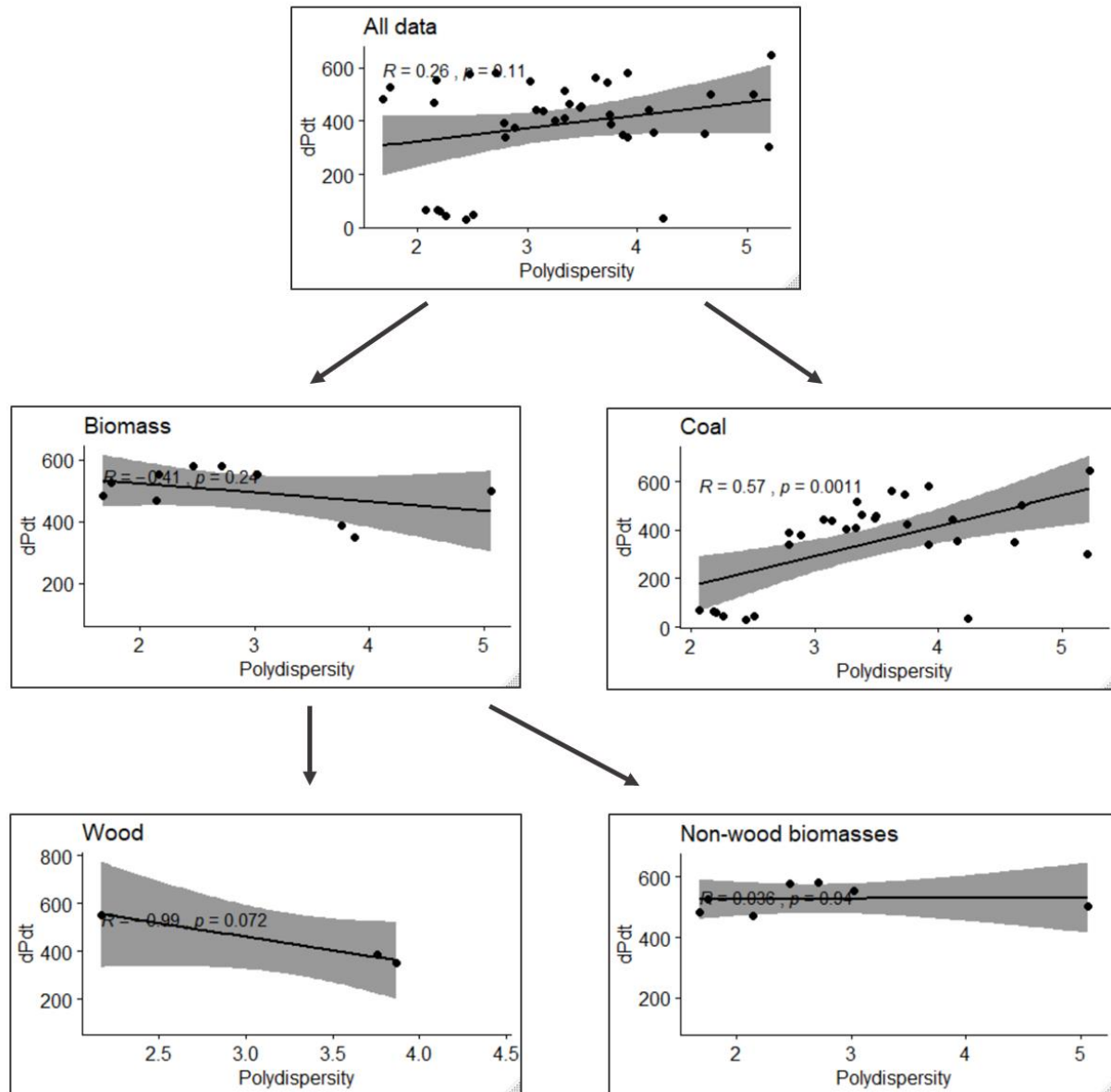


Figure 34: Scatterplots showing correlations between the maximum rate of pressure rise and the polydispersity index

dP/dt and moisture

All the plots show positive correlation, indicating that with a higher percentage of moisture the rate of pressure rise will also increase. For the complete data set and coal, the correlations are quite strong and have a high significance. The plot for biomass shows some positive correlation for biomass. There is Insufficient data for wood.

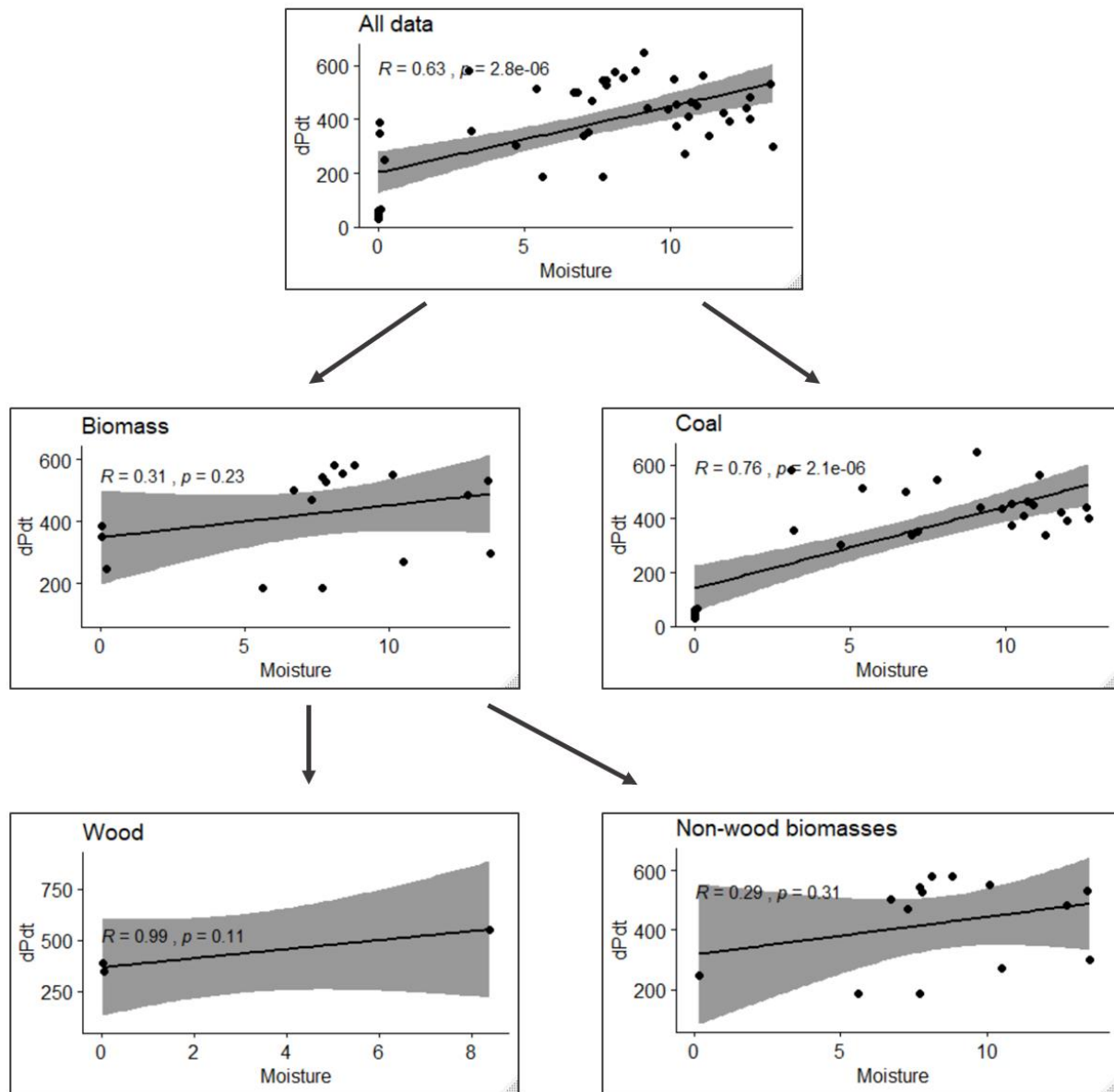


Figure 35: Scatterplots showing correlations between the maximum rate of pressure rise and moisture content

MIT and d10

From the complete dataset a significant negative correlation can be observed, indicating that an increase in the d10 will lower the minimum ignition temperature, making a dust cloud easier to ignite. A breakdown into coal and biomass reveals that these two again show opposite correlation. Coal has a weak negative correlation with low significance, while biomass has a weak positive correlation with even lower significance. A further breakdown of the biomass shows that there is too little data.

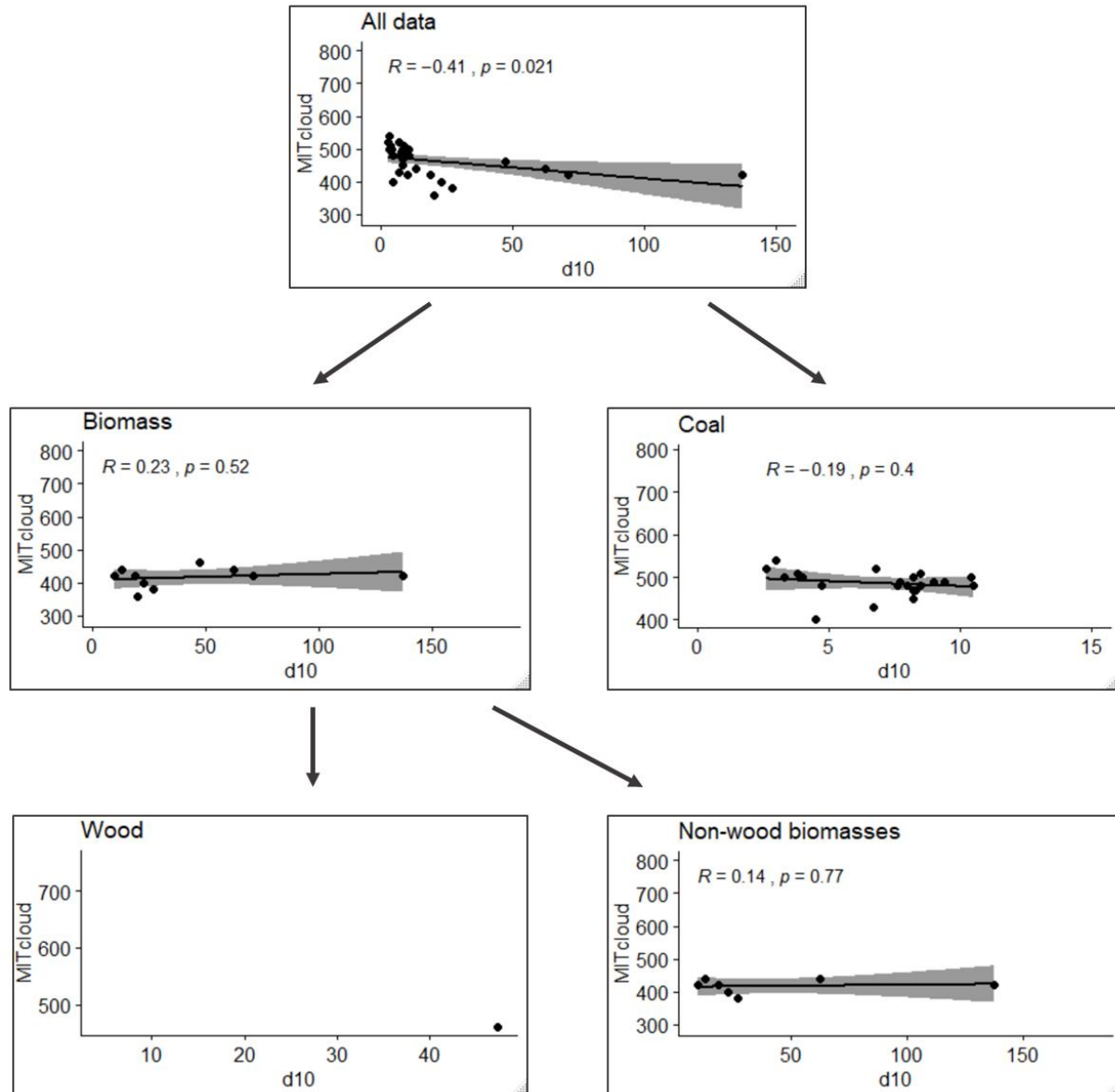


Figure 36: Scatterplots showing correlations between the minimum ignition temperature and d10

MIT and d50

MIT and d50 show no correlation. The correlation factors are all close to zero, and the p-values are all 0,1 or above, meaning there is little significance to the correlations. However, all the plots have a negative trend, so there is some indication that a higher median diameter will decrease the minimum ignition temperature. This is not in line with expectations.

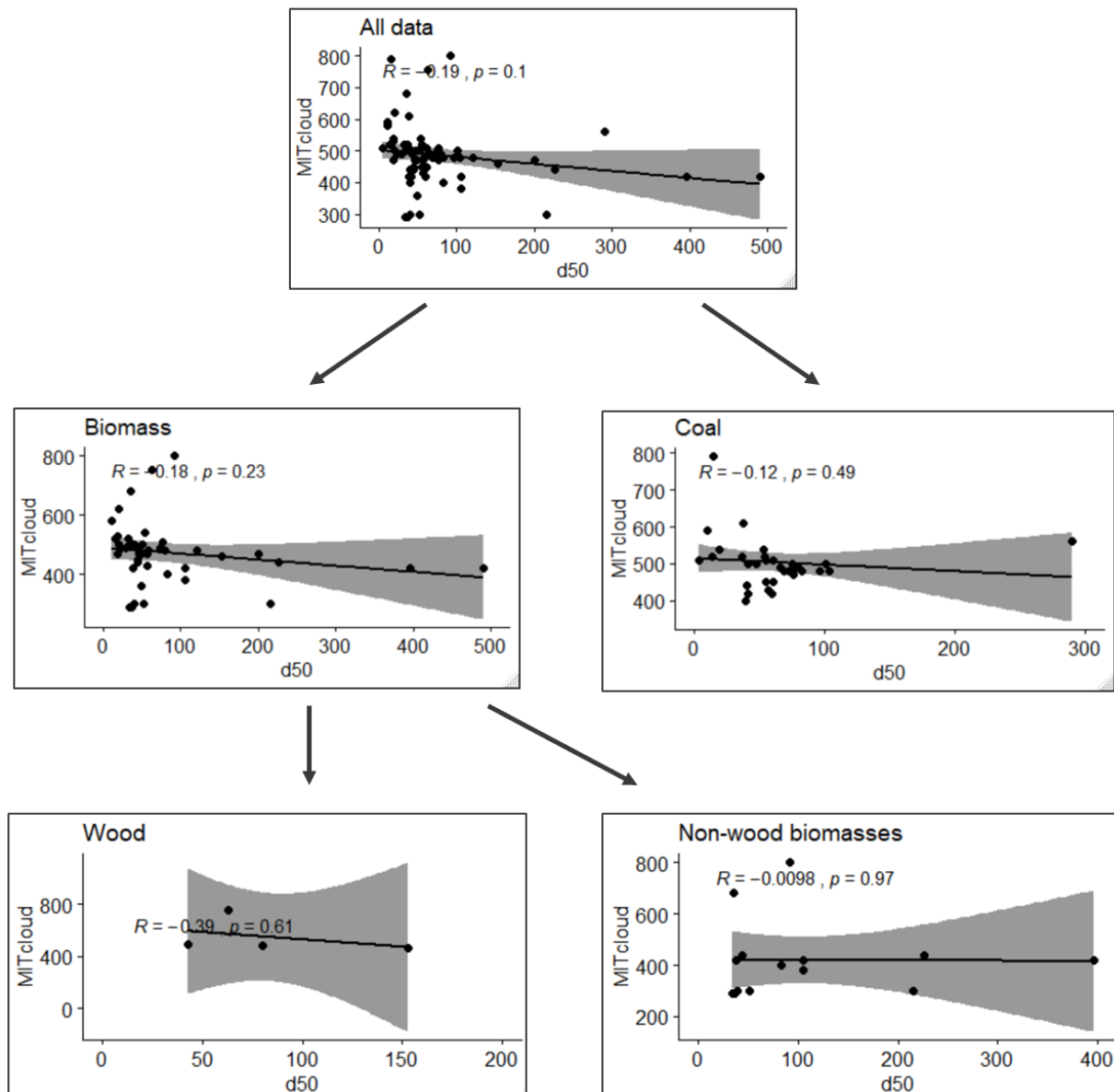


Figure 37: Scatterplots showing correlations between the minimum ignition temperature and d50

MIT and d90

With the exceptions of non-wood biomass all correlations are negative. For the complete dataset this correlation is also quite significant. Like for the correlations between MIT and d50 and MIT and d10, this implies that larger particles require lower temperature to be ignited.

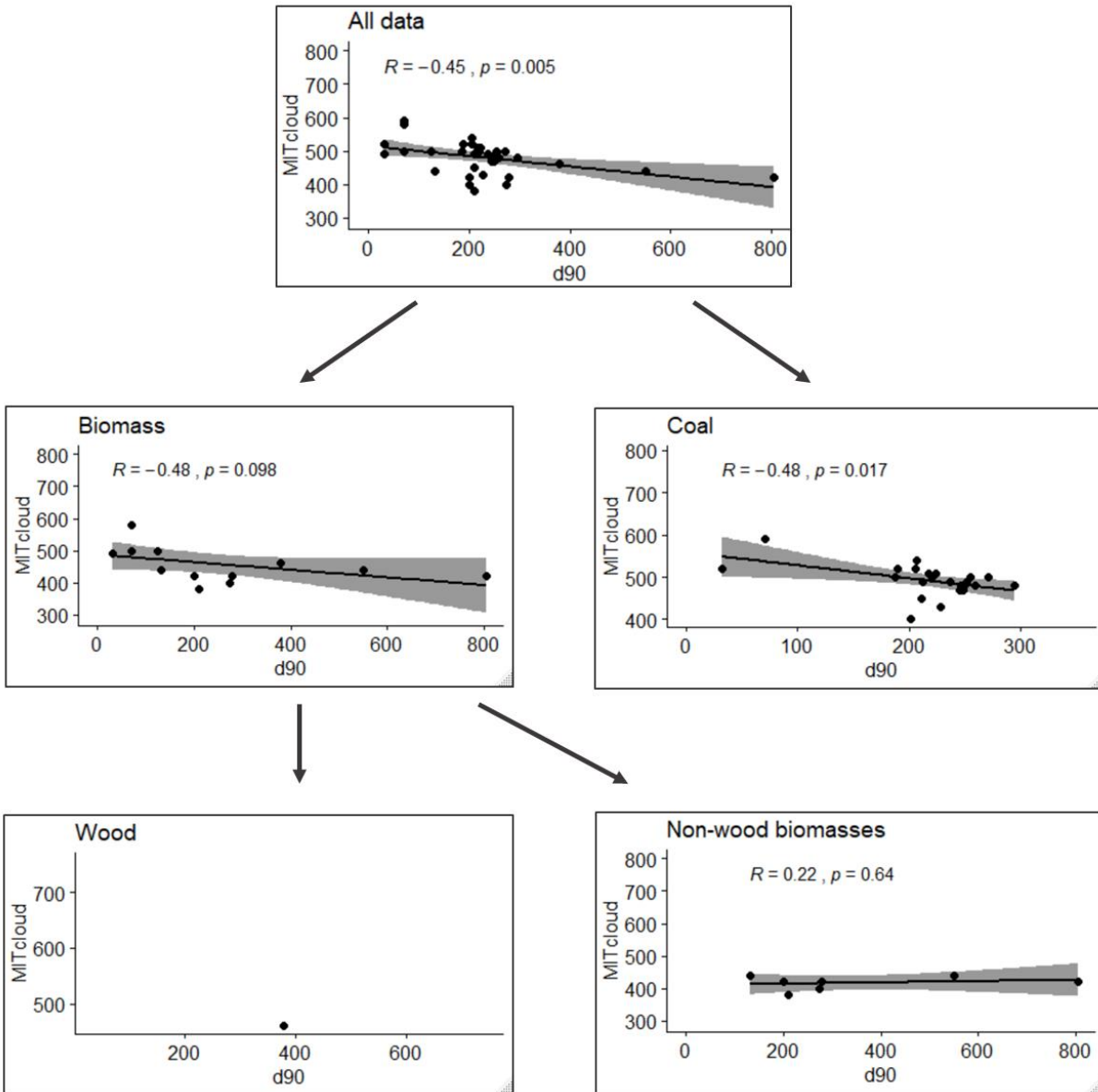


Figure 38: Scatterplots showing correlations between the minimum ignition temperature and d90

MIT and the polydispersity index

The plot for the complete dataset shows some positive correlation between MIT and the polydispersity index, though not very significant. For all the plots the datapoints are closely gathered along the nearly horizontal trend line, indicating that the MIT is not dependent on the polydispersity index. There are very little data in general, and even less for biomass. Still, it can appear like the MIT is constant between about 400 and 550 °C.

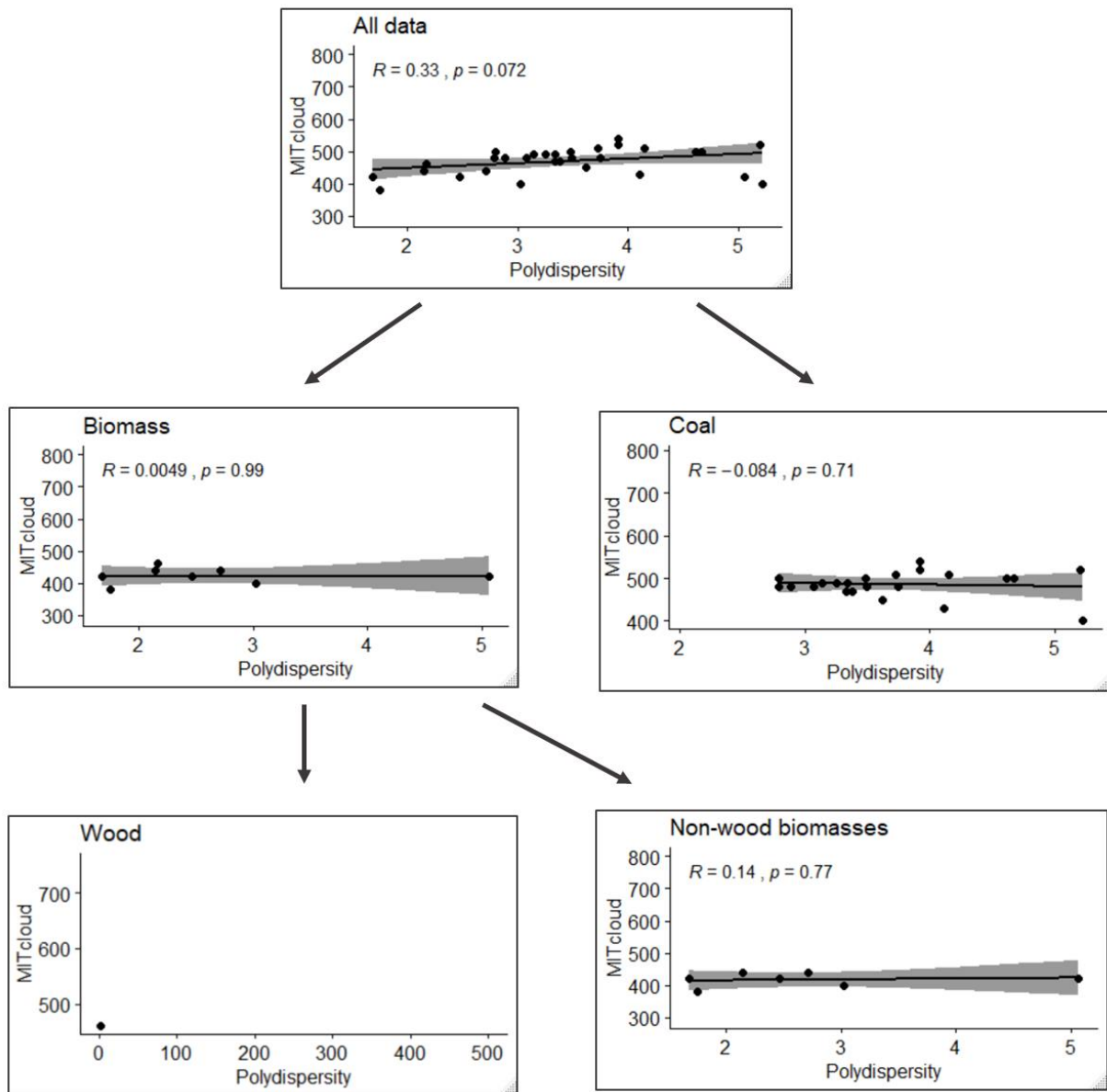


Figure 39: Scatterplots showing correlations between the minimum ignition temperature and the polydispersity index

MIT and moisture

These plots show that there is some clear negative correlation between moisture content and minimum ignition temperature. This means that as the moisture content increases the MIT decreases, making lower temperatures necessary to ignite the dust cloud. These correlations have a very high significance, despite being against expectation.

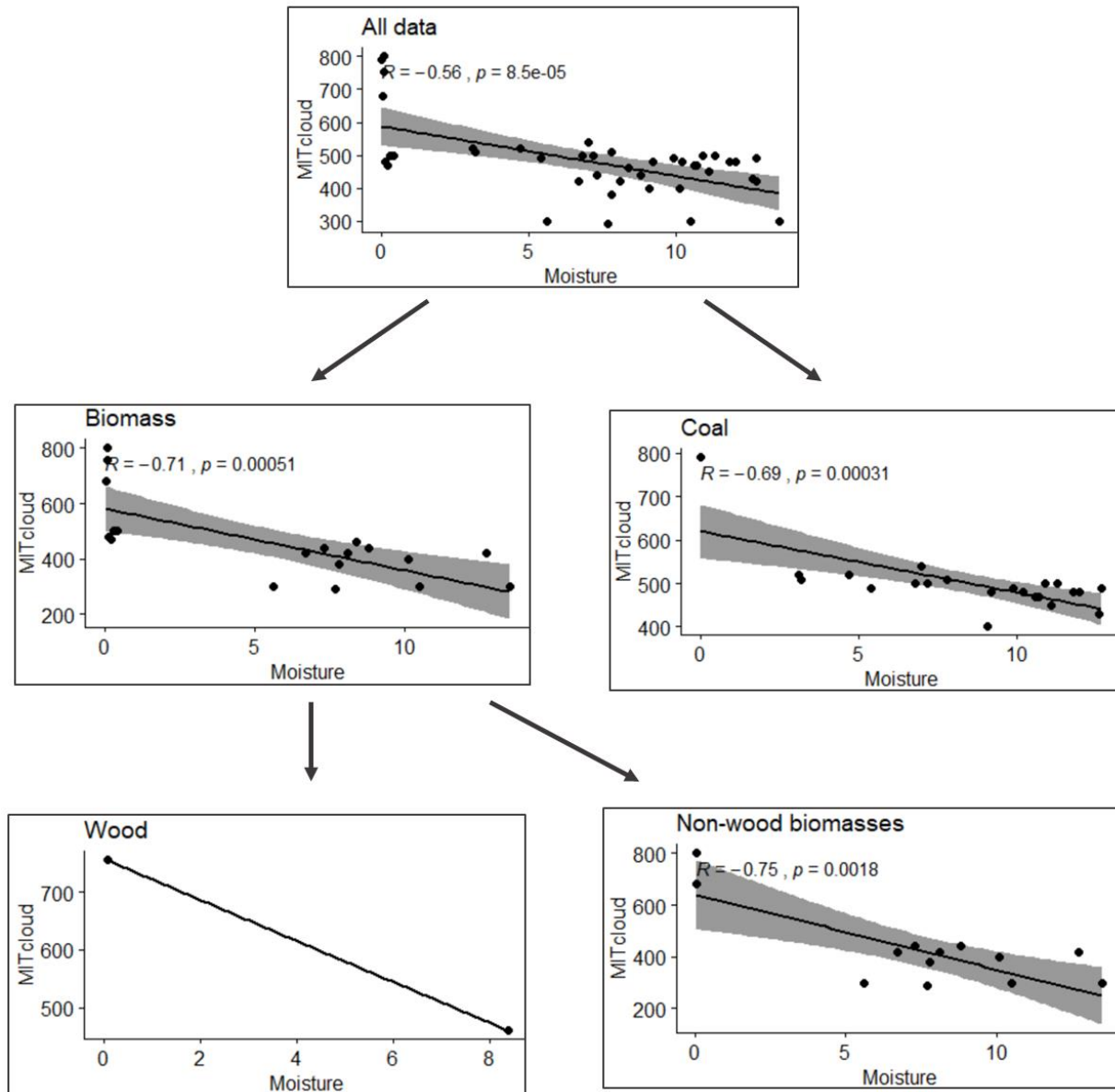


Figure 40: Scatterplots showing correlations between the minimum ignition temperature and moisture content

Specific surface area

There are only a few of the samples in the collection that have a reported specific surface area.

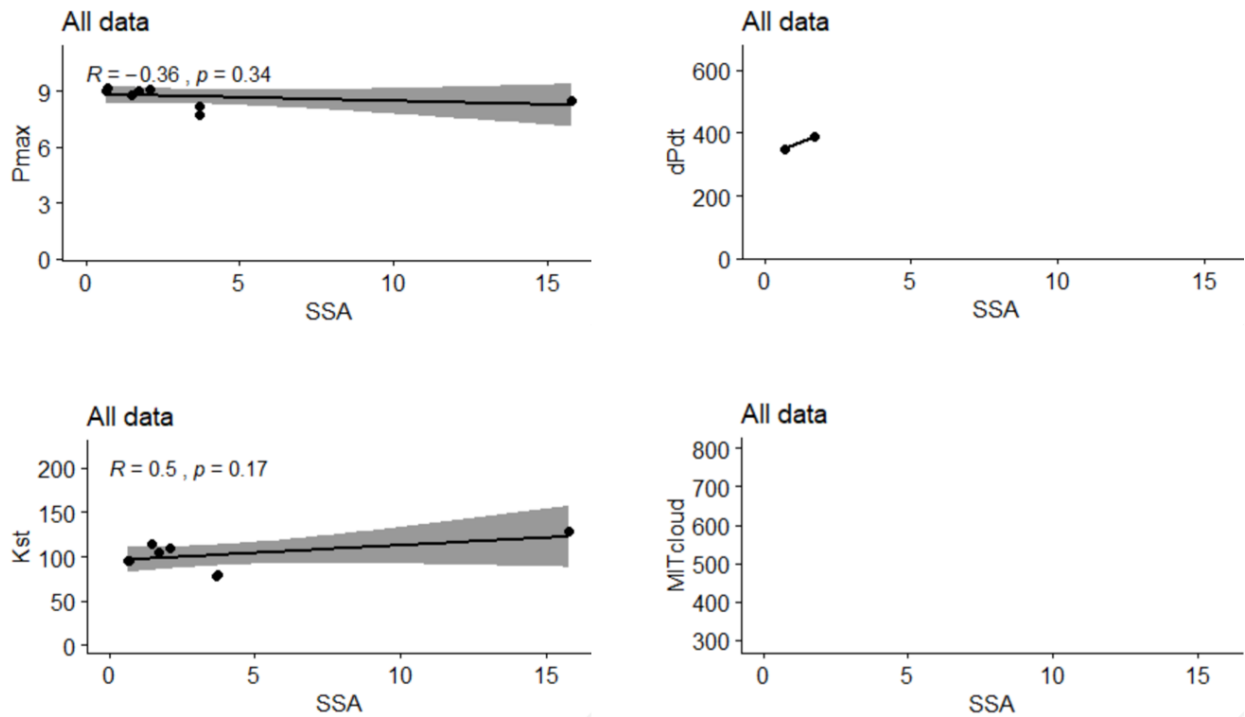


Figure 41: Scatterplots for specific surface area and explosion parameters

5. Discussion

The literature speaks quite confidently of the effect of particle size and other material properties: why is this effect not found in the data analysis? Is it simply a lack of data?

The data available is simply not enough to draw any conclusions from. However: there are more data than what is available to the general public (i.e. student researchers). Wood processing facilities are obligated to test their material, which is often done by sending samples to private/independent laboratories. The data resulting from these tests are owned by either the lab or the company that purchased their services and are therefore not publicly available. Yet, the data exists and if its owners could be persuaded to share that would be very valuable. It could bring the scientific communities many steps forward in understanding how certain materials behave. Each facility is likely consistent in their testing procedure and comparing similar data from different facilities can clarify how the procedure influences the result.

In the data collected for this thesis there is close to no samples with a median diameter of 500 μm which is the criterion set in NFPA 664. One possible reason can be that the available testing equipment is not suitable for particles this size. It is also possible that these larger particles have not been prioritized because of the assumption that they cannot explode. But that raises the question of how they would know that they cannot explode if they are not being tested. This does not mean the NFPA's claim is untrue, 500 μm is among the largest median diameters in this data collection, and 25 % moisture is more than double the moisture content of any of the studied samples. There should still be some form of documentation to a criterion that is this specific.

The P_{max} is more or less constant, or if not constant the values are mainly within a narrow range between approximately 7 and 10 bar. but relatively unaffected by factors that were expected to have a significant impact (such as particle size and moisture content). The biomass in this data collection has a higher P_{max} than coal. One factor that has not been controlled for is the amount of fuel in the explosion chamber. This could mean either increasing the amount of fuel without changing the test chamber or changing the chamber size and changing the amount of fuel so that the concentration is constant. Theoretically, if the concentration is the same, and procedure is done according to standards the results should also stay the same. This is because part of the reason the 20L-sphere is accepted as an alternative to the 1 m^3 -chamber is because it can be calibrated to give the same results. Still, intuitively it would seem like a larger amount of fuel should make a more severe explosion, since more fuel has more potential energy. But assuming one had the optimum concentration of a fuel and tested it in two explosion chambers of different size, would the larger one have a more violent explosion? Supposedly no, because of the calibrations, however, as has been pointed out previously in this work, there are discrepancies between chambers of different sizes. Some of this is due to the relative heat loss to the chamber walls, so that is one of the factors that needs to be controlled for.

Coal and biomass need to be studied separately, in the scatterplot they often show contradicting outputs, and the histograms and boxplot show differences in material properties as well as explosion properties.

Biomass has a higher maximum explosion pressure while coal has higher maximum rate of pressure rise and deflagration index, suggesting that biomass has more powerful explosions while coal has more severe explosions. One would expect those two things to go hand in hand. In this data collection the coal samples are in general smaller, as seen in Figure 14 coal has lower values for d10, d50 and d90. This could lead one to believe coal should have a higher P_{max} , which is not the case here. However, from the scatterplots it appears that P_{max} is less dependent on particle size than previously assumed. Coal *does* have higher values for $(dP/dt)_{max}$, which is an important factor in determining the severity of an explosion.

The data analysis was not able to include shape as a factor. Shape could be the factor that gives biomass a higher P_{max} compared to coal. By the expectations set by the literature review coal, having the smaller particles, should have the higher maximum pressure. Since coal is assumed to be more spherical and therefore have a smaller specific surface area.

The correlation results for moisture are very counter-intuitive. The expectation is that since it requires a significant amount of energy for water to be heated and go through phase change, increased moisture content should hinder the explosion. This is supported in Yuan et al.'s research paper [52] where they specifically looked at how moisture influences explosion parameters. Their results clearly state that increased moisture content gives a less severe explosion both in terms of maximum pressure and rate of pressure rise, as illustrated in Figure 8. In the scatterplots however, moisture correlates positively with $(dP/dt)_{max}$ and K_{St} and negatively with P_{max} and MIT. Of these four only the negative correlation to P_{max} is expected.

The negative correlation between moisture and minimum ignition temperature is the hardest to explain, because to ignite the dust it has to be heated to the point of devolatilization and this includes heating the water too. Though looking at the scatterplots there are some outliers with very high MIT and moisture content close to zero. These could be skewing the data and are certainly affecting the outcome of the correlation analysis. Excluding these data may make the correlation analysis more acceptable and in line with expectation, however, it would not mean those data would cease to exist.

Most of the scientific literature behind the data collection does not focus on moisture content, in general if it is tested for it is often treated as a constant. That is, they did not as a rule repeat a test under the exact same conditions only with a different level of moisture in the sample. More typically they tested an entirely different sample, a different type of coal or some other form of biomass. This seems likely to have some impact on the results, but it doesn't sufficiently explain in three of four cases the correlation is opposite of what the scientific literature describes. A hypothesis could be that as moisture go through phase change this contributes to increasing the pressure. But then that should also be the case in the above-mentioned study by Yuan et al.

Alternatively, the molecular structure of the moisture-dust mix could lead to incorrect results. As noted in chapter 2.4 there are different types of moisture, and not all types of moisture will be revealed by the methods typically used for finding moisture content. Finding moisture content is done by heating a sample so the moisture evaporates and then calculating the percentage of moisture by the weight that was lost. However, if the moisture is bound to the dust particles on a molecular level, it will not evaporate and therefore not be accounted for. While this will lead to inaccurate reports of moisture content, it seems unlikely that it would affect the results to such a degree that they defy all expectation, since the expectations are not solely based on theory, but also confirmed by experiments. Though this is a topic that remains largely unexplored.

6. Conclusion

The main conclusion to draw from this thesis is that more research is needed. This report shows an urgent need for the wood industry to develop and implement a new methodology to classify the risk of deflagration other than relying on d50. However, as this thesis has uncovered, to achieve this goal there are several necessary steps to be performed in advance.

Researchers need to agree on methodologies. Of course, this is more easily said than done, since to find out which methods are better, more research is needed. First, the methodology for how to measure particles must be established. This must be a method that does not assume sphericity but considers the particle shape as a parameter. The median diameter does not tell us everything we need to know, and even though the polydispersity index shows more promising results, with a stronger correlation to explosion parameters, it still assumes sphericity and is only an indication of the span of a sample, not the actual size of the particles.

Samples should always be collected in similar locations to ensure that all variables can be controlled for, and the complete sample should be studied, including the finest particles that are formed by abrasion. This is so that the full range of possible values that can appear in the wood working facilities can be evaluated. Once these samples are collected, testing should also be homogenized. There are several procedures and types of equipment used for determining particle size. This equipment is not based in the same principles, so the results it gives are not comparable to results obtained by a different method and may substantially differ. A standard procedure should be established to clarify this.

Coal and biomass are different and should be studied separately. Are the differences between coal and biomass because they are fundamentally different material or can they be explained by the testing procedure, or the sampling procedure? It is clear that biomass and coal should be studied separately, and that what we have learned from studying coal particles and coal dust explosions should not automatically be assumed to be true for wood or other biomasses. Testing equipment developed to study explosion parameters of coal should be redesigned to accommodate the bulkier biomass particles.

Nothing in this project has confirmed the NFPA 664's claim that dust cannot explode if the median particle size is more than 500 μm and the moisture content exceeds 25%. However, only two of the biomass samples have a d50 above 400 μm , and none of the samples approach 25% in moisture content, so there also is no evidence to the contrary.

7. Further work

There is much work to be done:

- Find out how to best measure particle size for biomass. d50 that has been commonly used is not very helpful. The polydispersity index has better results, but it would likely function even better in combination with another factor.
- Study the effect of particle shape on explosion parameters. This data analysis should have included a correlation analysis for specific surface area, and it does, however, what is evident from Figure 1 is that there are too little data for SSA.
- Standardize explosion test equipment for biomass. In some cases, researchers have taken it upon themselves to adapt equipment to be more suitable for biomass dust. This means their results are not comparable to other results, because they are not obtained under the same conditions.
- Generate a database from existing data. An initiative to gather the already existing data from explosion tests from independent facilities would help us gain a better understanding of how different materials behave in an explosion scenario. Each facility is likely consistent in their testing procedure and comparing similar data from different facilities can clarify how the procedure influences the result.
- The correlation analysis for moisture content did not align with expectations. The reasons for this could be about this particular dataset, but there is no certain explanation, which is cause for further investigation.
- Looking into existing standards. Most of the research articles referenced in this thesis does not put any emphasis on standards when describing their methodology. This suggest that standards are not being used as they should. Finding out if this is true, and the reasons for it, seems like a good step.
- Assigning a single value for all the different wood species and the different facilities and situation that we can encounter would be too simplistic and not accurate enough. This is why, once these steps have been taken, a great improvement in the field would be to create a mathematical model to define the risk of deflagration of wood dusts, which can simulate the behavior in the particular case of each facility and in different moments of the process.

8. References

- [1] Hughes Environmental, “Don’t Repeat A History Of Combustible Dust Explosions,” 20 October 2015. [Online]. Available: <https://hughesenv.com/history-of-combustible-dust-explosions/>. [Accessed 28 May 2019].
- [2] U.S. Chemical Safety and Hazard Investigation Board, “Investigation Report, Sugar dust explosion and fire,” 2009.
- [3] Cheshire Fire and Rescue Service, “Explosion in a Bosley wood mill,” 17 July 2015. [Online]. Available: <https://www.cheshirefire.gov.uk/home/ongoing-explosion-in-a-bosley-woodmill>. [Accessed 20 May 2019].
- [4] J. S. Forrester, “Hopper Eyed as Cause of Fire at Spice Plant,” Powder and bulk solids, 5 April 2016. [Online]. Available: <https://www.powderbulksolids.com/news/Hopper-Eyed-as-Cause-of-Fire-at-Spice-Plant-04-05-2016>. [Accessed 22 May 2019].
- [5] GenDisasters.com, “Litchfield, IL Flour Mill Explosion, Mar 1893,” [Online]. Available: <http://www.gendisasters.com/illinois/8352/litchfield-il-flour-mill-explosion-mar-1893>. [Accessed 30 May 2019].
- [6] J. Sutton, “Six dead from weekend grain elevator explosion in Kansas,” CNN, 1 November 2011. [Online]. Available: <https://edition.cnn.com/2011/10/31/us/kansas-grain-explosion/>. [Accessed 28 May 2019].
- [7] CBC News, “Burns Lake sawmill explosion and fire called preventable,” CBC, 16 January 2014. [Online]. Available: <https://www.cbc.ca/news/canada/british-columbia/burns-lake-sawmill-explosion-and-fire-called-preventable-1.2499632>. [Accessed 22 May 2019].
- [8] T. C. Gordon Hoekstra, “Two dead, 22 injured after massive explosion destroys Prince George sawmill,” Vancouver Sun, 25 April 2012. [Online]. Available: <http://www.vancouversun.com/dead+injured+after+massive+explosion+destroys+prince+george+sawmill/6506952/story.html>. [Accessed 22 May 2019].
- [9] L. V. Mette Finborud Børresen, “Fabrikktak blåst bort i eksplosjon,” NRK, 13 September 2013. [Online]. Available: <https://www.nrk.no/ho/stoveksplosjon-pa-forestia-1.11240633>. [Accessed 30 May 2019].
- [10] C. Cloney, “Explosion Incidents,” My dust explosion research, 2016. [Online]. Available: <https://www.mydustexplosionresearch.com/explosion-incidents/>. [Accessed 23 May 2019].
- [11] Dust Safety Science, “Explosion During Grain Silo Demolition Kills Seven in Aqaba, Jordan,” 2018. [Online]. Available: <https://dustsafetyscience.com/grain-silo-explosion-aqaba-jordan/>. [Accessed 28 May 2019].
- [12] National Fire Protection Association, “About NFPA - overview,” [Online]. Available: <https://www.nfpa.org/overview>. [Accessed 1. March 2019].

- [13] P. Amyotte, *An Introduction to Dust Explosions*, Oxford: Butterworth-Heinemann, 2013.
- [14] R. A. Ogle, *Dust explosion dynamics*, Oxford: Elsevier Inc., 2017.
- [15] N. F. P. Association, “NFPA 68. Standard on explosion protection by deflagration venting,” NFPA, 2018.
- [16] T. Abbasi and S. A. Abbasi, “Dust explosions—Cases, causes, consequences, and control,” *Journal of hazardous materials*, February 2007.
- [17] R. Zalosh, “Dust Explosions,” in *SFPE handbook of fire protection engineering*, 5th ed., M. J. Hurley, Ed., New York, Springer, 2016, pp. 2766-2792.
- [18] B. Beamish and A. Arisoy, “Effect of mineral matter on coal self-heating rate,” *Fuel*, vol. 87, pp. 125-130, 2008.
- [19] E. Kaymakci and V. Didari, “Relations between coal properties and spontaneous combustion parameters,” *Turkish journal of engineering and environmental sciences*, vol. 26, pp. 59-64, 2002.
- [20] C. Huéscar Medina, H. Phylaktou, G. Andrews and B. Gibbs, “Explosion characteristics of pulverised torrefied and raw Norway spruce (*Picea abies*) and Southern pine (*Pinus palustris*) in comparison to bituminous coal,” *Biomass and bioenergy*, August 2015.
- [21] J. Garcia-Torrent, E. Conde-Lazaro, C. Wilen and A. Rautalin, “Biomass dust explosibility at elevated initial pressures,” *Fuel*, vol. 77, pp. 1093-1097, 1998.
- [22] R. Eckhoff, “Understanding dust explosions. The role of powder science and technology,” *Journal of loss prevention in the process industries*, vol. 22, pp. 105-116, 2009.
- [23] R. K. Eckhoff, *Dust explosions in the process industries*, USA: Elsevier Science, 2003.
- [24] W. Gao, T. Mogi, J. Yu, X. Yan, J. Sun and R. Dobashi, “Flame propagation mechanisms in dust explosions,” *Journal of loss prevention in the process industries*, vol. 36, pp. 186-194, 2015.
- [25] R. Dobashi and K. Senda, “Mechanisms of flame propagation through suspended combustible particles,” *Journal de Physique*, vol. 12, no. 7, pp. 459-465, 2002.
- [26] A. Di Benedetto, P. Russo, P. Amyotte and N. Marchand, “Modelling the effect of particle size on dust explosions,” *Elsevier: Chemical Engineering Science*, January 2010.
- [27] G. Rice, L. Jones, W. Egly and H. Greenwald, “Coal-dust explosion tests in the experimental mine 1913--1918, inclusive,” Bureau of Mines, Department of Interior, Washington, 1922.

- [28] S. Callé, L. Klabá, D. Thomas, L. Perrin and O. Dufaud, "Influence of the size distribution and concentration on wood dust explosions: Experiment and reaction modelling," *Elsevier: Powder Technology*, September 2005.
- [29] A. Fumagalli, M. Derudi, R. Rota, J. Snoeys and S. Copelli, "Prediction of the deflagration index for organic dusts as a function of the mean particle diameter," *Journal of loss prevention in the process industries*, vol. 50, pp. 67-74, 2017.
- [30] K. L. Cashdollar, "Overview of dust explosibility characteristics," *Elsevier: Journal of Loss Prevention in the Process industries*, 2000.
- [31] D. P. Mishra and S. Azam, "Experimental investigation on effects of particle size, dust concentration and dust-dispersion-air pressure on minimum ignition temperature and combustion process of coal dust clouds in a G-G furnace," *Elsevier: Fuel*, October 2016.
- [32] N. Kalkert and H.-G. Schecker, "Explosionsgrenzen von Ammoniak in Mischungen mit Methan," *Chemie ingenieur technik*, vol. 51, no. 9, pp. 895-895, 1979.
- [33] R. K. Eckhoff, "Does the dust explosion risk increase when moving from μm -particle powders to powders of nm-particles?," *Elsevier: Journal of loss prevention in the process industries*, November 2011.
- [34] P. Amyotte, M. J. Pegg, F. I. Khan, M. Nifuku and T. Yingxin, "Moderation of dust explosions," *Elsevier: Journal of Loss Prevention in the Process Industries*, May 2007.
- [35] N. Fernandez-Anez and J. Garcia-Torrent, "Influence of particle size and density on the hot surface ignition of solid fuel layers," *Fuel technology*, vol. 55, no. 1, pp. 175-191, 2019.
- [36] W. Gao, T. Mogi, J. Sun, J. Yu and R. Dobashi, "Effects of particle size distributions on flame propagation mechanism during octadecanol dust explosions," *Elsevier: Powder Technology*, August 2013.
- [37] D. Castellanos, V. Carreto-Vazquez, C. Mashuga, R. Trottier, A. Mejia and M. Mannan, "The effect of particle size polydispersity on the explosibility characteristics of aluminium dust," *Powder technology*, vol. 254, pp. 331-337, 2014.
- [38] A. Tascón, "Influence of particle size distribution skewness on dust explosibility," *Elsevier: Powder Technology*, October 2018.
- [39] D. Castellanos, V. H. Carreto-Vazquez, C. V. Mashuga, R. Trottier, A. F. Mejia and M. S. Mannan, "The effect of particle size polydispersity on the explosibility characteristics of aluminum dust," *Elsevier: Powder Technology*, March 2014.
- [40] Q. Li, K. Wang, Y. Zheng, M. Ruan, X. Mei and B. Lin, "Experimental research of particle size and size dispersity on the explosibility characteristics of coal dust," *Elsevier: Powder Technology*, May 2016.

- [41] A. Klippel, M. Scheid and U. Krause, "Investigations into the influence of dustiness on dust explosions," *Elsevier: Journal of loss prevention in the process industries*, November 2013.
- [42] C. Huéscar Medina, H. N. Phylaktou, H. Sattar, G. E. Andrews and B. M. Gibbs, "The development of an experimental method for the determination of the minimum explosible concentration of biomass powders," *Elsevier: Biomass and bioenergy*, March 2013.
- [43] R. K. Eckhoff, "Influence of dispersibility and coagulation on the dust explosion risk presented by powders consisting of nm-particles," *Elsevier: Powder Technology*, May 2013.
- [44] G. Grant, J. Brenton and D. Drydale, "Fire suppression by water sprays," *Progress in energy and combustion science*, vol. 26, no. 2, pp. 79-130, 2000.
- [45] B. Ewan and M. Moatamedi, "The study of induced water flow devices in the suppression of gas explosions," *Process safety and environmental protection transactions of the Institution of Chemical Engineers, Part B*, vol. 80, no. 3, pp. 126-134, 2002.
- [46] P. Amyotte, F. Khan and A. Dastidar, "Reduce dust explosions the inherently safer way," *Chenucak engineering progress*, vol. 99, no. 10, pp. 36-43, 2003.
- [47] G. Thomas, "On the conditions required for explosion mitigation by water sprays," *Process safety and environmental protection*, vol. 78, no. 5, pp. 339-354, 2000.
- [48] Z. Jiang, W. Chow and S. Li, "Review on additives for new clean fire suppressants," *Environmental engineering science*, vol. 24, no. 5, 2007.
- [49] M. Traore, O. Dufaud, L. Perrin, S. Chazelet and D. Thomas, "Dust explosions: How should the influence of humidity be taken into account?," *Process safety and environment protection*, vol. 87, pp. 14-20, 2009.
- [50] J. Yuan, W. Wei, W. Huang, B. Du, L. Liu and J. Zhu, "Experimental investigations on the roles of moisture in coal dust explosion," *Journal of the Taiwan Institute of chemical engineers*, vol. 45, no. 5, pp. 2325-2333, 2014.
- [51] F. Lees, *Loss prevention in the process industries: hazard identification, assessment and control*, London: Butterworth-Heinemann, 1980.
- [52] J. Yuan, W. Wei, W. Huang, B. Du, L. Liu and J. Zhu, "Experimental investigations on the roles of moisture in coal dust explosion," *Elsevier: Journal of the Taiwan Institute of chemical engineers*, September 2014.
- [53] M. Gil, E. Teruel and I. Arauzo, "Analysis of standard sieving method for milled biomass through image processing. Effects of particle shape and size for poplar and corn stover," *Fuel*, 15 January 2014.
- [54] C. Igathinathane, S. Melin, S. Sokhansanj, X. Bi, C. Lim, L. Pordesimo and E. Columbus, "Machine vision based particle size and size distribution determination of airborne," *Powder Technology*, pp. 202-211, 11 August 2009.

- [55] O. Laitinen and P. Karinkanta, "Use of tube flow fractionation in wood powder characterisation," *Biomass and bioenergy*, 9 March 2017.
- [56] H. Lu, E. Ip, J. Scott, P. Foster, M. Vickers and L. L. Baxter, "Effects of particle shape and size on devolatilization of biomass particle," *Elsevier: Fuel*, 7 November 2008.
- [57] Q. Guo, X. Chen and H. Liu, "Experimental research on shape and size distribution of biomass particle," *Fuel*, 28 November 2011.
- [58] V. Chaloupková, T. Ivanova and B. Havrland, "Sieve analysis of biomass: accurate method for determination of particle size," Elsevier, 2016.
- [59] C. H. Medina, B. MacCoitir, H. Sattar, D. J. F. Slatter, H. N. Phylaktou, G. E. Andrews and B. M. Gibbs, "Comparison of the explosion characteristics and flame speeds of pulverised coals and biomass in the ISO standard 1 m³ dust explosion equipment," *Elsevier: Fuel*, 20 January 2015.
- [60] D. Castellanos, V. Carreto, T. Skjold, S. Yuan, P. Chaudhari, M. S. Mannan and C. Mashuga, "Construction of a 36L dust explosion apparatus and turbulence flow field comparison with a standard 20L dust explosion vessel," *Elsevier: Journal of Loss Prevention in the Process Industries*, September 2018.
- [61] T. Skjold, "Selected aspects of turbulence and combustion in 20-litre explosion vessels - Development of experimental apparatus and experimental investigation," University of Bergen, Bergen, 2003.
- [62] M. Azam Saeed, M. Farooq, G. E. Andrews, H. N. Phylaktou and B. M. Gibbs, "Ignition sensitivity of different compositional wood pellets and particle size dependence," *Elsevier: Journal of Environmental Management*, February 2019.
- [63] Y. Yang, "Image and Sieve Analysis of Biomass Particle Sizes and Separation after Size Reduction," University of Tennessee, Knoxville, 2007.
- [64] G. G. Løvås, *Statistikk for universiteter og høyskoler*, 3. ed., Oslo: Universitetsforlaget, 2013.
- [65] G. E. Andrew, H. Sattar, C. Heuscar-Medina, D. M. Slatter, M. A. Saeed, H. N. Phylaktou and B. M. Gibbs, "Recent developments including pulverised biomass," University of Leeds, Leeds, 2016.
- [66] M. C. Lee, Y. S. Kim and D. H. Rie, "Analysis of explosion characteristics of combustible wood dust in confined system using the thermal decomposition rate and mass loss rate," *Elsevier: Applied Thermal Engineering*, October 2016.
- [67] C. Huéscar Medina, H. Sattar, H. N. Phylaktou, G. E. Andrews and B. M. Gibbs, "Explosion reactivity characterisation of pulverised torrefied spruce wood," *Elsevier: Journal of loss prevention in the process industries*, December 2014.
- [68] S. Hosseinzadeh, J. Berghmans, J. Degreve and F. Verplaetsen, "A model for the minimum ignition energy of dust clouds," *Elsevier: Process Safety and Environmental Protection*, 10 October 2018.

- [69] Á. Ramírez, J. García-Torrent and P. J. Aguado, “Determination of parameters used to prevent ignition of stored materials and to protect against explosions in food industries,” *Elsevier: Journal of hazardous materials*, August 2009.
- [70] N. Fernandez-Anez and J. Garcia-Torrent, “Influence of particle size and density on the hot surface ignition of solid fuel layers,” *Springer: Fire Technology*, October 2018.
- [71] J. G. Torrent, Á. Ramírez-Gómez, N. Fernandez-Anez, L. M. Pejic and A. Tascón, “Influence of the composition of solid biomass in the flammability and susceptibility to spontaneous combustion,” *Elsevier: Fuel*, November 2016.
- [72] S.-H. Liu, Y.-F. Cheng, X.-R. Meng, H.-H. Ma, S.-X. Song, W.-J. Liu and Z.-W. Shen, “Influence of particle size polydispersity on coal dust explosibility,” *Elsevier: Journal of loss prevention in the process industries*, November 2018.
- [73] J. Garcia-Torrent, N. Fernandez-Anez, L. Medic-Pejic, A. Blandon-Montes and J. M. Molina-Escobar, “Ignition and explosion parameters of Colombian coals,” *Journal of loss prevention in the process industries*, September 2016.
- [74] K. L. Cashdollar, “Coal dust explosibility,” *Journal of loss prevention in the process industries*, 1996.

9. Appendix A – data collection

Table 4: Data collection part 1/2 – dust parameters

Sample	d10	d50	d90	SSA	Moisture	Poly-dispersity	Volatile content	Fixed carbon	Ash	Vessel	Material	Wood	Ref.
Wood		95									biomass	yes	[65]
Bark		57									biomass	yes	
Spanish pine		247									biomass	yes	
Wood dust from the production of particleboard (silo dust)	18,96	56,02	113,07		1,74 %	2,36				20L	biomass	yes	[66]
Wood dust from the production of particleboard (hammer mill dust)	4,43	15,96	37,74		3,88 %	2,64				20L	biomass	yes	
Radiata Pine	37,25	92,08	210,1		1,18 %	2,69				20L	biomass	yes	
Raw Norway spruce	28	149	603		5,80 %	4,23	79,00 %	11,1 %	4,1 %	1 m ³	biomass	yes	[67]
Torrified Norway spruce	15	67	281		2,70 %	4,42	77,00 %	15,9 %	4,2 %	1 m ³	biomass	yes	
Norway spruce		148,5		0,65	5,80 %		79,00 %	11,1 %	4,1 %	1 m ³	biomass	yes	[20]
Torrified Norway spruce		38,5		2,1	2,70 %		69,40 %	22,1 %	5,8 %	1 m ³	biomass	yes	
Southern pine		53,2		1,71	5 %		78,50 %	14 %	2,5 %	1 m ³	biomass	yes	
Torrified southern pine		36,6		1,47	3,30 %		70,30 %	22,1 %	4,3 %	1 m ³	biomass	yes	
Wood			700							1 m ³	biomass	yes	[59]
Bark			700							1 m ³	biomass	yes	
Forest residue			500							1 m ³	biomass	no	
Spanish pine			500							1 m ³	biomass	yes	
Barley straw			500							1 m ³	biomass	no	
Miscanthus			350							1 m ³	biomass	no	
Sorghum			650							1 m ³	biomass	no	
Rape seed straw			500							1 m ³	biomass	no	
Wood dust - beech oak mix			125							20 L	biomass	yes	
Forest residue - wood + bark			275							20 L	biomass	no	
Wood dust chipboard			43							20 L/1 m ³	biomass	yes	

Sample	d10	d50	d90	SSA	Moisture	Poly-dispersity	Volatile content	Fixed carbon	Ash	Vessel	Material	Wood	Ref.
Wheat grain dust		500								20 L/1 m ³	biomass	no	[59]
Cellulose		125								20 L/1 m ³	biomass	no	
British Colombia wood pellets		63								ASTM E1226	biomass	yes	
Nova Scotia wood pellets		63								ASTM E1226	biomass	yes	
Southern yellow pine		63								ASTM E1226	biomass	yes	
Fibrous wood		75								20 L	biomass	yes	
Dry Douglas fir and Western red cedar		250								20 L	biomass	yes	
Dry mountain pine and Lodgepole pine		200								20 L	biomass	yes	
Dry spruce and pine and fir			200							20 L	biomass	yes	
Southern pine	25,4	189,8	739	1,7	5 %	3,76	78,50 %	14 %	2,5 %	1 m ³	biomass	yes	
Norway spruce	28,4	148,5	603	0,7	5,80 %	3,87	79 %	11,10 %	4,1 %	1 m ³	biomass	yes	
Cacao		92			7,80 %					Hartmann	biomass	no	[68]
Oakwood		62,9			7,70 %					Hartmann	biomass	yes	
Lycopodium		35,9			5,80 %					Hartmann	biomass	no	
Icing sugar		17,9			0,2						biomass	no	[69]
Maize grain dust		215,1			13,5						biomass	no	
Wheat grain dust		36,4			7,7						biomass	no	
Barley grain dust		33,9			7,7						biomass	no	
Alfalfa		39			5,6						biomass	no	
Bread-making wheat		55,6			13,4						biomass	no	
Soybean dust		51,7			10,5						biomass	no	
Wood pellets	43,4	152,9	378,9	0,0069		2,19					biomass	yes	[70]

Sample	d10	d50	d90	SSA	Moisture	Poly-dispersity	Volatile content	Fixed carbon	Ash	Vessel	Material	Wood	Ref.
Stubble	180	830	1800			1,95					biomass	no	[70]
Wood chips	46,5	146,6	404,1	0,0065		2,44					biomass	yes	
Straw	43,7	171,2	474,5	0,076		2,52					biomass	no	
Almond shell	14,8	44,3	143	0,227		2,89					biomass	no	
Olive pit	20,5	68,2	196,7	0,155		2,58					biomass	no	
Torrefied wood pellets	22,3	104	326,9	0,13		2,93					biomass	yes	
Woodchips	47,3	152,7	378,5		8,4	2,17					biomass	yes	[71]
Straw	18,8	105,4	279,4		8,1	2,47					biomass	no	
Almond shell	13,2	44,2	133,2		8,8	2,71					biomass	no	
Pine cone	27	105	211		7,8	1,75					biomass	no	
Coconut	22,8	83,3	274,7		10,1	3,02					biomass	no	
Orange peel	62,4	226,6	549,7		7,3	2,15					biomass	no	
Cooperage residues	137,2	396,2	804		12,7	1,68					biomass	no	
Vine shoot	9,9	37,5	199,7		6,7	5,06					biomass	no	
Cellulose		51	125									no	[23]
Wood dust		33	71									no	
Wood dust		80										yes	
Wood dust (chipboard)		43										yes	
Lignin dust		18										no	
Paper dust		10	71									no	
Paper tissue dust		54										no	
Paper (phenolresin treated)		23	32									no	
Peat		58			15 %							no	
Peat		46			22 %							no	
Peat		38			31 %							no	
Peat		39	125		41 %							no	
Peat (from bottom of sieve)		74										no	
Peat (dust deposit)	20	49										no	

Sample	d10	d50	d90	SSA	Moisture	Poly-dispersity	Volatile content	Fixed carbon	Ash	Vessel	Material	Wood	Ref.
Paper pulp		29										no	[23]
Barley grain dust	63	240										no	
Oats grain dust	63	295										no	
Wheat grain dust		80										no	
Rye flour		29										no	
Soy bean flour		20										no	
Potato starch		32										no	
Maize starch		16										no	
Rice starch (hydrolyzed)		120										no	
Rice starch		18										no	
Wheat starch		20										no	
Tobacco		49										no	
Tapioca pellets		44										no	
Tea					6 %							no	
Tea (black, from dust collector)		76										no	
Wheat flour		57										no	
Wheat flour 550		56										no	
Hops, malted	71	490										no	
Grass dust		200										no	
Kellingley coal	5	26	65		1,70 %		29,20 %	50 %	19,10 %	1 m ³	coal	no	[67]
Kellingley coal		25,51		3,69	1,70 %		29,20 %	50 %	19,10 %	1 m ³	coal	no	[20]
Morwell coal		22								20 L	coal	no	[59]
Brown coal		32								1 m ³	coal	no	
Yallourn coal		36								20 L	coal	no	
Prince mine coal		125								20 L	coal	no	
Phalen mine coal		125								20 L	coal	no	
Lingan mine coal		125								20 L	coal	no	
Russian anthracite		53								20 L	coal	no	
Sulcis lignite		53								20 L	coal	no	

Sample	d10	d50	d90	SSA	Moisture	Poly-dispersity	Volatile content	Fixed carbon	Ash	Vessel	Material	Wood	Ref.	
South African coal		53								20 L	coal	no	[59]	
Polish coal		53								20 L	coal	no		
Snibston coal		53								20 L	coal	no		
Spanish lignite		40								1 m ³	coal	no		
German lignite		58								1 m ³	coal	no		
Pittsburgh coal		75								20 L	coal	no		
Pocahontas coal		75								20 L	coal	no		
Sebuku coal		15								20 L	coal	no		
Kellingley coal	5	25,5	65,3	3,7	1,70 %		29,20 %	50,00 %	19,1 %	1 m ³	coal	no		
Colombian coal	6,8	28,1	85,2	15,8	3,20 %		33,70 %	47,80 %	15,3 %	1 m ³	coal	no		
Sebuku coal		14,9			3 %						coal	no	[68]	
Blend 1	47,81	95,56	160,92			2,18				20 L	coal	no	[72]	
Blend 2	19,42	94,52	180,46			2,11				20 L	coal	no		
Blend 3	11,05	94,81	196,47			2,19				20 L	coal	no		
Blend 4	4,21	95,22	236,13			2,52				20 L	coal	no		
Tiefa - 1	12,37	55,94	103,4		9,76 %	2,07	40,97 %	42,44 %	28,12 %	20 L	coal	no	[40]	
Tiefa - 2	9,63	37,33	71,95		9,76 %	2,19	40,97 %	42,44 %	28,12 %	20 L	coal	no		
Lvliang - 1	17,11	51,13	111,2		1,03 %	2,51	23,38 %	71,32 %	6,92 %	20 L	coal	no		
Lvliang - 2	16,67	52,36	205,4		1,03 %	4,24	23,38 %	71,32 %	6,92 %	20 L	coal	no		
Neimeng	9,54	45,37	101,4		1,48 %	2,45	14,03 %	73,72 %	14,25 %	20 L	coal	no		
Ningxia	7,14	43,69	91,62		1,58 %	2,26	33,51 %	47,51 %	28,54 %	20 L	coal	no		
Huaibei	7,92	45,2	91,66		2,16 %	2,20	35,77 %	51,03 %	20,55 %	20 L	coal	no		
Coal 1	9,4	78,3	236,4		9,9	3,139208					coal	no		[73]

Sample	d10	d50	d90	SSA	Moisture	Poly-dispersity	Volatile content	Fixed carbon	Ash	Vessel	Material	Wood	Ref.	
Coal 2	8,2	60,5	211,1		11,1	3,624793					coal	no	[73]	
Coal 3	8,2	76,1	245,5		10,6	3,333771					coal	no		
Coal 4	3,3	41,2	186,9		7,2	4,616505					coal	no		
Coal 5	9	80,1	251,6		12,7	3,253433					coal	no		
Coal 6	3	53,5	206,5		7	3,915888					coal	no		
Coal 7	10,4	100,6	270,8		11,3	2,795229					coal	no		
Coal 8	6,7	57,2	228,3		12,6	4,108392					coal	no		
Coal 9	8,3	76,1	248,7		10,7	3,377135					coal	no		
Coal 10	7,7	65,6	211,3		5,4	3,338415					coal	no		
Coal 14	8,5	60,5	216,8		7,8	3,723967					coal	no		
Coal 15	10,5	96,6	258,9		12	2,78882					coal	no		
Coal 16	7,6	72,8	246,8		10,2	3,494505					coal	no		
Coal 18	4,7	103,7	294,7		10,2	2,887175					coal	no		
Coal 19	4,5	39,4	201,3		9,1	5,22335					coal	no		
Coal 20	8,5	68,8	249,3		11,8	3,747093					coal	no		
Coal 22	3,8	54,7	223,1		3,2	4,14808					coal	no		
Coal 23	8	82,6	245,9		9,2	3,07385					coal	no		
Coal 24	8,2	75,3	254,2		10,9	3,484728					coal	no		
Coal 25	4	48,1	220,6		6,8	4,669439					coal	no		
Coal 26	6,8	54,3	205,9		3,1	3,917127					coal	no		
Coal 27	2,6	36,9	189,3		4,7	5,200542					coal	no		
Pittsburgh coal 1		163									coal	no		[74]
Pittsburgh coal 2		68									coal	no		
Pittsburgh coal 3		48									coal	no		
Pittsburgh coal 4		32									coal	no		
Pittsburgh coal 5		28									coal	no		
Pittsburgh coal 7		11									coal	no		
Pocahontas coal 1		52									coal	no		
Pocahontas coal 2		47									coal	no		

Sample	d10	d50	d90	SSA	Moisture	Poly-dispersity	Volatile content	Fixed carbon	Ash	Vessel	Material	Wood	Ref.
Pocahontas coal 4		27									coal	no	[74]
Pocahontas coal 5		22									coal	no	
Pocahontas coal 6		14									coal	no	
Pocahontas coal 7		10									coal	no	
Brown coal		41									coal	no	[23]
Brown coal (from electrostatic filter)		55									coal	no	
Brown coal (dust from grinding)		60									coal	no	
Brown coal/anthracite (80:20)		40									coal	no	
Brown coal/anthracite (20:80)		10	71								coal	no	
Brown coal coke		290									coal	no	
Brown coal (graphitized)		28									coal	no	
Char coal		14	32								coal	no	
Char coal		19									coal	no	
Char coal		500									coal	no	
Bituminous coal		10									coal	no	
Bituminous coal (Petchora)		38									coal	no	
Bituminous coal (high volat.)		4									coal	no	

Table 5: Data collection part 2/2 – combustion properties of the dusts

Sample	P_{max}	K_{St}	dP/dt	MIT_{layer}	MIT_{cloud}	MEC	LEL	MIE	Vessel	Material	Wood	Ref.
Wood						29,4				biomass	yes	[65]
Bark						27,8				biomass	yes	
Spanish pine						83,1				biomass	yes	
Wood dust from the production of particleboard (silo dust)									20L	biomass	yes	[66]
Wood dust from the production of particleboard (hammer mill dust)									20L	biomass	yes	
Radiata Pine									20L	biomass	yes	
Raw Norway spruce	9	96							1 m ³	biomass	yes	[67]
Torrified Norway spruce	9,1	122				63			1 m ³	biomass	yes	
Norway spruce	9	96							1 m ³	biomass	yes	[20]
Torrified Norway spruce	9,1	110				54			1 m ³	biomass	yes	
Southern pine	9	105							1 m ³	biomass	yes	
Torrified southern pine	8,8	115				55			1 m ³	biomass	yes	
Wood	8,8	87	321			30			1 m ³	biomass	yes	[59]
Bark	9,7	98	361			30			1 m ³	biomass	yes	
Forest residue	9,1	84	309			60			1 m ³	biomass	no	
Spanish pine	8,2	23	85			90			1 m ³	biomass	yes	
Barley straw	9,3	58	214			90			1 m ³	biomass	no	
Miscanthus	8,1	31	114			120			1 m ³	biomass	no	
Sorghum	8,2	28	103			120			1 m ³	biomass	no	
Rape seed straw	8,2	32	118			210			1 m ³	biomass	no	
Wood dust - beech oak mix	7,7	136	501			-			20 L	biomass	yes	
Forest residue - wood + bark	9,1	92	339			20			20 L	biomass	no	
Wood dust chipboard	8,7	102	376			60			20 L/1 m ³	biomass	yes	
Wheat grain dust	9,3	112	413			60			20 L/1 m ³	biomass	no	
Cellulose	9,3	66	243			60			20 L/1 m ³	biomass	no	
British Colombia wood pellets	8,1	146	538			70			ASTM E1226	biomass	yes	

Sample	Pmax	Kst	dP/dt	MIT _{layer}	MIT _{cloud}	MEC	LEL	MIE	Vessel	Material	Wood	Ref.
Nova Scotia wood pellets	8,4	162	597			70			ASTM E1226	biomass	yes	[59]
Southern yellow pine	7,7	98	361			25			ASTM E1226	biomass	yes	
Fibrous wood	8,2	149	549			20			20 L	biomass	yes	
Dry Douglas fir and Western red cedar	8,5	43	158						20 L	biomass	yes	
Dry mountain pine and Lodgepole pine	8,8	40	147						20 L	biomass	yes	
Dry spruce and pine and fir	8,2	51	188						20 L	biomass	yes	
Southern pine	9	105	387						1 m ³	biomass	yes	
Norway spruce	9,2	95	350						1 m ³	biomass	yes	
Cacao						800		350	Hartmann	biomass	no	[68]
Oakwood						755		42	Hartmann	biomass	yes	
Lycopodium						680		4	Hartmann	biomass	no	
Icing sugar	7,5	68	249	400			210			biomass	no	[69]
Maize grain dust	7,5	81	298	420	300		150			biomass	no	
Wheat grain dust	8,1	148	544	510	290		30			biomass	no	
Barley grain dust	7,1	50	185	480	290		180			biomass	no	
Alfalfa	7	50	186	460	300		150			biomass	no	
Bread-making wheat	8,1	144	530	440			60			biomass	no	
Soybean dust	7	73	270	560	300					biomass	no	
Wood pellets				300						biomass	yes	
Stubble										biomass	no	
Wood chips				360						biomass	yes	
Straw				320						biomass	no	
Almond shell				290						biomass	no	
Olive pit				300						biomass	no	
Torrefied wood pellets				320						biomass	yes	
Woodchips	7,4	150	553	350	460		60	160		biomass	yes	[71]
Straw	7,2	157	579	320	420		60	440		biomass	no	
Almond shell	7,1	157	580	290	440		60	610		biomass	No	

Sample	P _{max}	K _{st}	dP/dt	MIT _{layer}	MIT _{cloud}	MEC	LEL	MIE	Vessel	Material	Wood	Ref.
Pine cone	7,1	143	527	320	380		60	260		biomass	no	[71]
Coconut	7,3	150	552	280	400		60	220		biomass	no	
Orange peel	7,3	127	469	300	440		125	1000		biomass	no	
Cooperage residues	7,3	131	484	350	420		750	1000		biomass	no	
Vine shoot	7,2	136	501	300	420		125	260		biomass	no	
Cellulose	9,3	66			500					biomass	no	[23]
Wood dust					500					biomass	no	
Wood dust					480					biomass	yes	
Wood dust (chipboard)	9,2	102			490					biomass	yes	
Lignin dust	8,7	208			470					biomass	no	
Paper dust	5,7	18			580					biomass	no	
Paper tissue dust	8,6	52			540					biomass	no	
Paper (phenolresin treated)	9,8	190			490					biomass	no	
Peat	10,9	157			480					biomass	no	
Peat	8,4	69			470					biomass	no	
Peat	8,1	64			500					biomass	no	
Peat					500					biomass	no	
Peat (from bottom of sieve)	8,3	51			490					biomass	no	
Peat (dust deposit)	9,5	144			360					biomass	no	
Paper pulp	9,8	168								biomass	no	
Barley grain dust										biomass	no	
Oats grain dust	6	14								biomass	no	
Wheat grain dust	9,3	112								biomass	no	
Rye flour	8,9	79			490					biomass	no	
Soy bean flour	9,2	110			620					biomass	no	
Potato starch	9,4	89			520					biomass	no	
Maize starch	9,7	158			520					biomass	no	
Rice starch (hydrolyzed)	9,3	190			480					biomass	no	
Rice starch	10	190			530					biomass	no	
Wheat starch	9,8	132			500					biomass	no	

Sample	P _{max}	K _{st}	dP/dt	MIT _{layer}	MIT _{cloud}	MEC	LEL	MIE	Vessel	Material	Wood	Ref.
Tobacco	4,8	12			470					biomass	no	[23]
Tapioca pellets	9	53			450					biomass	no	
Tea	8,1	68								biomass	no	
Tea (black, from dust collector)	8,2	59			510					biomass	no	
Wheat flour	8,3	87			430					biomass	no	
Wheat flour 550	7,4	42			470					biomass	no	
Hops, malted	8,2	90			420					biomass	no	
Grass dust	8	47			470					biomass	no	
Kellingley coal	8,2	78				91			1 m ³	coal	no	[67]
Kellingley coal	7,7	78				91			1 m ³	coal	no	[20]
Morwell coal	7,6	220							20 L	coal	no	[59]
Brown coal	10	151							1 m ³	coal	no	
Yallourn coal	6,7	91							20 L	coal	no	
Prince mine coal	6,5	44				70			20 L	coal	no	
Phalen mine coal	6	30				120			20 L	coal	no	
Lingan mine coal	7	44				90			20 L	coal	no	
Russian anthracite	5	68							20 L	coal	no	
Sulcis lignite	6,8	162							20 L	coal	no	
South African coal	6	81							20 L	coal	no	
Polish coal	6,8	135							20 L	coal	no	
Snibston coal	6,5	149							20 L	coal	no	
Spanish lignite	8,8	107				90			1 m ³	coal	no	
German lignite	8,7	105				60			1 m ³	coal	no	
Pittsburgh coal	6,7	41				65			20 L	coal	no	
Pocahontas coal	6,5	31				80			20 L	coal	no	
Sebuku coal	6,6	114				63			20 L	coal	no	
Kellingley coal	8,2	80				120			1 m ³	coal	no	
Colombian coal	8,5	129				75			1 m ³	coal	no	
Sebuku coal					790			55		coal	no	[68]
Blend 1	4,9	3,46							20 L	coal	no	[72]

Sample	Pmax	Kst	dP/dt	MIT _{layer}	MIT _{cloud}	MEC	LEL	MIE	Vessel	Material	Wood	Ref.
Blend 2	5,1	3,86							20 L	coal	no	[72]
Blend 3	5,3	4,31							20 L	coal	no	
Blend 4	5,6	4,99							20 L	coal	no	
Tiefa - 1	7		68						20 L	coal	no	[40]
Tiefa - 2	7,7		65						20 L	coal	no	
Lvliang - 1	7,9		47						20 L	coal	no	
Lvliang - 2	7,6		36						20 L	coal	no	
Neimeng	6,1		28						20 L	coal	no	
Ningxia	6,8		44,5						20 L	coal	no	
Huaibei	8,2		61						20 L	coal	no	
Coal 1	7,3	119	438		490		60	220		coal	no	[73]
Coal 2	7,1	153	563		450		60	1000		coal	no	
Coal 3	6,8	112	411		470		60	1000		coal	no	
Coal 4	6,8	96	352		500		60	1000		coal	no	
Coal 5	7,3	110	404		490		60	1000		coal	no	
Coal 6	6,6	92	339		540		125	1000		coal	no	
Coal 7	7	92	340		500		60	1000		coal	no	
Coal 8	7,3	121	444		430		60	1000		coal	no	
Coal 9	7,4	126	463		470		60	1000		coal	no	
Coal 10	7,2	140	515		490		60	470		coal	no	
Coal 14	7,7	148	547		510		30	220		coal	no	
Coal 15	7,3	106	391		480		60	1000		coal	no	
Coal 16	7,3	124	458		480		60	1000		coal	no	
Coal 18	7,1	102	377		480		125	1000		coal	no	
Coal 19	7,9	176	647		400		30	500		coal	no	
Coal 20	7,5	115	424		480		30	1000		coal	no	
Coal 22	6,7	97	357		510		125	1000		coal	no	
Coal 23	7,1	121	444		480		60	1000		coal	no	
Coal 24	7,2	122	450		500		30	1000		coal	no	
Coal 25	7,4	136	502		500		30	1000		coal	no	

Sample	Pmax	Kst	dP/dt	MIT _{layer}	MIT _{cloud}	MEC	LEL	MIE	Vessel	Material	Wood	Ref.
Coal 26	7,4	157	580		520		30	79		coal	no	[73]
Coal 27	6,7	82	303		520		60	1000		coal	no	
Pittsburgh coal 1	6					130				coal	no	[74]
Pittsburgh coal 2	6,3					85				coal	no	
Pittsburgh coal 3	6,6					80				coal	no	
Pittsburgh coal 4	6,7					65				coal	no	
Pittsburgh coal 5	6,8					75				coal	no	
Pittsburgh coal 7	7,7					85				coal	no	
Pocahontas coal 1	6					120				coal	no	
Pocahontas coal 2	6,3					130				coal	no	
Pocahontas coal 4	6,3					90				coal	no	
Pocahontas coal 5	6,2					80				coal	no	
Pocahontas coal 6	6,5					80				coal	no	
Pocahontas coal 7	6,5					80				coal	no	
Brown coal	9,1	123			420					coal	no	[23]
Brown coal (from electrostatic filter)	9	143			450					coal	no	
Brown coal (dust from grinding)	8,9	107			420					coal	no	
Brown coal/antracite (80:20)	8,6	108			440					coal	no	
Brown coal/antracite (20:80)	0,4	1			590					coal	no	
Brown coal coke	8,4	115			560					coal	no	
Brown coal (graphitized)										coal	no	
Char coal	9	10			520					coal	no	
Char coal	8,5	119			540					coal	no	
Char coal										coal	no	
Bituminous coal	9	55			590					coal	no	
Bituminous coal (Petchora)	8,6	86			610					coal	no	
Bituminous coal (high volat.)	9,1	59			510					coal	no	

10. Appendix B – EGU poster and abstract

10.1. Abstract

To participate in the EGU General Assembly 2019 the following abstract was submitted: *Explosion risks on biomass materials: how to work with particle size* by Inger Marie Fanebust and Nieves Fernandez-Anez to ERE2.5 – “Biomass in future energy and resource systems: impact on land use, climate and environmental services”.

Explosion risks on biomass materials: how to work with particle size

Inger Marie Fanebust and Nieves Fernandez-Anez

The Oxford dictionary defines biomass as all “organic matter used as a fuel, especially in a power station for the generation of electricity”. This broad term includes solid substances from wood to waste: several materials with diverse characteristics that are currently grouped together. However, many properties of these solid substances depend on characteristics as particle shape, size or mechanic properties, which affect the bulk properties of the materials and their relationship to processes such as flow, compaction or fluidization.

If we focus on the treatment of these materials, safety should be one of the first terms that come to our mind. Making a safe working environment is essential and requires an enormous investment. One of the main risks observed in this type of plants is the fire and explosion risk. Biomass materials are easily dispersible and highly flammable, so the rate of incidents and accidents that these facilities present is higher than many others. In order to make this process easier, the National Fire Protection Energy developed the Standard 664 for the prevention of fires and explosions in wood processing and woodworking facilities. It is important to notice that this standard covers several biomass, as it defines wood as “the cellulosic material derived from trees, and other cellulosic materials including, but not limited to, wheat straw, flax, bagasse, coconut shell, corn stalks, hemp, rice hulls, and paper or other cellulosic fiber used as a substitute or additive to wood”.


The measurements and requirements established in this standard are based on the median particle size of the materials to distinguish between materials with a potential fire and explosion risk from those without it. This consideration is based on the previous knowledge on coal particulates, which proved in several occasions that the diameter of the almost-rounded particulates heavily influences the explosion and self-ignition risks associated with these materials. For these materials, the terms d10, d50 and d90 have been widely used, describing the diameter where 10, 50 or 90% of the material’s mass is comprised of particles with a diameter less than this value, respectively.

However, the elongated particle shape of biomass makes this assumption inaccurate. One of the dimensions of these particles is comparatively much longer than the other two, making incorrect to assume one unique value for the whole particle.

Once this problem is identified, we face a new one: find a correct concept that fits with these particles and that can be used to define the fire and explosion risks of these materials. Specific surface area, polydispersity, skewness are terms that are now under consideration. Pros and cons are considered, and a discussion is open in order to find the right concept that ensure a safe working space to treat all types of biomass materials.


10.2. Poster

This poster was presented at the EGU conference 2019 in the session “Biomass in future energy and resource systems: impact on land use, climate and environmental services”.



Explosion risks on biomass materials: how to work with particle size

Inger Marie Fanebust* & Nieves Fernandez-Anez



Background

Much of the knowledge concerning dust explosion is based on incidents and experiments involving coal dust. Much less research is done on biomass, and the data from this research is often not publicly available. Lack of available data is not the only problem that needs solving. There is also a question of how to measure the size of non-spherical particles.

NFPA 664

Standard for the Prevention of Fires and Explosions in Wood Processing and Woodworking Facilities

Deflagrable wood dust is defined as any dust that will propagate a flame front when suspended in air. Wood particulate with a mass median particle size of 500 µm or less, with a moisture content of less than 25 % are considered deflagrable. Meaning that if a dust has larger particles or more moisture it should not pose an explosion hazard.

Particle size

The influence of particle size on dust explosions has been thoroughly studied for coal. It is clear that particle size is one of the most important factors affecting explosion parameters. Smaller particles are considered more dangerous.

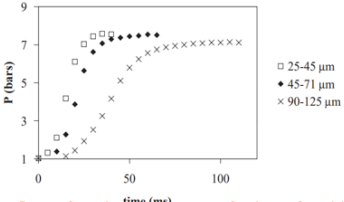


Figure 1. Influence of particle size on the severity of explosion of wood dust [1]

Decreased particle size leads to

- more violent explosions
- easier suspension and dispersion
- easier ignition of a dust cloud
- more rapid flame propagation (until a certain point)

Particle shape

In most cases particles are treated as *spheres*. However, biomass particles are very rarely spherical. More often biomass particles are described as *needle-like* or *fibrous*. The figures to the right are examples of some actual shapes biomass particles can have [2].

This means particles often have a bigger surface area than what might be assumed based on a single parameter, such as a diameter. Sometimes an equivalent diameter is used, though this can also give many different results depending on which parameter is kept constant (Figure 3).

SSA (specific surface area) is the surface area per mass unit. This parameter has shown a correlation to explosions parameters.

Particle size distribution

Since dust is rarely (if ever) made up of single-size particles it is necessary to look at the size distribution for the whole sample. To express this the median particle size, D_{50} , has traditionally been used. If D_{50} is 500 µm this means 50 % of the particles are 500 µm or smaller. To get a more complete picture if a sample's size distribution, D_{10} and D_{90} are also being used. These three parameters together can be used to find the polydispersity index:

$$\sigma_D = \frac{D_{90} - D_{10}}{D_{50}}$$

The *polydispersity index* gives the width of the distribution, however, it cannot tell whether a wide distribution is due to an increase in D_{90} or decrease in D_{10} . An alternative to this is the skewness index, which gives an indication for whether there is an abundance of smaller or larger particles. When applying the skewness index to datasets this shows a correlation to explosion violence [3]




Figure 2. View of particle shapes of poplar and corn stover from image analysis [2]

Findings

The data available is not sufficient to define a certain upper limit for when dust poses a deflagration hazard. Moreover, my findings suggest that using the diameter as a parameter is inadequate as well.

A consensus is needed both in the parameters to study and in the methodology to be used to define them. Several researchers are currently investigating both, but a common standard is needed.

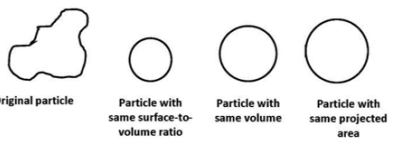



Figure 3. Equivalent spherical diameters [4]

Acknowledgements

I would like to thank the NFPA research foundation for giving me this project and for letting me be at this conference.

And I would very much like to thank Nieves Fernandez-Anez, my counsellor for this project, whose guidance and encouragement have been invaluable.



References

- [1] S. Callé, L. Klabá, D. Thomas, L. Perrin og O. Dufaud (2005) Powder technology.
- [2] Miguel Gil, Enrique Teruel, Inmaculada Arauzo, (2014). Fuel.
- [3] Alberto Tascón (2018). Powder technology.
- [4] Russell A. Ogle (2017). *Dust explosion dynamics*. Elsevier Inc.